RESULTS AND DISCUSSION

CHAPTER IV
RESULTS AND DISCUSSION

4.1. Introduction

Results pertaining to the current study on **"Adsorption Behaviour and Corrosion Inhibitive Potential of Imidazoline Derivatives on Mild Steel/Acid Interface"** is presented and discussed on the basis of objectives setforth.

The influence of the addition of imidazoline derivatives (P2I, TMP2I, DMP2I, OCP2I, PNDM2I, PNP2I) on the electrochemical behaviour of steel in 0.5M H_2SO_4 and 1M HCl was investigated by the weight loss, electrochemical and surface analytical techniques.

Experimental results are explained on the following headings:

a) **Weight loss method:**

The following parameters were investigated:

- **Effect of concentration (40 ppm to 200ppm)**
- **Effect of immersion time (½ h, 1h, 3h, 6h, 12h and 24h)**
- **Temperature variation (303K, 313K, 323K, 333K, 343K)**

b) **Electrochemical Measurements**

The following techniques were carried out in this method

- **Linear Polarisation Resistance technique**
- **Tafel Intercept Method**
- **Electrochemical Impedance Spectroscopy**

c) **Surface Analysis Techniques:**

The following surface analytical techniques were used to study the surface of the mild steel in the presence and absence of the inhibitors.

- **Scanning Electron Microscope**
- **Fourier Transform Infra Red Spectroscopy**

d) **d) UV Spectroscopy studies were conducted to find out possibility of Fe complex on mild steel surface.**

4.2 WEIGHT LOSS METHOD

4.2.1 Effect of Concentration of the Inhibitors - P2I, TMP2I, DMP2I, OCP2I, PNDMP2I, PNP2I in Sulphuric acid and Hydrochloric acid on mild steel surface :

The imidazoline derivatives were investigated in a wide interval of concentration ranging from 40 ppm to 200 ppm. The limits of this interval were determined for each compound by its solubility (the maximum concentration studied) and the protective effect reached (the minimum concentration of experimental interest). After reaching a definite concentration value, specific for each inhibitor studied, the subsequent increase of concentration, does not significantly change the protective effect,

The weight loss measurements and inhibition efficiencies for varying concentrations of **P2I,TMP2I, DMP2I, OCP2I, PNDM2I, PNP2I** in 0.5M H_2SO_4 and in 1M HCl are presented in Tables (2-7) and in Figures (15- 20).

A maximum efficiency of 88.8 % in H_2SO_4 and 91.4 % in HCl was obtained at 200 ppm for P2I.

TMP2I showed an inhibition efficiency of 98.2 % and 98.2 % in H_2SO_4 and HCl respectively at 200 ppm.

The inhibition efficiency attained a maximum of 93.4 % and 94.6 % in H_2SO_4 sulphuric acid and HCl for DMP2I at 200 ppm .

Maximum efficiency afforded by OCP2I in H_2SO_4 medium was 90.6 % at 200 ppm concentration and in HCl medium was 93.6 % at 120 ppm concentration.

Highest inhibition efficiency of 85.4 % and 90.1% 200 for PNDM2I was observed at 200 ppm for H_2SO_4 and HCl medium.

PNP2I showed increased inhibition efficiency with increasing concentration reaching 81.7 % in H_2SO_4 and 83.6 % in HCl at 200 ppm .

TABLE – 2 Effect of concentration of P2I on mild steel corrosion at various time intervals in 0.5M H_2SO_4 and 1M HCl

ACID MEDIA	Conc in ppm	1/2 h		1 h		3 h		6 h		12 h		24 h	
		CR mpy	IE %	CR mpy	IE %	CR mpy	IE %	CR mpy	IE %	CR mpy	IE %	CR mpy	IE %
H_2SO_4	Blank	1290	-	1347		1508		5309		2331		1790	
	40	1168	18.4	1139	38.2	1022	57.1	4034	72.0	1832	51.8	1645	48.9
	50	1053	20.5	1036	41.7	766	66.7	3760	75.2	1696	67.5	1559	52.0
	60	1014	21.5	859	46.7	728	71.4	3520	81.5	1594	68.1	1462	57.1
	70	924	25.1	773	48.8	625	76.5	3209	81.9	1534	70.4	1410	62.6
	80	808	27.1	621	51.3	559	78.3	2871	83.3	1367	74.6	1358	65.3
	100	744	31.6	581	56.3	478	79.4	2641	84.2	1212	76.5	1232	68.7
	120	686	36.1	521	62.4	422	79.5	2335	84.6	1097	77.9	1100	72.9
	140	609	39.5	491	68.3	350	81.7	2190	84.8	1035	80.0	1052	74.3
	160	549	41.4	347	71.3	283	82.1	1768	85.4	903	82.3	846	77.8
	200	515	45.8	344	74.1	186	84.3	1636	88.8	760	83.8	754	81.2
HCl	Blank	1140		1235		1546		1840		1256		1138	
	40	859	24.6	884	28.4	1072	30.7	1097	40.3	783	37.7	814	28.4
	50	759	33.4	807	34.6	1000	35.3	742	59.7	573	54.3	759	33.3
	60	661	42.0	685	44.5	820	46.9	703	61.8	549	56.3	606	46.7
	70	594	47.9	633	48.7	786	49.1	657	64.3	468	62.7	496	56.4
	80	541	52.5	567	54.1	673	56.4	471	74.4	408	67.5	405	64.4
	100	468	58.9	487	60.5	596	61.4	425	76.9	323	74.3	342	69.9
	120	427	62.5	446	63.8	536	65.3	272	85.2	265	78.9	284	75.0
	140	390	65.7	381	69.1	450	70.9	185	89.9	190	84.8	245	78.4
	160	354	68.9	358	71.0	402	74.0	165	91.0	135	89.2	232	79.5
	200	323	71.6	294	76.1	330	78.6	118	91.4	117	90.7	201	82.3

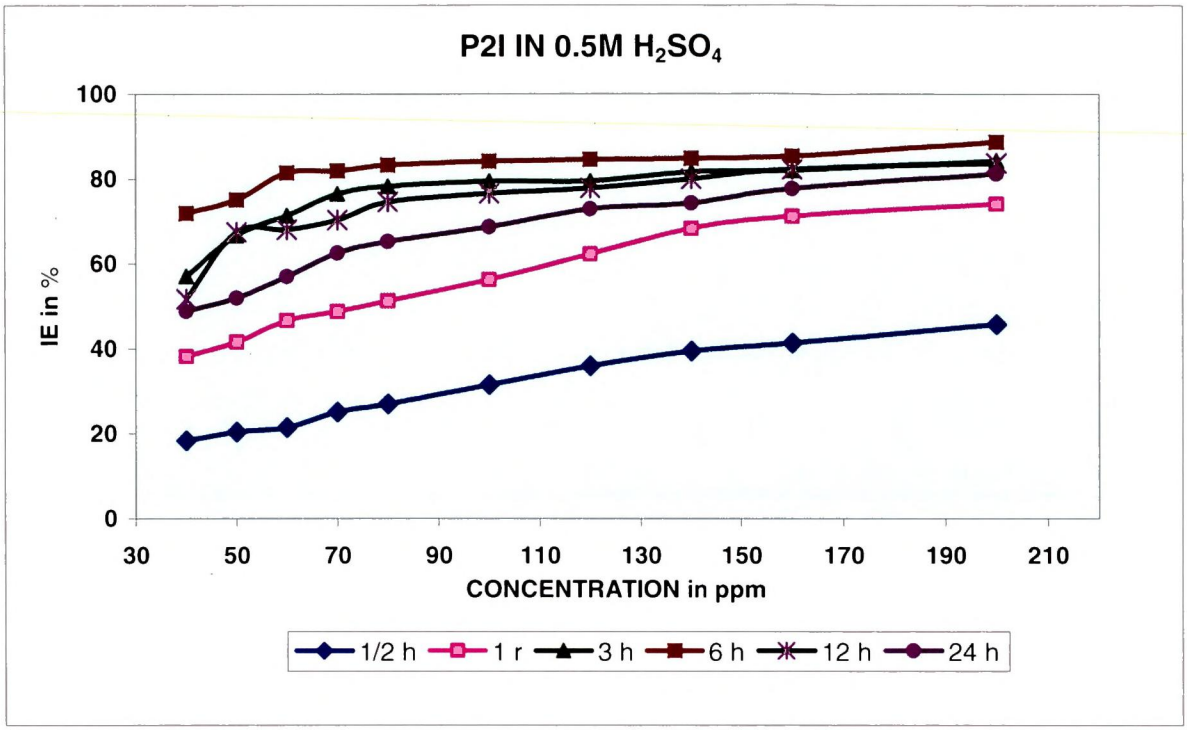

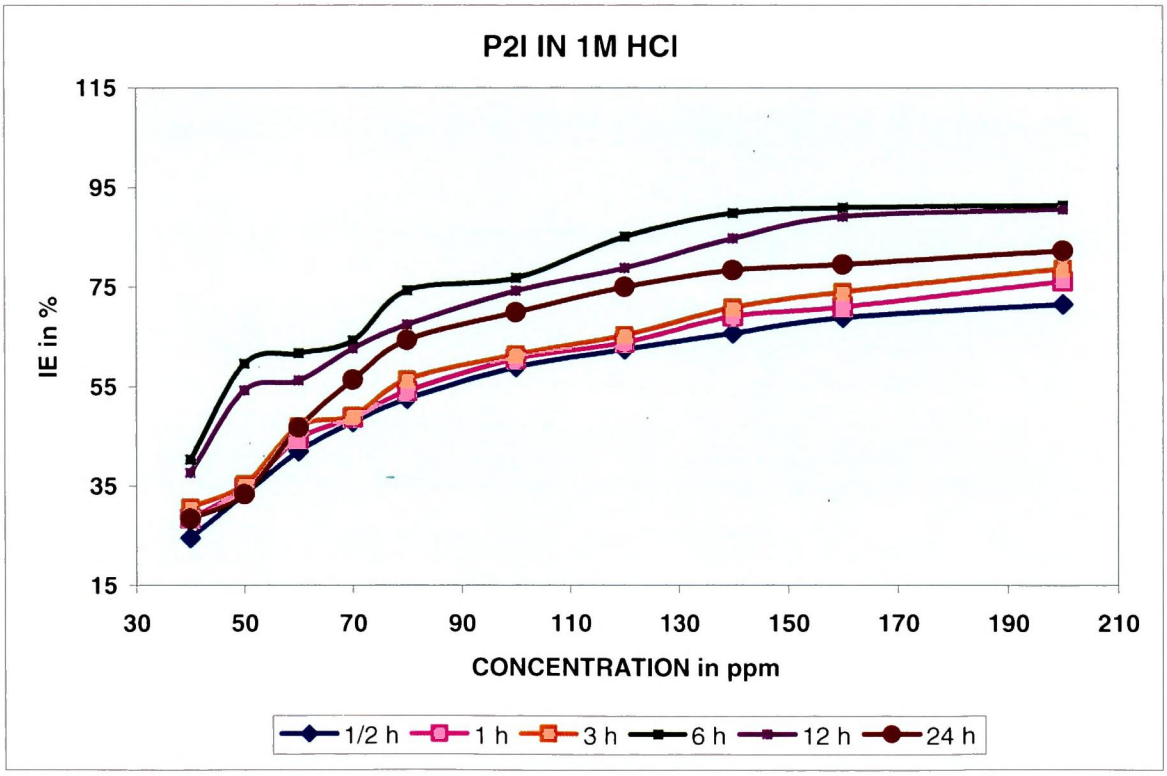

Figure - 15 Effect of concentration and exposure time on the inhibition efficiency of P2I for mild steel corrosion in 0.5M H_2SO_4 and 1M HCl.

Table – 3 Effect of concentration of TMP2I on mild steel corrosion at various time intervals in 0.5M H_2SO_4 and 1M HCl

ACID MEDIA	Conc in ppm	1/2 h		1 h		3 h		6 h		12 h		24 h	
		CR mpy	IE %	CR mpy	IE %	CR mpy	IE %	CR mpy	IE %	CR mpy	IE %	CR mpy	IE %
H_2SO_4	Blank	1290	-	1347		1508		5309		2331		1790	
	40	1237	4.1	1141	15.2	1278	68.5	2494	53.0	1732	25.7	652	12.6
	50	995	22.8	920	31.6	1030	71.6	2088	60.7	1278	45.2	601	24.8
	60	772	40.1	677	49.7	758	74.9	1775	66.6	807	65.4	509	43.4
	70	716	44.4	570	57.6	639	76.5	1525	71.3	782	66.4	342	50.1
	80	607	52.9	471	65.0	528	78.9	1298	75.6	606	75.0	318	68.4
	100	569	55.8	471	71.3	528	83.4	1138	75.6	584	75.0	305	72.5
	120	517	59.9	386	76.6	432	86.7	1102	79.2	582	75.0	283	74.2
	140	482	62.6	315	78.0	353	89.9	1002	81.1	520	77.7	242	76.7
	160	448	65.2	296	80.1	331	95.8	830	84.4	486	79.2	222	79.0
	200	425	67.0	238	82.3	267	98.2	375	92.9	330	85.8	200	81.8
HCl	Blank	1140		1235		1546		1840		1256		1138	
	40	1032	9.6	1180	4.4	873	43.5	491	73.3	336	73.2	414	63.6
	50	645	43.5	1126	18.8	203	86.9	410	77.7	309	75.4	382	66.4
	60	607	46.8	970	21.4	200	87.1	288	84.3	282	77.5	324	71.5
	70	552	51.6	871	29.4	152	90.1	260	85.9	223	82.2	218	80.8
	80	460	59.7	635	48.5	133	91.4	237	87.1	208	83.4	202	82.2
	100	454	60.2	370	70.0	114	92.6	197	89.3	200	84.0	194	82.9
	120	428	62.4	344	72.1	97	93.7	163	91.1	154	87.7	180	84.2
	140	395	65.4	314	74.6	79	94.9	114	93.8	150	88.1	154	86.5
	160	372	67.4	260	78.9	53	96.6	105	94.3	111	91.1	141	87.6
	200	342	70.0	251	79.6	28	98.2	104	94.3	78	93.8	127	88.8

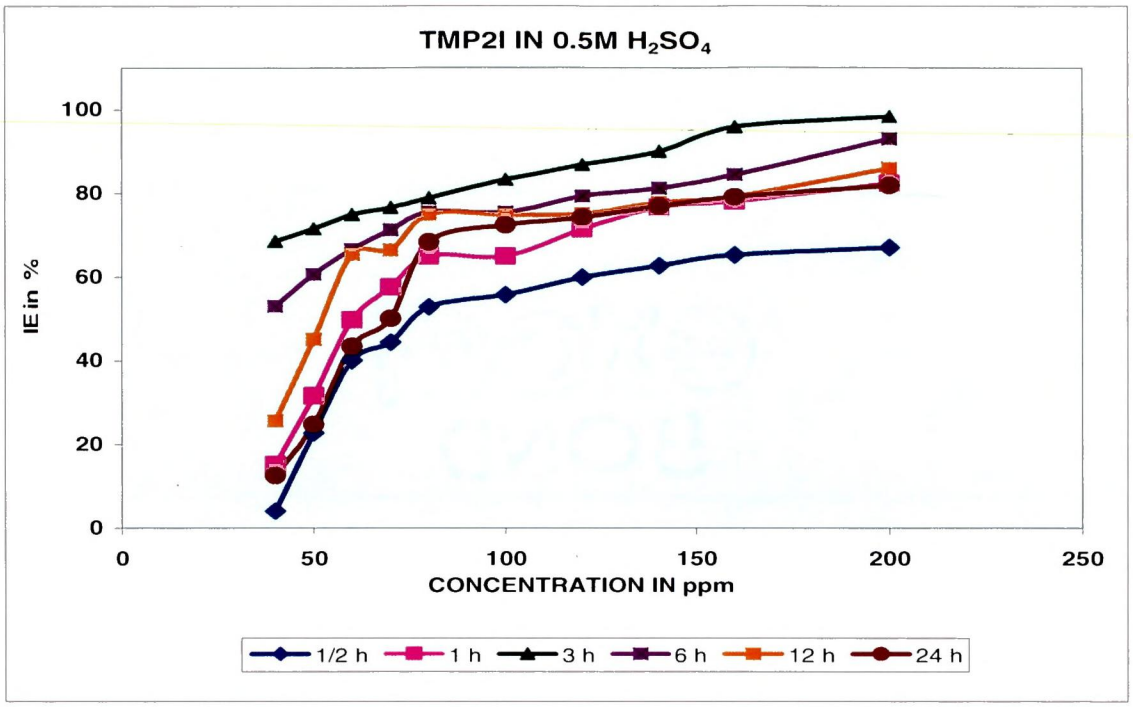

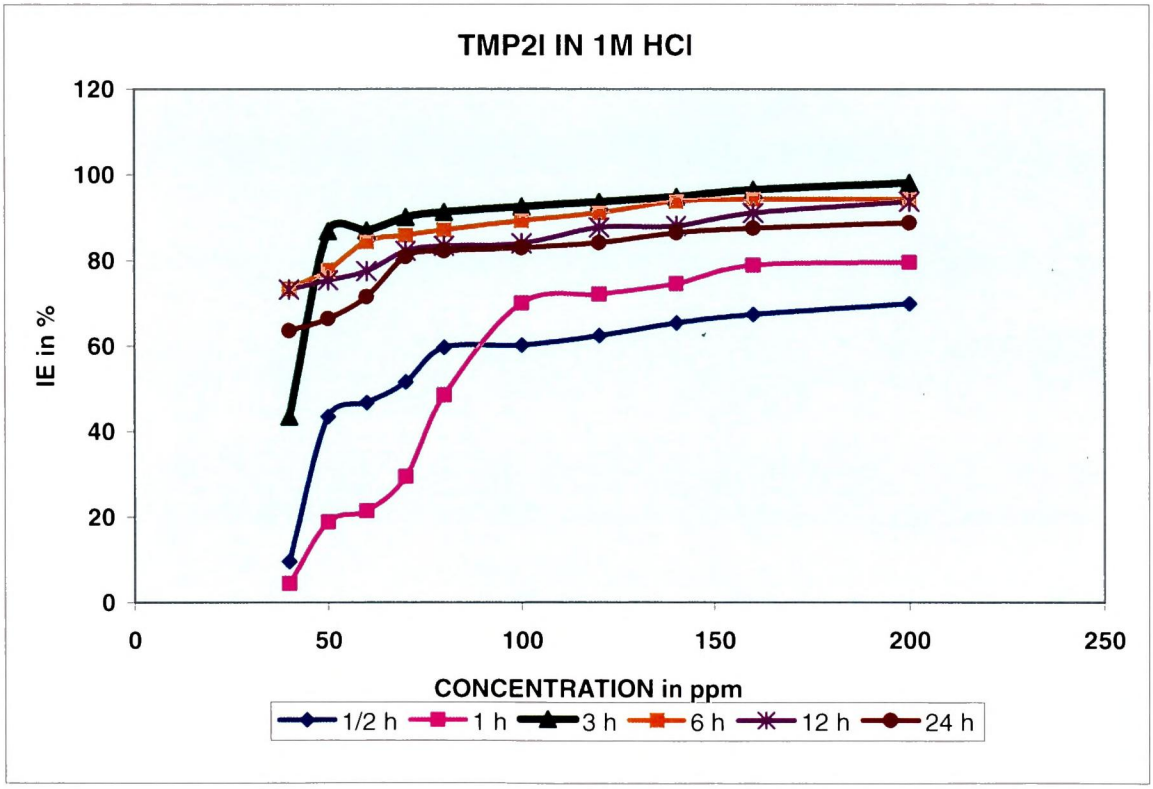

Figure – 16 Effect of concentration and exposure time on the inhibition efficiency of TMP2I for mild steel corrosion in 0.5M H_2SO_4 and 1M HCl.

TABLE – 4 Effect of concentration of DMP2I on mild steel corrosion at various time intervals in 0.5M H_2SO_4 and 1M HCl

ACID MEDIA	Conc in ppm	1/2 h		1 h		3 h		6 h		12 h		24 h	
		CR mpy	IE %	CR mpy	IE %	CR mpy	IE %	CR mpy	IE %	CR mpy	IE %	CR mpy	IE %
H_2SO_4	Blank	1290		1347		1508		5309		2331		1790	
	40	1042	19.2	1068	20.7	628	58.3	1933	63.6	1085	53.5	882	50.7
	50	984	23.7	1022	24.1	494	67.2	1473	72.3	957	58.9	811	54.7
	60	888	31.1	893	33.7	471	68.8	1381	74.0	651	72.0	682	61.9
	70	814	36.9	835	37.9	414	72.5	1353	74.5	624	73.2	639	64.3
	80	775	39.9	792	41.1	381	74.7	1221	77.0	563	75.8	579	67.6
	100	745	42.2	717	46.8	341	77.4	1135	78.6	528	77.3	551	69.2
	120	724	43.8	672	50.1	313	79.2	998	81.2	474	79.6	472	73.6
	140	663	48.5	587	56.4	277	81.6	890	83.2	449	80.7	407	77.3
	160	602	53.3	540	59.9	214	85.8	615	88.4	291	87.5	334	81.3
	200	546	57.6	500	62.8	162	89.3	352	93.4	218	90.6	257	85.6
HCl	Blank	1290		1347		1508		5309		2331		1790	
	40	930	9.4	762	15.4	663	32.2	515	30.3	606	21.4	707	8.1
	50	906	18.3	720	23.1	514	49.2	456	39.2	408	27.2	664	12.9
	60	894	21.3	658	36.2	441	51.7	340	43.7	400	31.6	595	18.3
	70	853	28.3	631	42.6	363	58.5	332	49.5	371	34.2	518	21.2
	80	831	37.3	601	53.8	335	62.9	307	55.9	318	41.3	481	24.1
	100	779	42.3	539	56.8	317	68.3	291	60.3	294	48.0	433	31.1
	120	728	46.8	464	61.3	316	72.0	283	66.0	278	52.9	375	38.5
	140	689	52.8	391	63.5	283	76.7	280	68.7	251	55.6	356	41.2
	160	667	57.4	354	74.2	276	81.2	269	76.7	221	61.2	308	52.7
	200	617	60.01	319	81.4	243	94.6	243	89.2	203	67.4	260	57.8

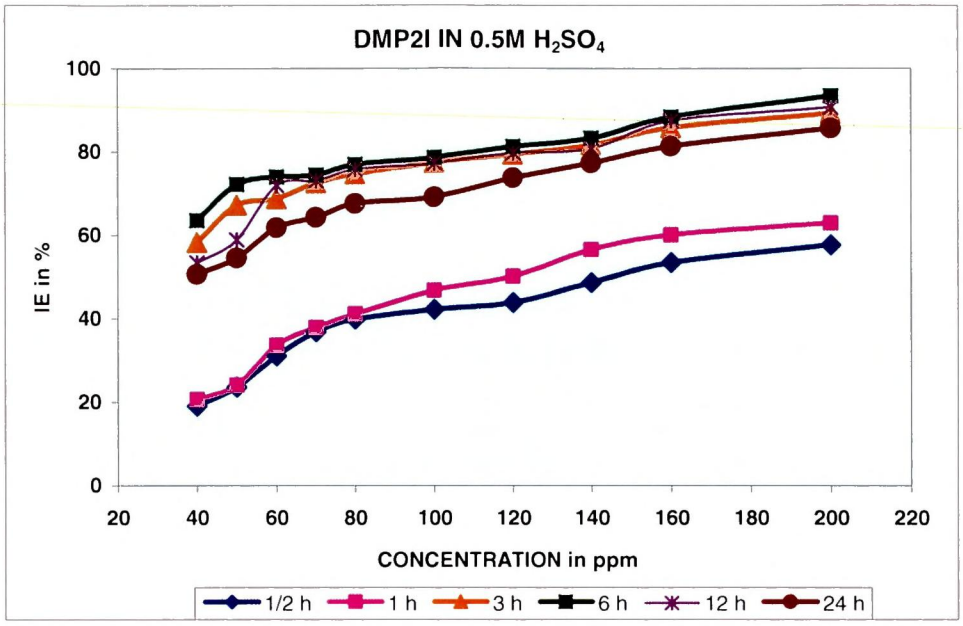

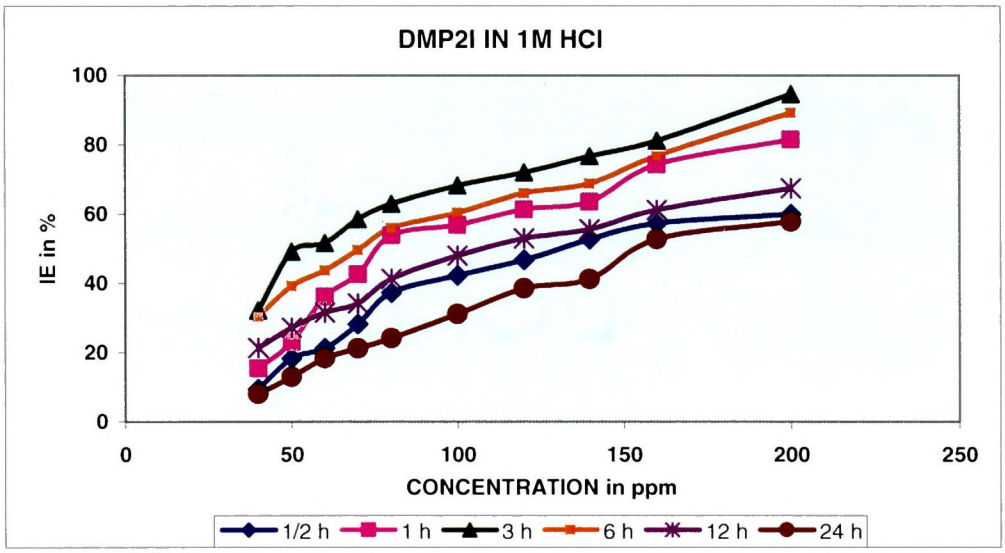

Figure - 17 Effect of concentration and exposure time on the inhibition efficiency of DMP2I for mild steel corrosion in 0.5M H_2SO_4 and 1M HCl.

TABLE – 5 Effect of concentration of OCP2I on mild steel corrosion at various time intervals in 0.5M H_2SO_4 and 1M HCl

ACID MEDIA	Conc in ppm	1/2 h		1 h		3 h		6 h	12 h			24 h	
		CR mpy	IE %	CR mpy	IE %	CR mpy	IE %	CR mpy	IE %	CR mpy	IE %	CR mpy	IE %
	Blank	1290	-	1347	-	1508	-	5309	-	2331	-	1790	-
	40	840	34.8	924	41.4	739	51.0	3749	39.4	1441	38.2	1716	4.1
	50	742	42.4	800	50.6	438	70.9	2951	54.4	1241	46.7	1409	21.3
	60	703	45.5	782	51.9	427	71.7	2314	66.4	1155	50.4	1363	23.8
	70	527	59.1	733	65.5	398	73.6	2140	69.7	1085	53.4	1232	31.2
H_2SO_4	80	488	62.1	728	65.9	349	76.8	1877	74.6	1082	53.6	1179	34.1
	100	365	71.7	720	76.5	329	78.1	1495	81.8	817	64.9	1179	34.1
	120	344	73.3	710	77.3	303	79.9	1343	84.7	750	67.8	937	47.6
	140	322	75.0	655	78.4	281	81.3	1324	85.1	740	68.2	799	55.3
	160	305	76.3	595	80.8	253	83.2	1261	86.2	663	71.5	749	58.1
	200	279	78.3	570	82.7	242	86.9	820	90.6	601	74.2	632	64.7
	Blank	1140	-	1235	-	1546	-	1840	-	1256	-	1138	-
	40	1010	11.4	771	37.5	924	40	453	75.4	375	70.1	400	64.8
	50	803	29.5	733	40.6	644	58	366	80.1	313	75.0	218	80.8
	60	647	43.2	617	50.0	474	69	309	83.2	256	79.6	182	83.9
	70	492	56.8	521	57.8	364	76	286	84.4	191	84.8	153	86.5
HCl	80	466	59.1	424	65.6	331	79	262	85.7	161	87.1	146	87.1
	100	380	66.6	308	75.0	220	86	252	90.3	135	89.2	124	88.1
	120	325	71.4	212	82.8	132	91	201	93.6	105	91.6	105	90.8
	140	271	76.2	173	85.9	257	83	286	84.4	301	76.0	272	76.0
	160	320	71.9	270	78.1	533	65	261	85.8	347	72.4	346	69.6
	200	396	65.2	328	73.4	801	48	286	84.4	382	69.6	574	49.5

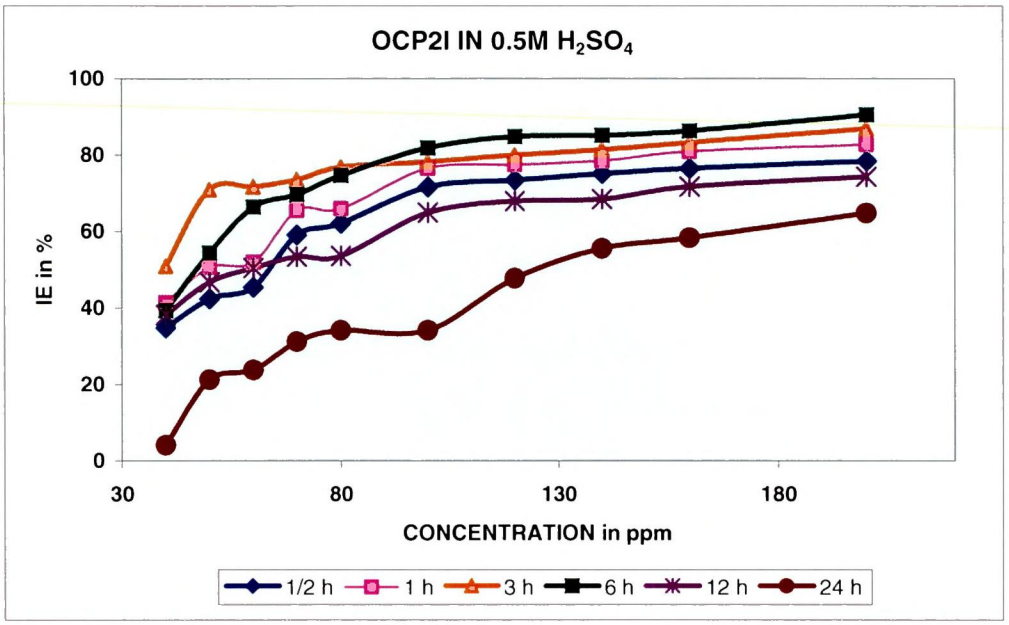

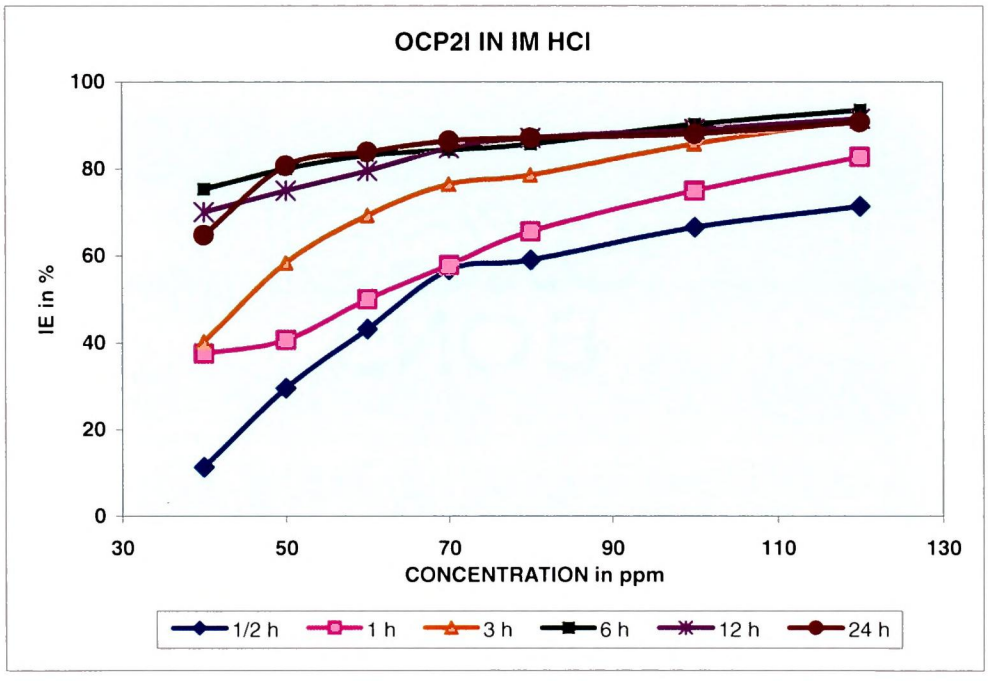

Figure – 18 Effect of concentration and exposure time on the inhibition efficiency of OCP2I for mild steel corrosion in 0.5M H_2SO_4 and 1M HCl.

Table - 6 Effect of concentration of PNDMP2I on mild steel corrosion at various time intervals in 0.5M H_2SO_4 and 1M HCl

ACID MEDIA	Conc in ppm	1/2 h		1 h		3 h		6 h		12 h		24 h	
		CR mpy	IE %	CR mpy	IE %	CR mpy	IE %	CR mpy	IE %	CR mpy	IE %	CR mpy	IE %
H_2SO_4	Blank	1290		1347		1508		5309		2331		1790	
	40	1047	18.8	1048	22.2	1167	22.6	3314	37.6	1628	30.1	1420	20.6
	50	882	31.6	903	33.0	1010	33.0	3114	41.3	1512	35.1	1216	32.1
	60	860	33.3	833	38.1	918	39.1	2300	56.7	1336	42.7	1075	39.9
	70	815	36.8	772	42.6	790	47.6	2105	60.4	1203	48.4	985	45.0
	80	716	44.4	693	48.5	755	49.9	1982	62.7	1101	52.7	894	50.0
	100	637	50.6	655	51.3	705	53.2	1704	67.9	983	57.8	844	52.8
	120	617	52.1	628	53.3	616	59.1	1508	71.6	932	60.0	802	55.2
	140	601	53.4	575	57.3	584	61.3	1180	77.8	804	65.5	774	56.7
	160	577	55.3	566	57.9	566	62.5	973	81.7	708	69.6	712	60.2
	200	564	56.3	547	59.3	517	65.7	666	85.5	633	72.8	552	69.1
HCl	Blank	1140		1235		1546		1840		1256		1138	
	40	1083	5.0	1017	17.6	1044	32.4	905	50.8	676	46.1	680	40.2
	50	1018	10.6	995	19.4	986	36.2	786	57.2	662	47.3	623	45.2
	60	974	14.6	940	23.8	822	46.8	828	55.0	607	51.6	570	49.9
	70	919	19.4	821	33.5	739	52.2	739	59.8	516	58.9	503	55.8
	80	867	23.9	809	34.5	603	61.0	602	67.3	476	62.1	464	59.2
	100	830	27.2	796	35.5	444	71.3	583	68.3	438	65.1	439	61.4
	120	819	28.1	723	41.4	355	77.0	539	70.7	434	65.4	402	64.6
	140	763	33.1	658	46.7	298	80.7	402	78.1	312	75.1	337	70.4
	160	678	40.5	585	52.6	235	84.8	240	86.9	249	80.1	319	72.0
	200	574	49.6	487	60.5	199	87.1	181	90.1	192	84.7	270	76.2

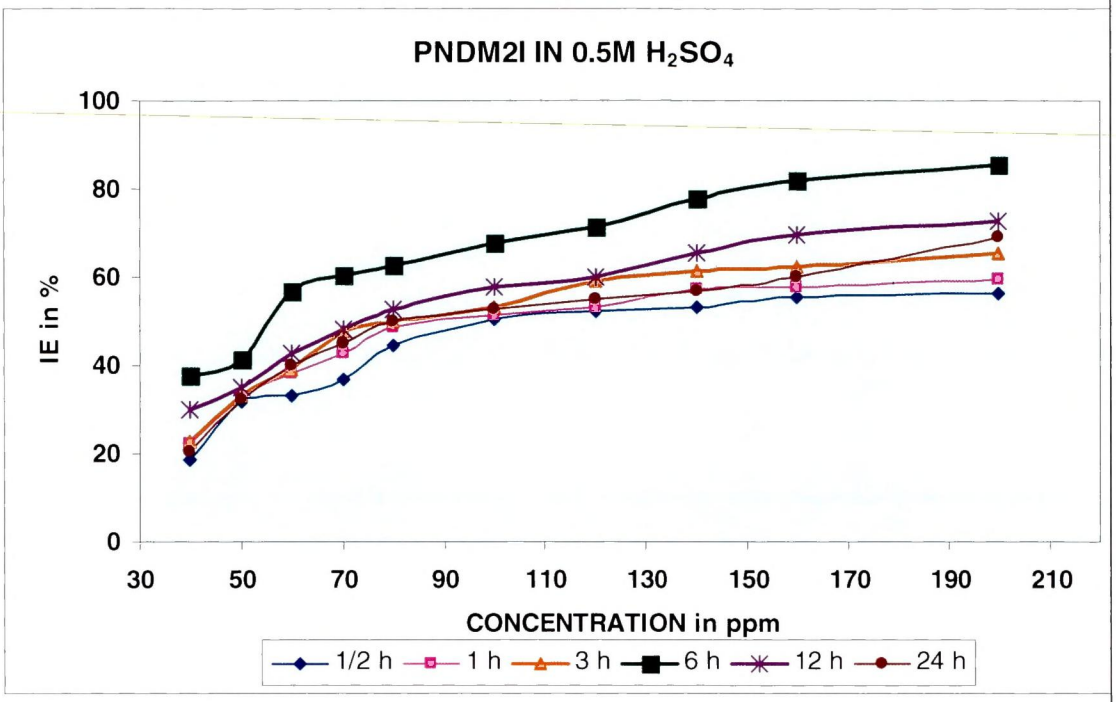

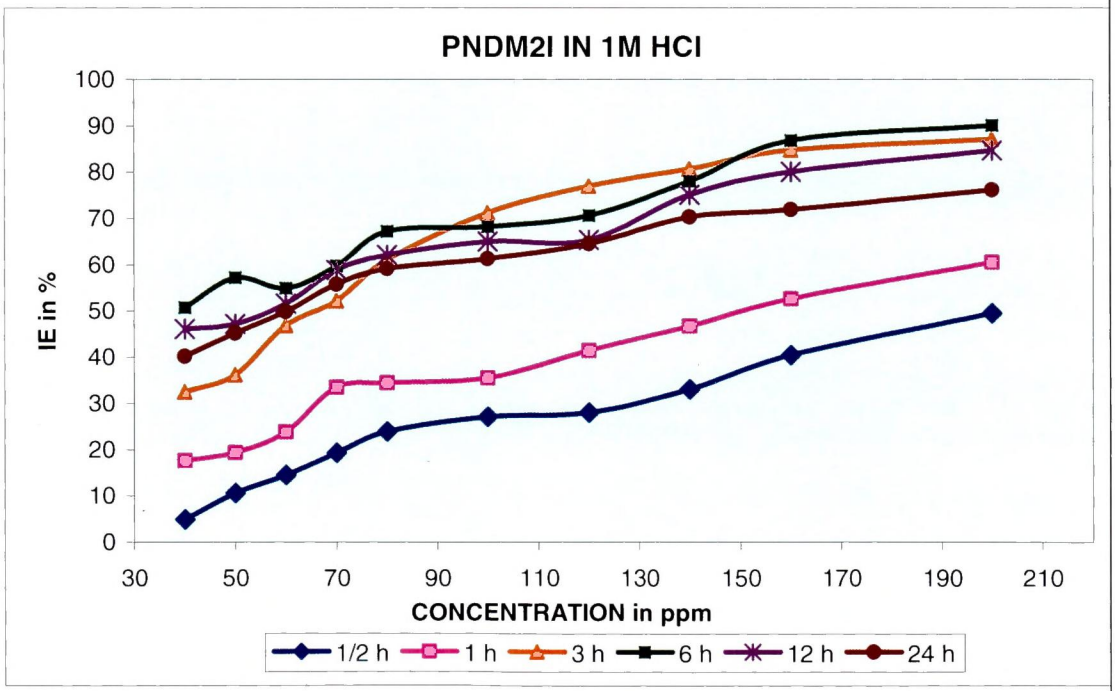

Figure - 19 Effect of concentration and exposure time on the inhibition efficiency of PNDM21 for mild steel corrosion in 0.5M H_2SO_4 and 1MHCl

Table – 7 Effect of concentration of PNP2I on mild steel corrosion at various time intervals in 0.5M H_2SO_4 and 1M HCl

ACID MEDIA	Conc in ppm	1/2 h		1 h		3 h		6 h		12 h		24 h	
		CR mpy	IE %	CR mpy	IE %	CR mpy	IE %	CR mpy	IE %	CR mpy	IE %	CR mpy	IE %
H_2SO_4	Blank	1290		1347		1508		5309		2331		1790	
	60	713	34.7	679	38.6	621	41.8	1986	49.6	910	40.9	1023	42.8
	80	698	38.9	660	41.9	550	43.5	1665	52.6	886	49.0	1003	43.9
	100	674	43.7	617	46.2	470	48.8	1311	55.3	858	52.2	946	47.2
	120	668	47.2	603	50.2	394	53.9	1152	60.3	815	56.0	863	51.7
	140	643	50.1	557	52.6	358	58.2	1024	63.7	798	59.7	797	55.5
	160	601	53.4	496	57.2	224	61.1	928	67.5	773	65.8	750	58.1
	180	543	57.9	417	62.0	209	64.1	528	70.1	732	68.6	688	61.6
	200	487	62.2	390	66.9	185	67.7	458	75.4	701	69.9	646	63.9
	240	442	65.7	361	69.2	155	70.7	391	79.6	627	73.1	557	68.8
	280	434	66.3	334	72.2	132	76.2	283	81.7	502	78.5	491	72.5
HCl	Blank	1140		1235		1546		1840		1256		1138	
	60	790	30.6	676	45.2	479	57.2	786	69.0	613	51.2	580	49.0
	80	756	33.6	649	47.4	459	62.0	699	70.3	544	56.7	538	52.7
	100	746	34.5	640	48.1	420	63.9	664	72.8	528	57.9	534	53.0
	120	714	37.4	618	49.9	413	65.1	642	73.2	484	61.4	502	55.9
	140	676	40.7	573	53.6	371	73.3	492	76.0	457	63.6	488	57.1
	160	645	43.4	530	57.0	340	74.3	472	78.0	395	68.5	429	62.2
	180	619	45.7	469	62.0	328	76.4	435	78.7	339	73.0	388	65.8
	200	602	47.2	445	63.9	322	77.8	408	79.1	335	73.3	379	66.7
	240	536	52.9	430	65.1	305	80.3	363	81.2	319	74.6	342	69.9
	280	459	59.7	384	68.9	279	81.9	356	83.6	313	75.1	328	71.1

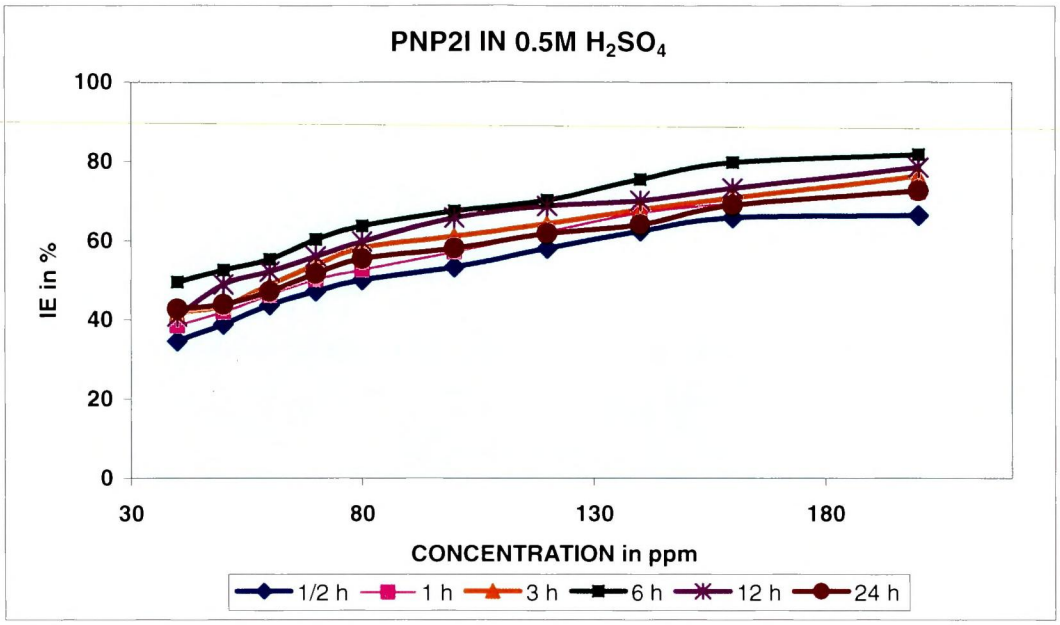

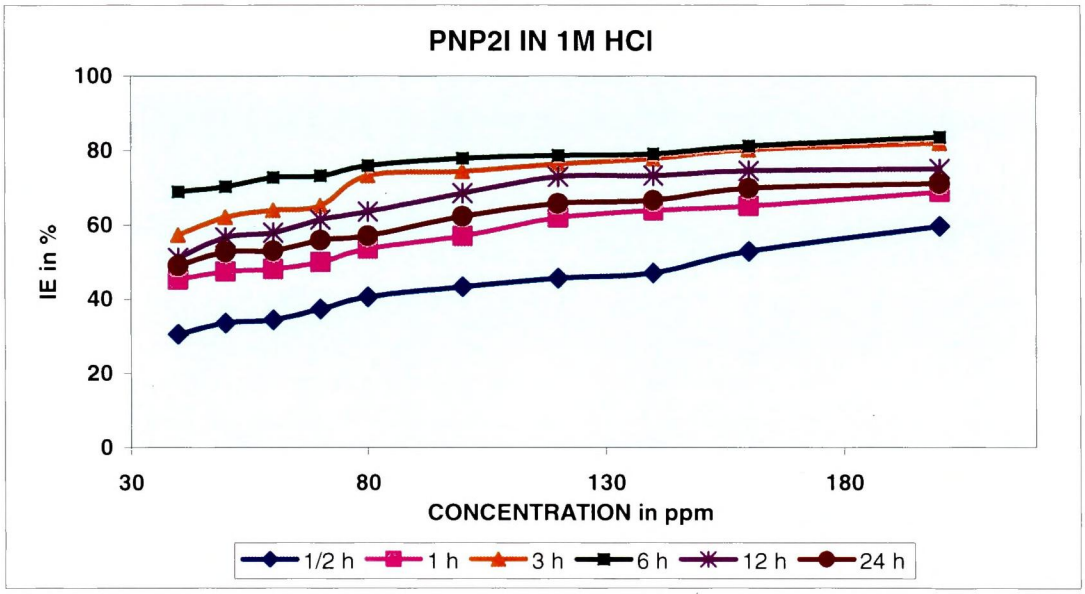

Figure - 20 Effect of concentration and exposure time on the inhibition efficiency of PNP2I for mild steel corrosion in 0.5M H_2SO_4 and 1M HCl.

It has been found that inhibition efficiency of the imidazoline derivatives increase with increase in concentration. Maximum efficiency was observed at 200 ppm (except for OCP2I in HCl medium, where the maximum efficiency was observed at 120 ppm) and further increase in the concentration did not cause any significant change in the performance of the inhibitors. The efficiency of the imidazoline derivatives may be due to the lone pair of electrons on the nitrogen atom and π-electrons of the aromatic ring, resulting in the adsorption of the compounds on the metal surface. **(Quaraishi *et al.*,2008).**

Better performance of TMP2I (98%) and DMP2I (93%) with reference to P2I (88%) may be attributed to the presence of electron releasing -OCH_3 group, which facilitates its greater adsorption on the metal surface, leading to more efficiency than other inhibitors in both acidic media. **(Quaraishi *et al.*,1996).**

The higher efficiency of chloro derivative, OCP2I with 91% is due to the fact that its dipole moment is greater than that of the parent compound P2I which furnished 88% inhibition efficiency.

Enhanced IE at 120 ppm for OCP2I in HCl medium is due to the synergistic effect of Chloride ions and also due to the chloro substituted product as inhibitor. This Chloro substituted product forms a protective layer on mild steel surface. **(Quaraishi *et al.*,1996)**

Although PNDMP2I has more reactive centres, the presence of lone pair of electrons on the nitrogen atom and the aromatic ring as compared to other imidazoline derivatives, its IE (85 % in H_2SO_4 and 90% in HCl) is less for the given concentration due to the steric hinderance of the two methyl groups present in the molecule.(**Suroor Athar *et al.*, 2001)**

The electron withdrawing nature of nitro group on the aromatic ring is responsible for the observed reduction on the IE of PNP2I (82%) in both acidic media compared to the parent derivative.

Comparison of the inhibition efficiency of the investigated inhibitors by weight loss method at maximum concentration and maximum inhibition efficiency in both acidic media is shown in Figure – 21.

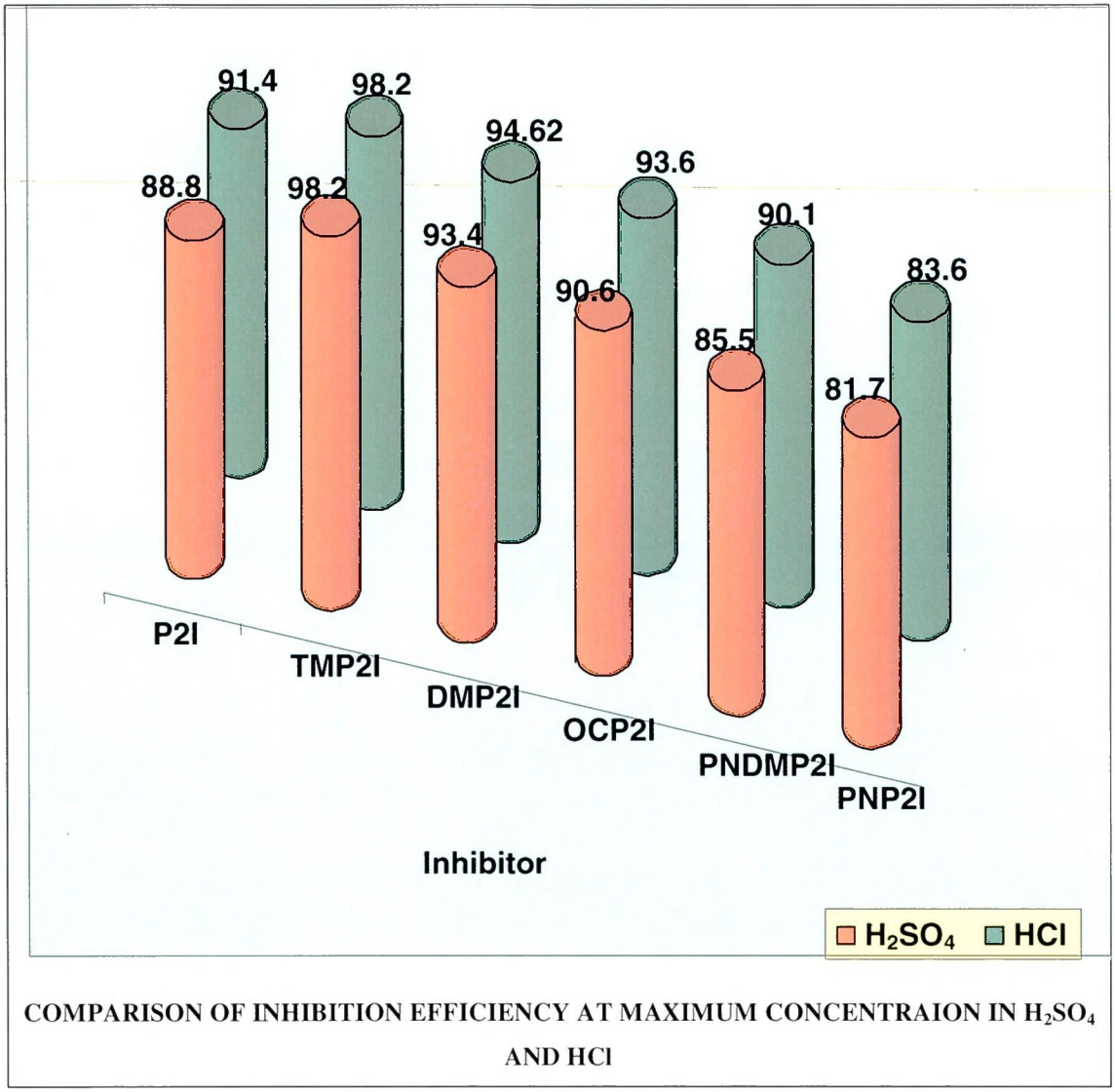

Figure - 21 Comparision of Inhibition Efficiency at Maximum Concentration in both acidic media

Reason for low Inhibition efficiency at low concentration:

Analysis of the tables, reveal, that inhibition efficiency was found to be low at low concentrations, for all the systems studied. This behaviour can be explained as follows: The inhibition efficiencies of the inhibitor in both acidic medium increase with increase in concentration of the investigated inhibitors. This also shows that adsorption of inhibitor increases with increase in inhibitor concentration. The adsorbed intermediate formed at the metal surface by interaction with inhibitor is probably a complex. At lower concentration of inhibitor the adsorption intermediate formed may be a soluble complex, leading to low values of inhibition efficiency. At higher concentrations the complex formed is insoluble and the higher values of

inhibition efficiency due to complex arise from the blocking of most of the active sites on the metal surface due to increased coverage. **(Ebenso *et al.*, 2003)**

4.2.2 Effect of Immersion Time

The effect of the exposure time on the corrosion rate ,weight loss studies were carried out at various intervals of time and the results are presented in Figures (22 - 27).

Maximum IE of 88.8% and 91.4% was observed for P2I for 6h of immersion time and after 6h the inhibition efficiency reduces to 81.2% and 82.3% for 24 h of immersion time in sulphuric acid and in hydrochloric acid respectively.

There was an increase in IE with increase in time of immersion, upto 3h (98.2%) then stabilized at 6h (92.9%), further reduced at 12h and 24h, resulting 85.8% and 81.8% respectively. TMP2I showed a maximum efficiency of 98.2 % and 98.2% in H_2SO_4 and HCl respectively.

Maximum IE was 93.4% in H_2SO_4 and 94.6% in HCl for 6h of immersion time in the presence of DMP2I. Thereafter the corrosion rate increases with increase in immersion time and the IE decreases to 85.6 % in H_2SO_4 and 57.8% in HCl for 24 h.

In the presence of OCP2I initially inhibition efficiency increases from 1/2h to 6h affording a maximum IE of 90.6% and 84.4% in 1M HCl and 0.5M H_2SO_4 and then there is a decline in inhibition at 6 hours.

For PNDMP2I, the inhibition efficiency reaches a maximum of 85.5% in sulphuric acid and 90.1% in hydrochloric acid medium for 6h of immersion time. After 6 hours the IE decreases in both the media. The IE reduces to 69.1% and 76.2% for 24 h.

For PNP2I, IE reaches a maximum of 81.7 % in H_2SO_4 and 83.6 % for 6h in HCl and reduces to 72.5% and 71.1% for 24h.

Immersion studies reveal that as the time of immersion increased from 1/2 h to 3 h the inhibition efficiency also increased. After 3 hours there is a slight decline in the inhibition efficiency at 12 h and 24 h. The decrease in inhibition efficiency at longer immersion time may be due to the desorption of the protective layer formed in the presence of the imidazoline derivatives on the mild steel surface. All the investigated inhibitors could furnish an efficiency of 90-98% at 3 h of immersion.

This behaviour can be discussed on the following basis. Prolonged immersion of steel in acidic solution allows the cathodic or hydrogen evolution kinetics to increase presumably as more cathodic or carbon containing sites are exposed by the corrosion process and increase the concentration of ferrous ion which is known for its stimulation of corrosion attack of the acid on the base metal. (Zakvi et al., 1988)

Figure- 22 Impact of Time of Immersion on Mild Steel Corrosion in 0.5M H_2SO_4 and in in 1M HCl at Various Concentrations of P2I

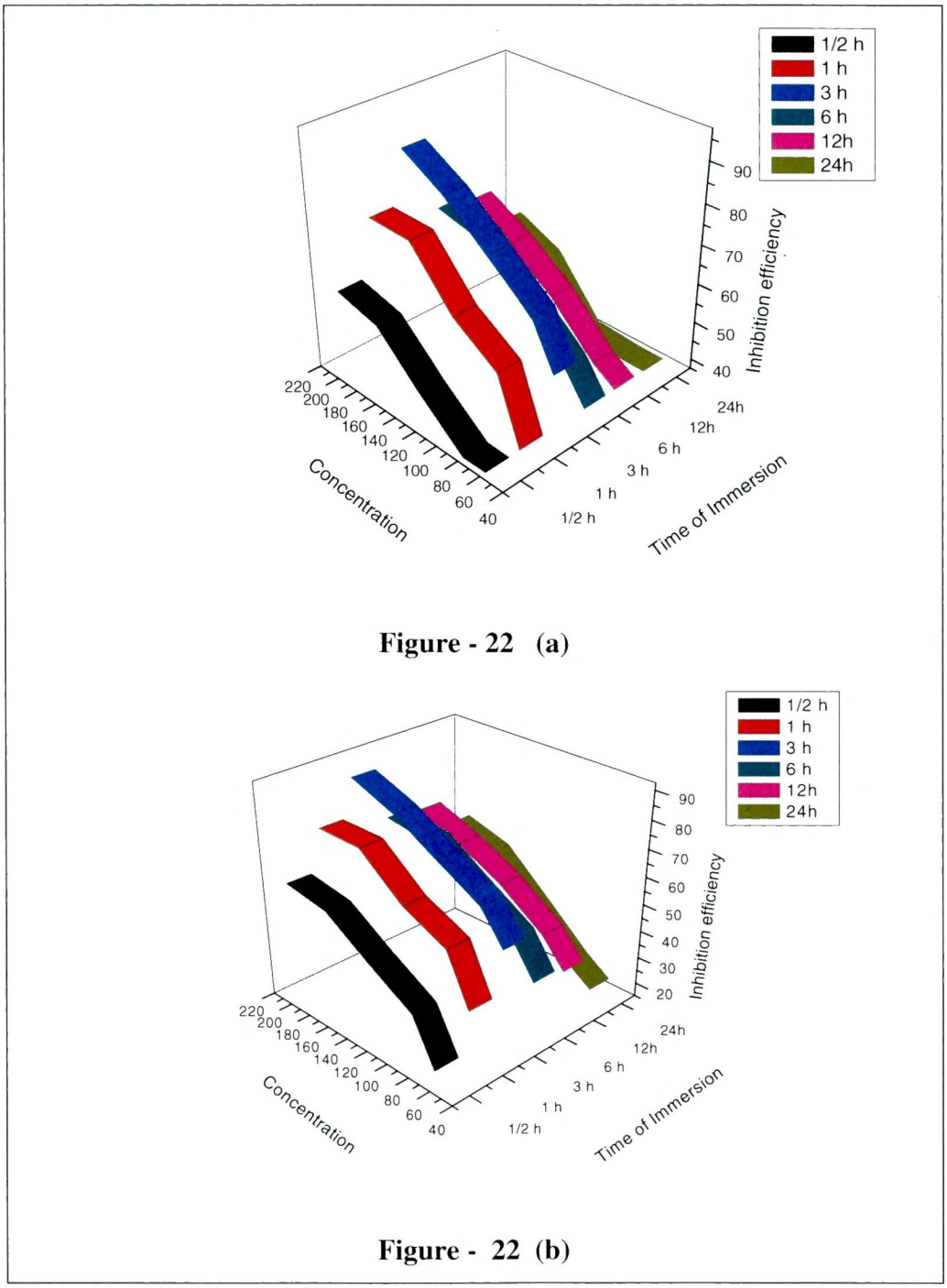

Figure - 22 (a)

Figure - 22 (b)

Figure - 23 Impact of Time of Immersion on Mild Steel Corrosion in 0.5M H_2SO_4 and in in 1M HCl at Various Concentrations of TMP2I

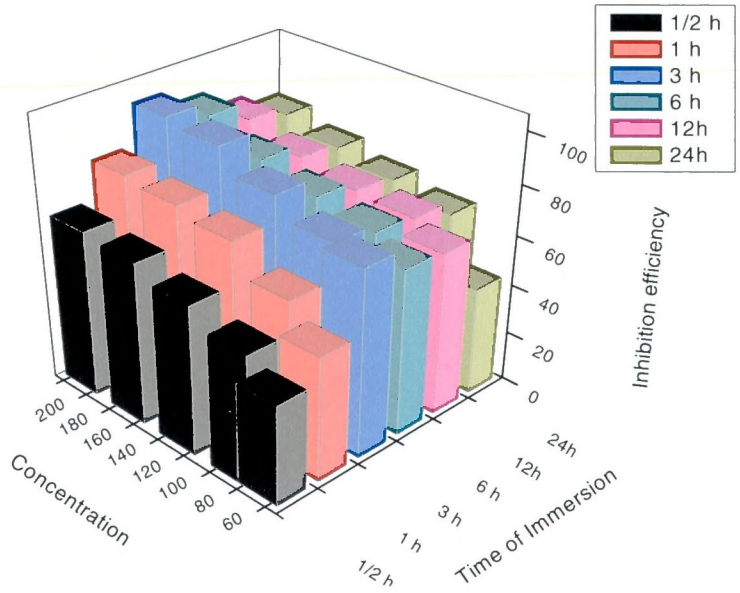

Figure - 23 (a)

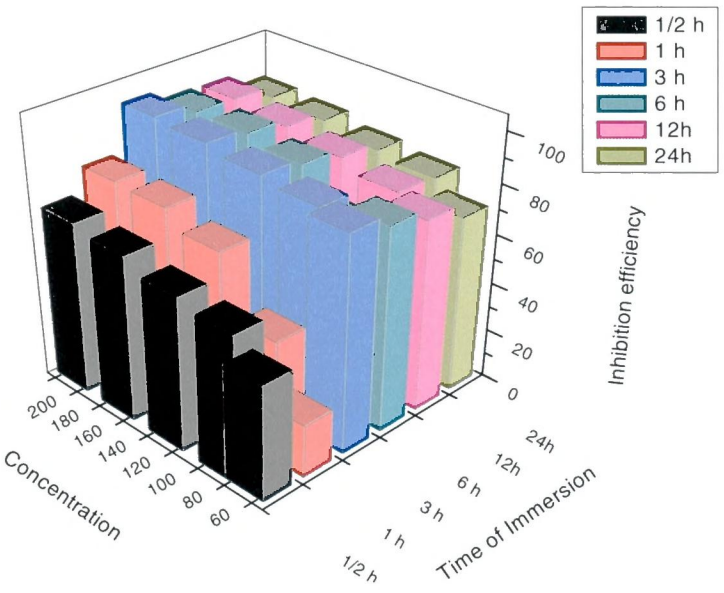

Figure - 23 (b)

Figure - 24 Impact of Time of Immersion on Mild Steel Corrosion in 0.5M H_2SO_4 and in in 1M HCl at Various Concentrations of DMP2I

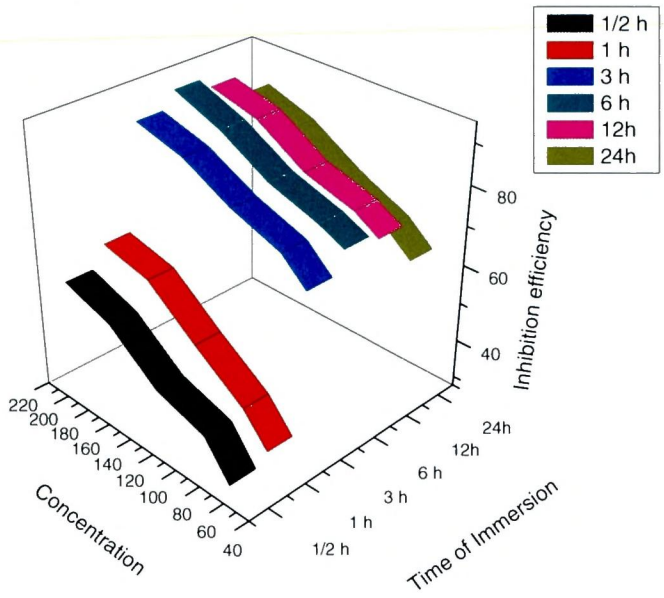

Figure - 24 (a)

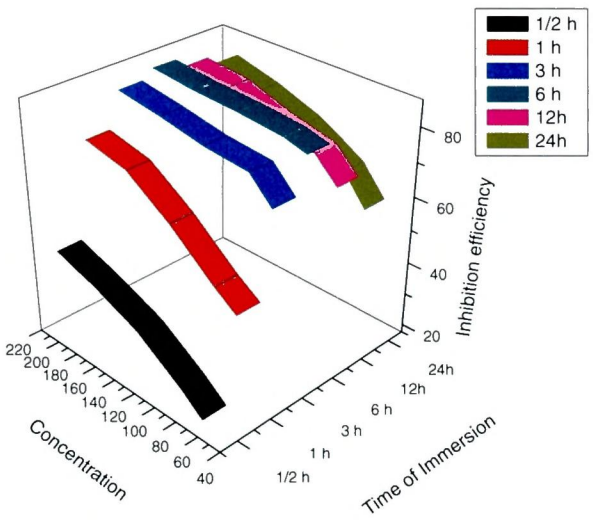

Figure – 24 (b)

Figure – 25 Impact of Time of Immersion on Mild Steel Corrosion in 0.5M H_2SO_4 and in in 1M HCl at Various Concentrations of OCP2I

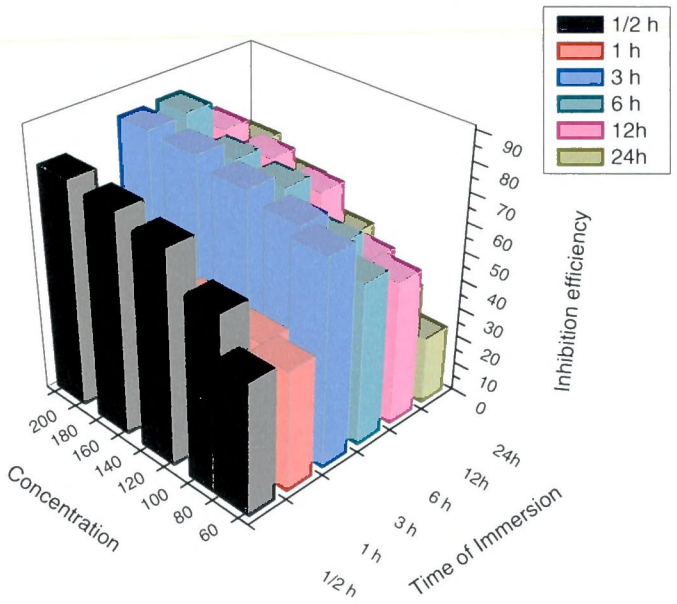

Figure - 25 (a)

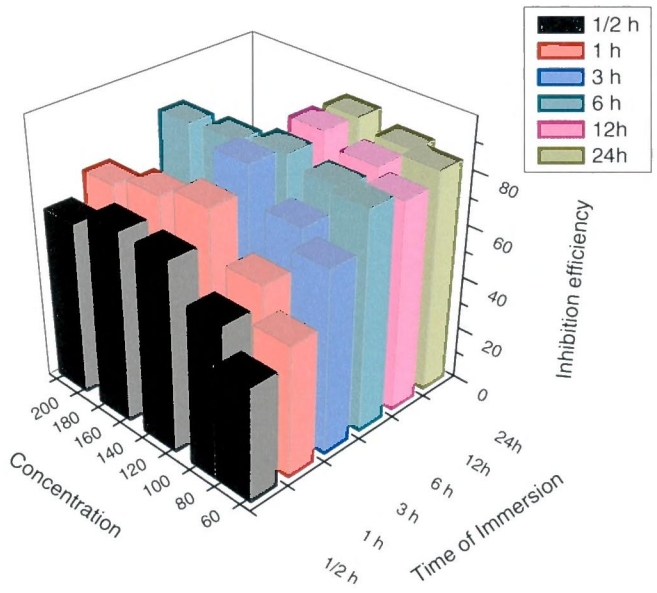

Figure - 25 (b)

Figure -26 Impact of Time of Immersion on Mild Steel Corrosion in 0.5M H_2SO_4 and in in 1M HCl at Various Concentrations of PNDMP2I

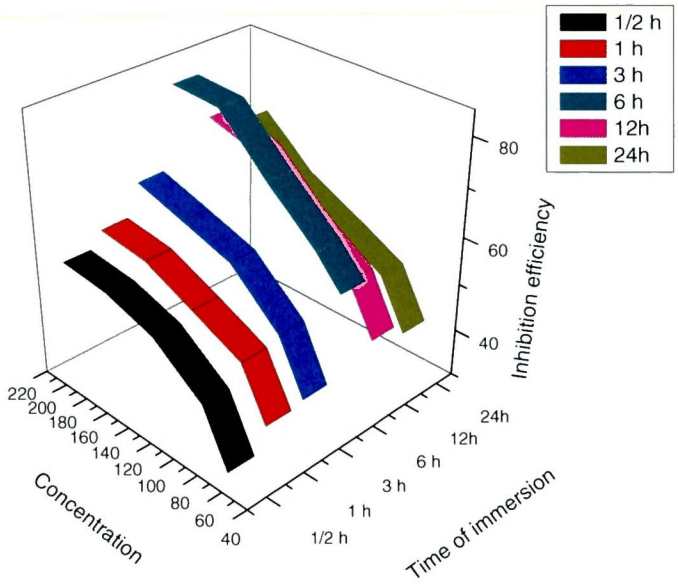

Figure -26 (a)

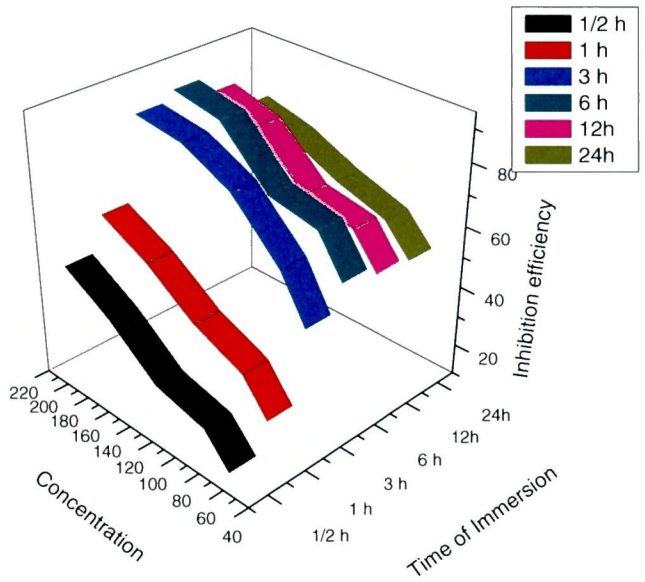

Figure - 26 (b)

Figure – 27 Impact of Time of Immersion on Mild Steel Corrosion in 0.5M H_2SO_4 and in in 1M HCl at Various Concentrations of PNP2I

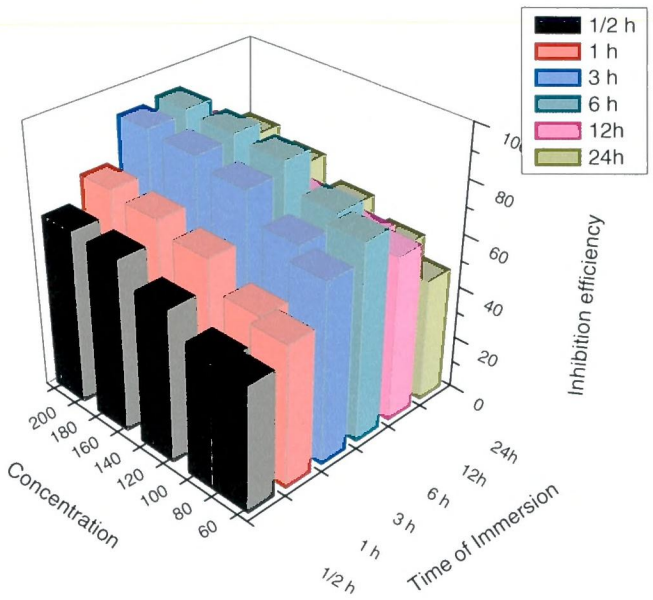

Figure- 27 (a)

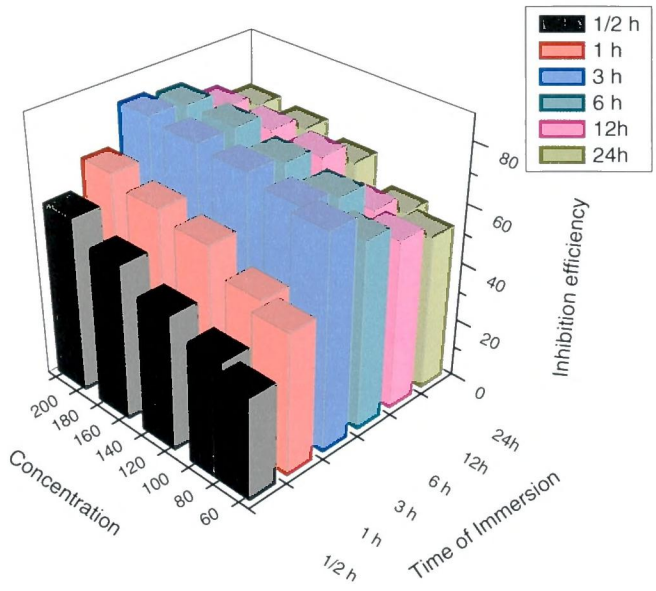

Figure – 27 (b)

Considering that adsorption is essentially controlled by electrostatic attraction, as the immersion time increases, more inhibitor molecules will be adsorbed on the surface helping to the formation of the inhibitor layer. However, as soon as all the active sites become saturated with the inhibition the development of the inhibitor layer is gradually slows down. Figures (22-27) depicts the inhibition efficiency at the specified time of immersion and concentration of the inhibitors.

The corrosion rate decreased with increasing the immersion time, then began to increase. The reasons may be the adsorptive film of imidazoline derivatives which is independent on the immersion time. At first, the adsorptive film becomes compact and uniform with the increase of immersion time. However, when the immersion time is longer, the adsorptive film is not more uniform because of the corrosion of acid media. Increasing time resulted in increasing IE from 1/2hr to 6hrs and then IE began to decrease with immersion time. The decrease in IE at long immersion time may be due to the deterioration of the protective layer formed in the presence of the imidazoline derivatives on the steel surface. **(Xianghong *et al.*, 2005)**

4.2.3 Effect of Temperature

The effect of temperature on a chemical reaction is of practical and theoretical important. Like most chemical reactions, the rate of corrosion of iron and steel increases with temperature especially in media in which evolution of hydrogen, e.g. during corrosion of steel in acids. Acid pickiling of steel is usually carried out at elevated temperature – up to 60° C in hydrochloric acid solutions and up to 90° C in sulphuric acid solutions. Accordingly, pickling inhibitors are expected to be chemically stable to provide high protective efficiency under the conditions mentioned above. Temperature effects on acidic corrosion and corrosion inhibition of iron and steel most often in HCl and H_2SO_4 solutions had been the object of a large number of investigations. Temperature dependence of the inhibitor efficiency (IE) and the comparison of the obtained thermodynamic data of the corrosion product both in absence and presence of inhibitors lead to some conclusions concerning the mechanism of inhibiting action.

To study the effect of temperature on inhibition efficiency , weight loss measurements were taken at various temperatures ranging from 303 K to 343 K in the absence and presence of the investigated imidazoline

derivatives after 1/2 h of immersion. The corresponding efficiency and corrosion rate are summarized in Tables (8-13) and the effect of Temperature Vs Inhibition efficiency are given in Figures(28-33).

4.2.3.1 Influence of temperature on the corrosion rate of mild steel and inhibition efficiency in the presence of imidazoline derivatives in studied acidic media :

P2I:

The effect of temperature on the weight loss and the corrosion rate of mild steel in 0.5 M H_2SO_4 and in 1 M HCl without inhibitor (blank) and with various concentration of P2I was examined at 303,313,323,333 and 343 K and the results are presented in table - 8 and in figure - 28.

A remarkable decrease in mild steel corrosion rate was observed with the addition of increasing amount of P2I at each studied temperature. As the temperature rises from 303 K to 313 K, IE was found to increase from 62.5% to 73.1% in H_2SO_4 at maximum concentration of 200 ppm. Further rise in temperature resulted in decrease in IE. Analysing the temperature effect of P2I in H_2SO_4, the IE increases with increase in temperature upto 313 K (88%) and slightly decreased at 323 K (80.4%) and stabilized at 343 K, furnishing 38.4% inhibition efficiency.

As the temperature rises from 303 K to 323 K, IE was found to increase from 79.8% to 88.0% in HCl at maximum concentration of 200 ppm. Further rise in temperature resulted in decrease in IE. Analysing the temperature effect of P2I in HCl the IE increases with increase in temperature upto 323 K (88.0%) and slightly decreased at 333 K (80.4%) and stabilized at 343 K, furnishing 74.7% inhibition efficiency.

TABLE - 8 Variation of Inhibition efficiency of P2I on mild steel corrosion as a function of temperature in 0.5M H_2SO_4 and in 1M HCl

ACID MEDIA	Conc. in ppm	303K		313K		323K		333K		343K	
		CR	IE	CR	IE	CR	IE	CR	IE	CR	IE
		mpy	%	mpy	%	mpy	%	mpy	%	mpy	%
H_2SO_4	Blank	941	---	2782	---	8015	---	10588	---	17060	---
	40	742	21.1	1794	35.5	6024	24.8	9391	11.3	15517	9.0
	50	665	29.3	1626	41.6	5739	28.4	9252	12.6	15287	10.4
	60	625	33.5	1439	48.2	5554	30.7	9116	13.9	15046	11.8
	70	574	39.0	1342	51.8	4997	37.7	8978	15.2	14929	12.5
	80	552	41.3	1271	54.3	4372	45.4	7664	27.6	14238	16.5
	100	503	46.5	1073	61.4	3828	52.2	7248	31.5	13197	22.6
	120	457	51.4	1014	63.5	3662	54.3	7020	33.7	12474	26.9
	140	415	55.9	893	67.9	3185	60.3	6601	37.7	11454	32.9
	160	378	59.8	830	70.1	2962	63.0	6094	42.4	10793	36.7
	200	352	62.5	748	73.1	2449	69.4	5885	44.4	10510	38.4
HCl	Blank	776		1334		1133		6585		15995	
	40	805	43.7	816	50.8	1827	51.8	4671	36.9	8271	26.9
	50	781	45.4	747	54.9	1473	61.2	4032	45.5	7817	31.0
	60	733	48.7	666	59.8	1340	64.7	3726	49.7	7536	33.4
	70	575	59.7	594	64.1	1318	65.2	3601	51.4	7380	34.8
	80	552	61.3	542	67.3	1156	69.5	3545	52.1	6390	43.6
	100	504	64.7	454	72.6	1016	73.2	3295	55.5	6184	45.4
	120	444	68.9	411	75.2	861	77.3	2753	62.8	5235	53.8
	140	420	70.6	367	77.8	676	82.2	2315	68.7	3879	65.7
	160	396	72.3	276	83.3	559	85.2	2023	72.7	3323	70.6
	200	288	79.8	243	85.3	456	88.0	1453	80.4	2861	74.7

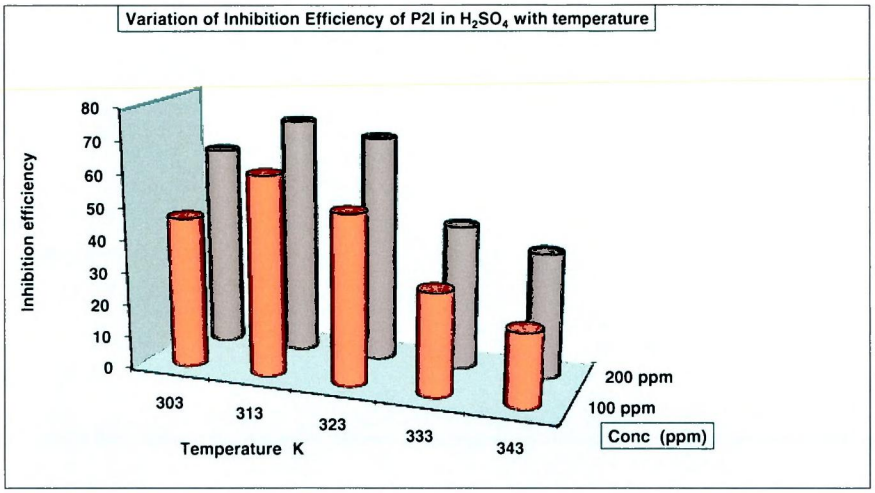

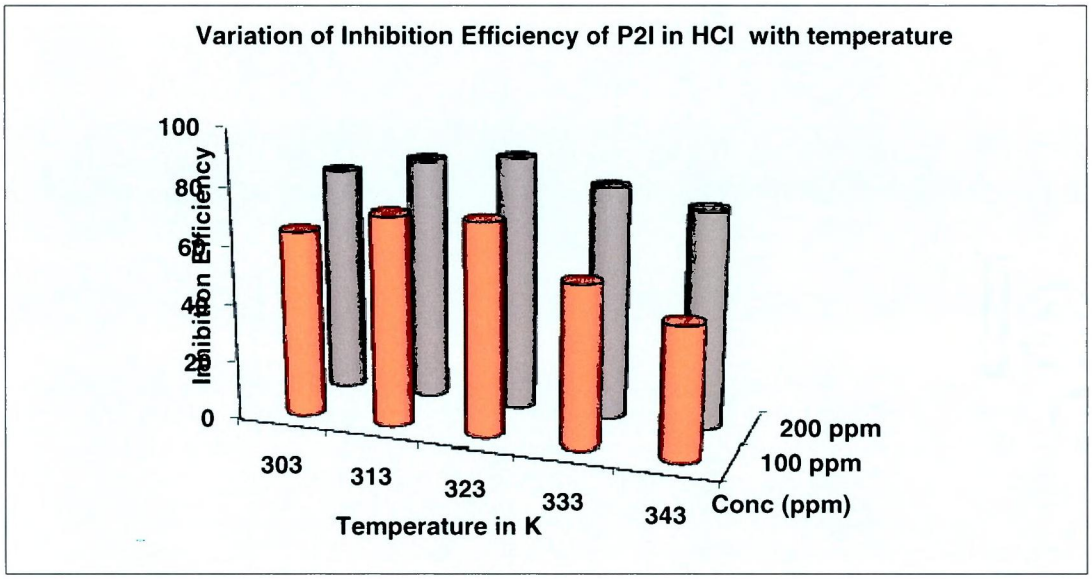

Figure – 28 Variation of inhibition efficiency of P2I with temperature

TMP2I:

Figure- 29 and Table - 9 present the variation of the inhibitor efficiency of TMP2I with temperature in both acidic media .

TABLE - 9 Variation of Inhibition efficiency of TMP2I on mild steel corrosion as a function of temperature in 0.5M H_2SO_4 and in 1M HCl

ACID MEDIA	Conc. in ppm	303K		313K		323K		333K		343K	
		CR	I.E	CR	I.E	CR	I.E	CR	I.E	CR	I.E
		mpy	%	mpy	%	mpy	%	mpy	%	mpy	%
H_2SO_4	Blank	941	---	2782	---	8015	---	10588	---	17060	---
	40	730	22.4	1588	42.9	3476	56.6	7413	30.0	14074	17.5
	50	624	33.6	1172	57.9	3017	62.4	6655	37.1	13762	19.3
	60	592	37.1	1120	59.7	2459	69.3	6515	38.5	12322	27.8
	70	551	41.4	1098	60.5	2145	73.2	4256	59.8	11952	29.9
	80	472	49.8	1001	64.0	2083	74.0	3507	66.9	11500	32.6
	100	411	56.3	813	70.8	1762	78.0	3201	69.8	10688	37.4
	120	399	57.5	775	72.1	1504	81.2	3131	70.4	7697	54.9
	140	289	69.3	701	74.8	1238	84.6	3073	71.0	5430	68.2
	160	267	71.5	667	76.0	1075	86.6	2263	78.6	4563	73.3
	200	251	73.3	575	79.3	659	91.8	1983	81.3	4160	75.6
HCl	Blank	776		1334		1133		6585		15995	
	40	1273	10.9	1220	26.3	3075	19.0	4227	42.9	7776	31.3
	50	1139	20.3	1131	31.7	2702	28.8	3265	55.9	7420	34.5
	60	1117	21.9	1099	33.7	2455	35.3	2796	62.2	7323	35.3
	70	960	32.8	562	66.1	2059	45.7	2527	65.9	7151	36.8
	80	869	39.2	520	68.6	1884	50.3	1945	73.7	6623	41.5
	100	759	46.9	496	70.0	804	78.8	717	90.3	6575	41.9
	120	644	54.9	454	72.6	624	83.5	504	93.2	3382	70.1
	140	588	58.8	430	74.0	540	85.8	457	93.8	3269	71.1
	160	574	59.8	354	78.6	396	89.6	393	94.7	2448	78.4
	200	532	62.7	342	79.3	312	91.8	339	95.4	1968	82.6

It is evident from the table, that the corrosion rate decreases with increase in inhibitor concentration at each studied temperature. TMP2I performed as an excellent inhibitor by giving a maximum of 91.8 % at 323 K in H_2SO_4 and 95.4 % at 333 K in HCl. This may be due to the adsorption of TMP2I on mild steel surface through non bonding electron pair on the nitrogen atom and the Π-electrons of the phenyl ring. After 323 K (H_2SO_4) and 333 K(HCl), the IE was found to decrease but stabilized to 75.6 % (H_2SO_4) and 82.6 % (HCl), respectively at 200 ppm.

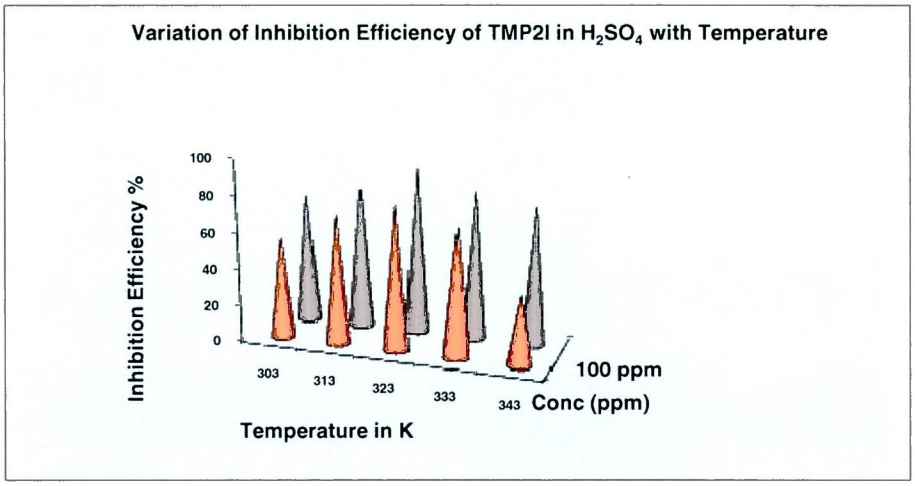

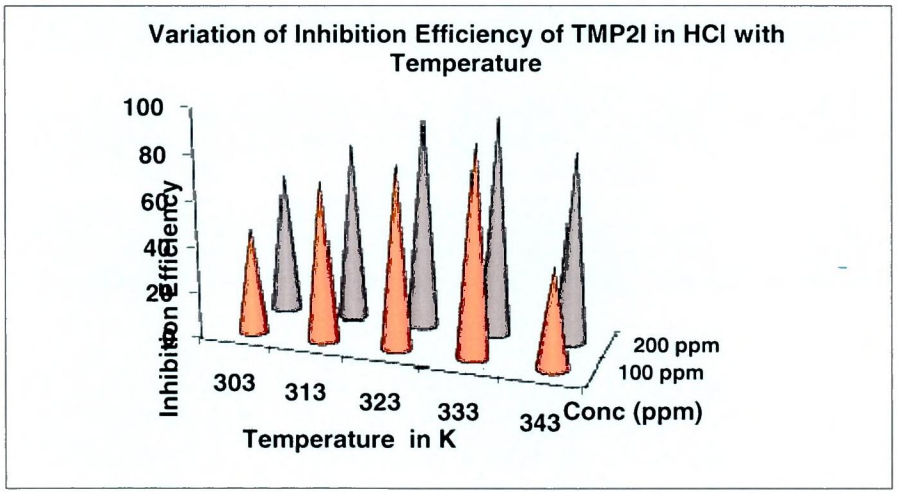

Figure – 29 Variation of inhibition efficiency of TMP2I with temperature

DMP2I:

The change of corrosion rate at various concentrations of the DMP2I for ½ h of immersion at different temperatures was studied in 0.5 M H_2SO_4 and in 1M HCl. It is clear from table-10 and Figure - 30, that the increase of corrosion rate is more pronounced with the rise of temperature for blank solution. DMP2I excellently protect mild steel from acid corrosion by furnishing 86.5% in H_2SO_4 (333 K) and 82.5% in HCl (333 K). In the presence of DMP2I molecules, the corrosion rate of mild steel decreases at any given temperature at all inhibitor concentrations due to the increase of the degree of surface coverage. In contrast at constant inhibitor concentration, the corrosion rate increases as temperature rises. Analysis of the table indicate that as the temperature increases IE increases upto 333 K and then decreases to 37.5 % (H_2SO_4) and 71.1 % (HCl) at 343 K. This behaviour can be interpreted on the basis that an increase in temperature resulted in the desorption of adsorbed molecules from the metal surface.

TABLE - 10 Variation of Inhibition efficiency of DMP2I on mild steel corrosion as a function of temperature in 0.5M H_2SO_4 and in 1M HCl

ACID MEDIA	Conc. in ppm	303K		313K		323K		333K		343K	
		CR	I.E	CR	I.E	CR	I.E	CR	I.E	CR	I.E
		mpy	%	mpy	%	mpy	%	mpy	%	mpy	%
H2SO4	Blank	941	---	2782	---	8015	---	10588	---	17060	---
	40	851	9.5	1875	32.6	4110	48.7	4302	59.4	15575	8.7
	50	770	18.1	1664	40.2	3926	51.0	3394	67.9	15064	11.7
	60	721	23.3	1627	41.5	3845	52.0	3146	70.3	15004	12.1
	70	667	29.1	1608	42.2	3693	53.9	3072	71.0	13474	21.0
	80	658	30.0	1527	45.1	3495	56.4	2741	74.1	12902	24.4
	100	481	48.8	1388	50.1	3415	57.4	2391	77.4	12667	25.8
	120	418	55.5	1322	52.5	2713	66.1	2004	81.1	11904	30.2
	140	393	58.1	975	65.0	2156	73.1	1598	84.9	11109	34.9
	160	324	65.5	925	66.7	2111	73.7	1581	85.1	10754	37.0
	200	317	66.3	825	70.3	1563	80.5	1433	86.5	10655	37.5
HCl	Blank	776		1334		1133		6585		15995	
	40	1315	8.0	1509	8.9	3375	11.0	3598	51.4	7898	30.2
	50	1285	10.1	1486	10.3	3235	14.7	2486	66.4	7615	32.7
	60	1226	14.2	1340	19.1	2700	28.8	2455	66.8	7278	35.7
	70	1186	17.0	1315	20.6	2537	33.1	2419	67.3	6253	44.8
	80	1152	19.4	1267	23.5	2164	42.9	2398	67.6	5742	49.3
	100	1143	20.0	1195	27.8	1815	52.2	2153	70.9	5203	54.0
	120	1034	27.6	1075	35.1	1585	58.2	2055	72.2	4731	58.2
	140	957	33.0	880	46.9	1513	60.1	1719	76.8	4137	63.5
	160	790	44.7	809	51.2	1396	63.2	1505	79.7	3612	68.1
	200	742	48.1	706	57.4	1340	64.7	1299	82.5	3270	71.1

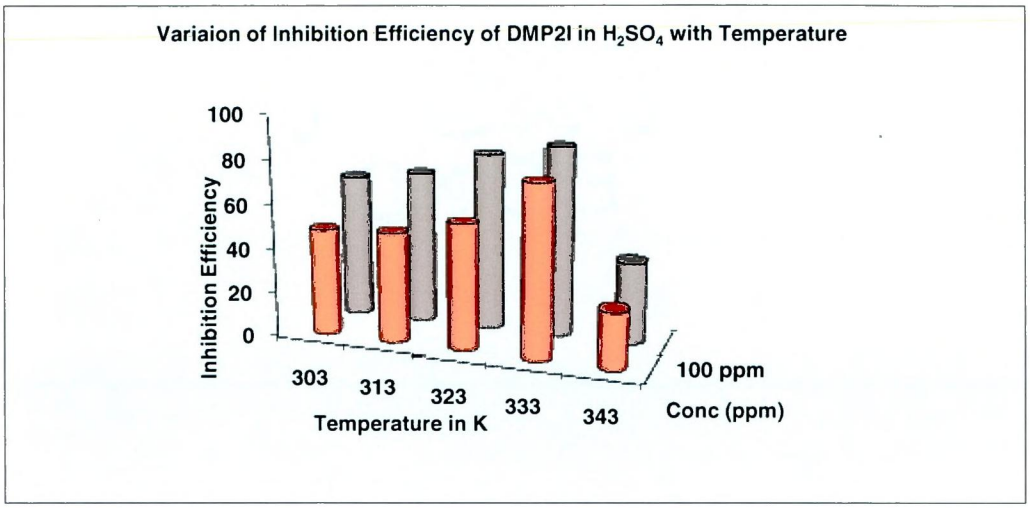

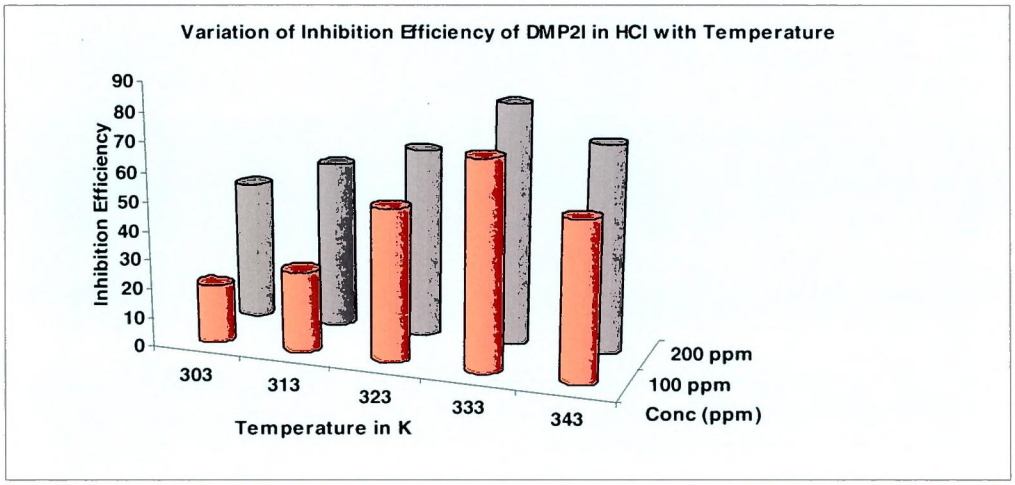

Figure –30 Variation of inhibition efficiency of DMP2I with temperature

OCP2I:

The effect of temperature on the weight loss and the corrosion rate of mild steel coupons in both the investigated acidic media without inhibitor (blank) and with various concentration of OCP2I was examined at 303,313,323,333, 343 K and the results are represented in table- 11 & figure -31

From the figure, it can be deduced that in the temperature range of 303K-343K OCP2I enhanced the IE upto 313K in H_2SO_4 medium and 333K for HCl medium. Data presented in Table -11 indicate that as the temperature increased IE increased

upto 313 K, then a slight decrease in IE at 323 K .Immediately after that the increase in temperature favors enhancement in IE at 333 K (86.2 %) and then stabilized to 84.7 % at 343 K in HCl solution. In H_2SO_4 solution as the temperature increased IE increased at 313 K (76.3 %) and stabilized at 343 K (33.3 %) .The enhanced inhibition efficiency of OCP2I in HCl solution as compared to H_2SO_4 solution may be attributed to the fact that chloride ions being less hydrated than sulphate ions are strongly adsorbed on the metal surface by creating an excess negative charge towards the solution phase, which favors synergistic adsorption on the metal surface.

TABLE - 11 Variation of Inhibition efficiency of OCP2I on mild steel corrosion as a function of temperature in 0.5M H_2SO_4 and in 1M HCl

ACID MEDIA	Conc. in ppm	303K		313K		323K		333K		343K	
		C.R	I.E	C.R	I.E	C.R	I.E	C.R	I.E	C.R	I.E
		mpy	%	mpy	%	mpy	%	mpy	%	mpy	%
H2SO4	Blank	941		2782		8015		10588		17060	
	40	826	12.2	1408	49.4	6962	13.1	7254	9.5	16090	5.7
	50	699	25.7	1383	50.3	6615	17.5	6219	22.4	15485	9.2
	60	526	44.1	1310	52.9	6311	21.3	5957	25.7	15125	11.3
	70	479	49.1	1294	53.5	5937	25.9	5314	33.7	14994	12.1
	80	470	50.0	1169	58.0	5097	36.4	4861	39.4	14098	17.4
	100	428	54.5	1091	60.8	4714	41.2	4626	42.3	13610	20.2
	120	419	55.4	1046	62.4	4028	49.7	4539	43.4	12365	27.5
	140	409	56.5	937	66.3	3286	59.0	4414	44.9	12363	27.5
	160	385	59.0	704	74.7	3073	61.7	4257	46.9	11399	33.2
	200	350	62.7	659	76.3	2693	66.4	3572	55.4	11382	33.3
HCl	Blank	776		1334		1133		6585		15995	
	40	841	41.1	1332	19.6	3239	14.6	3298	55.5	6696	40.9
	50	807	43.5	1246	24.8	2510	33.8	2618	64.6	4525	60.0
	60	726	49.2	898	45.8	2422	36.2	2099	71.7	3500	69.1
	70	657	54.0	866	47.7	2247	40.8	1844	75.1	2858	74.8
	80	576	59.7	779	52.9	2189	42.3	1726	76.7	2761	75.6
	100	565	60.5	758	54.2	2101	44.6	1637	77.9	2715	76.0
	120	495	65.3	628	62.1	1984	47.7	1431	80.7	2402	78.8
	140	438	69.4	530	68.0	1868	50.8	1314	82.3	2130	81.2
	160	426	70.2	509	69.3	1168	69.2	1255	83.0	2111	81.4
	200	334	76.6	379	77.1	1039	72.6	1020	86.2	1735	84.7

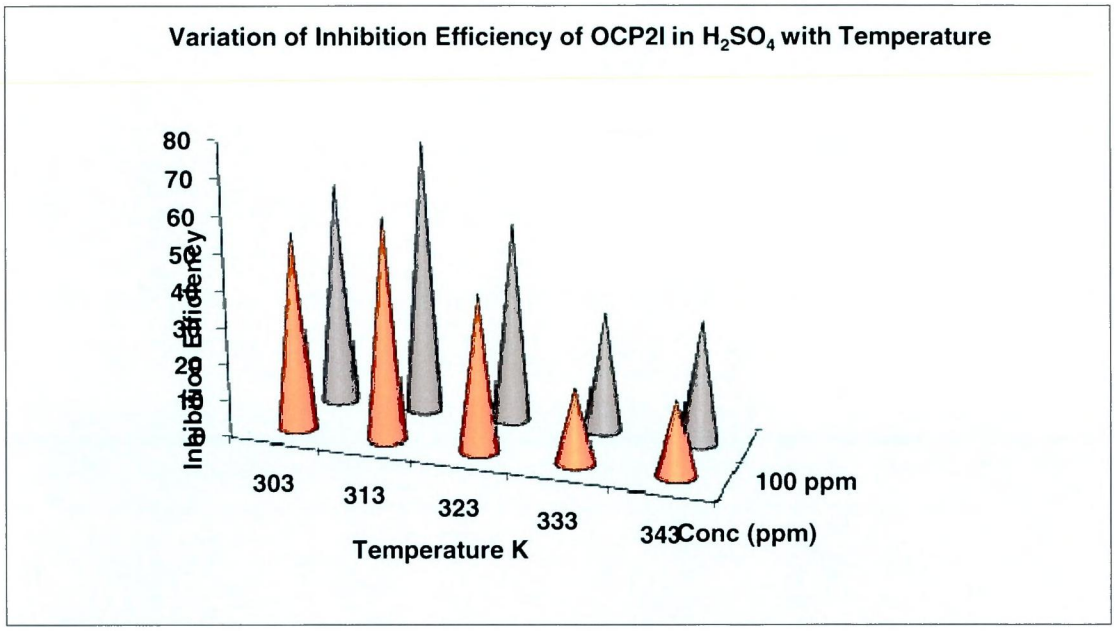

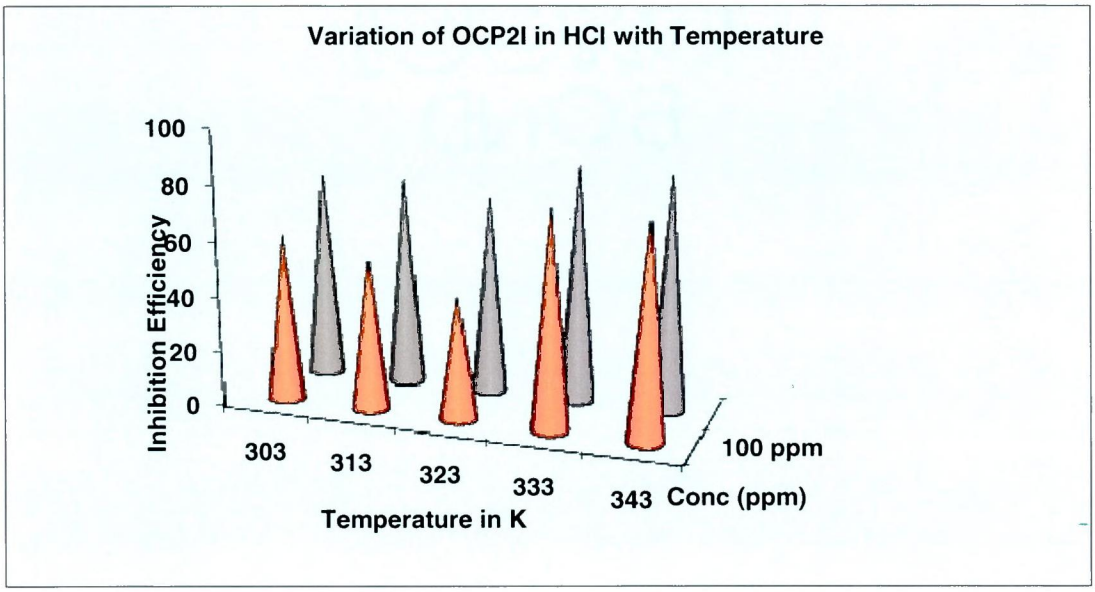

Figure – 31 Variation of inhibition efficiency of OCP2I with temperature

PNDMP2I:

The influence of temperature on inhibition efficiency was studied using weight loss measurements at 303 – 343K containing different concentrations of PNDMP2I

(Table - 12). Figure –32 shows the variation of percentage inhibition efficiency with temperature.

TABLE - 12 Variation of Inhibition efficiency of PNDMP2I on mild steel corrosion as a function of temperature in 0.5M H_2SO_4 and in 1M HCl

ACID MEDIA	Conc. in ppm	303K		313K		323K		333K		343K	
		C.R	I.E	C.R	I.E	C.R	I.E	C.R	I.E	C.R	I.E
		mpy	%	mpy	%	mpy	%	mpy	%	mpy	%
H_2SO_4	Blank	941	---	2782	---	8015	---	10588	---	17060	---
	40	811	13.8	2108	24.2	5865	26.8	7018	33.5	12194	28.5
	50	679	27.8	1869	32.8	5480	31.6	5414	48.7	11996	29.7
	60	609	35.2	1540	44.6	4818	39.9	5133	51.4	10816	36.6
	70	566	39.8	1324	52.4	4636	42.2	4549	56.9	9446	44.6
	80	505	46.3	1104	60.3	4546	43.3	4326	59.0	8748	48.7
	100	449	52.2	1020	63.3	4274	46.7	3577	66.1	7987	53.2
	120	439	53.3	936	66.3	4013	49.9	3494	66.9	7571	55.6
	140	427	54.5	835	70.0	3777	52.9	3376	68.0	7136	58.2
	160	412	56.2	741	73.3	3235	59.6	3295	68.8	6887	59.6
	200	395	57.9	671	75.9	2785	65.3	3527	66.6	6788	60.2
HCl	Blank	776		1334		1133		6585		15995	
	40	1328	7.1	1371	17.2	2776	26.8	5807	21.6	9506	16.0
	50	1302	8.9	1282	22.6	2594	31.6	5323	28.1	8788	22.4
	60	1220	14.6	1247	24.7	2280	39.9	4792	35.3	8120	28.3
	70	1154	19.3	1170	29.4	2194	42.2	4549	38.6	7971	29.6
	80	1050	26.6	1151	30.5	2151	43.3	4441	40.0	7760	31.5
	100	990	30.7	1067	35.6	2023	46.7	4067	45.1	7246	36.0
	120	962	32.7	1033	37.6	1900	49.9	3918	47.1	6938	38.7
	140	957	33.0	897	45.8	1788	52.9	3231	56.4	6810	39.8
	160	920	35.6	864	47.8	1531	59.6	3169	57.2	6606	41.6
	200	906	36.6	751	54.6	1318	65.3	2814	62.0	6382	43.6

Values of IE of PNDMP2I increase with increase in concentration at all investigated temperatures. Maximum IE was found to be 75.9 % at 313K (H_2SO_4) and 65.3 % (HCl) at 323K. Further increase in temperature stabilized furnishing inhibition efficiency of 60.2% (H_2SO_4) and 43.6 % (HCl) at 343K respectively. This PNDMP2I

effectively inhibits corrosion of Mild steel at all temperatures. PNDMP2I has a significant decrease in its protective properties with raising temperature. This trend in the inhibition properties of PNDMP2I with increase of temperature may be connected with two effects: decreasing the PNDMP2I strength of adsorption (shifting the adsorption and desorption equilibrium towards desorption) and roughening of the mild steel surface which results from enhanced corrosion.

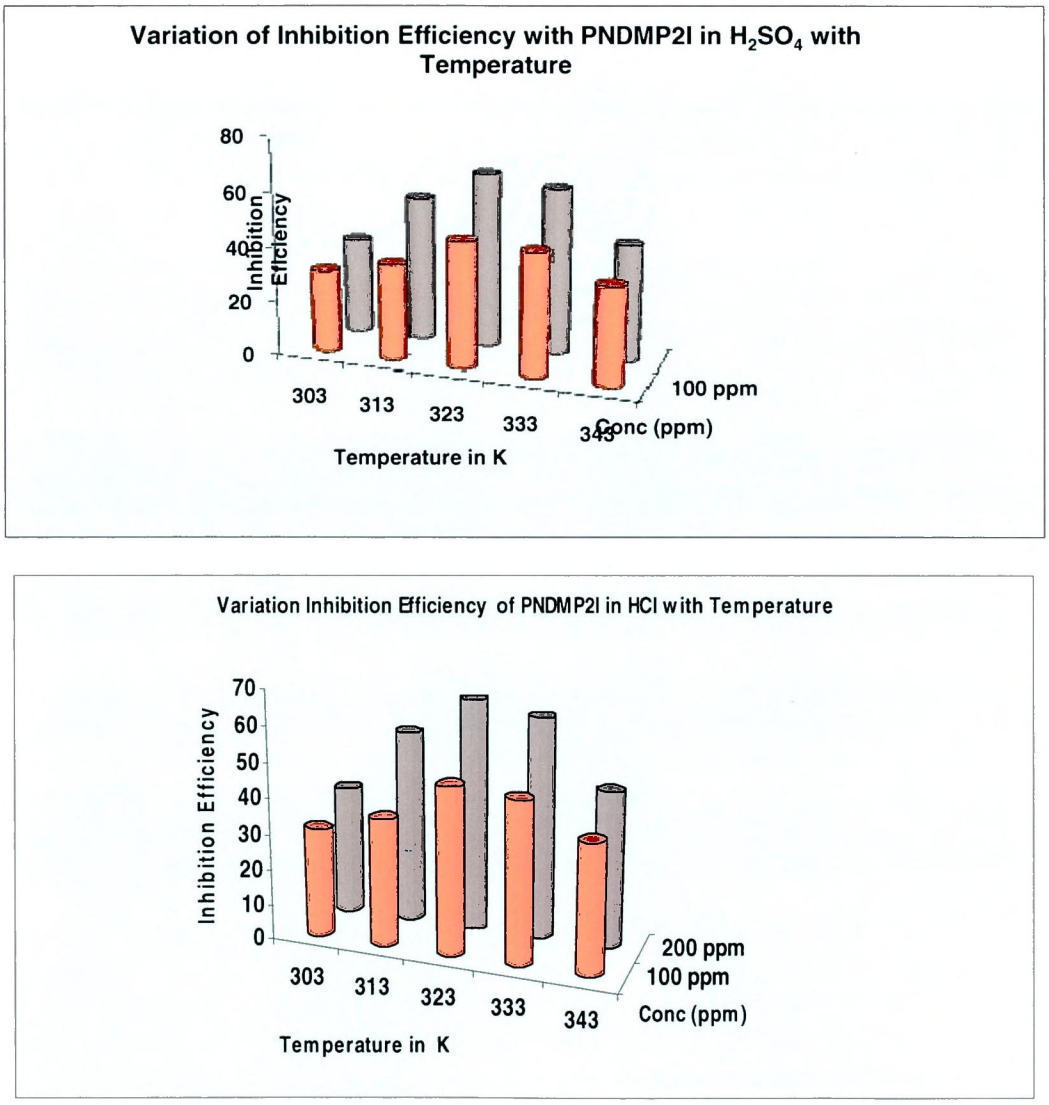

Figure – 32 Variation of inhibition efficiency of PNDMP2I with temperature

PNP2I:

Table – 13 & Figure - 33 represent the variation of inhibition efficiency of PNP2I in both acidic media with temperature.

The obtained data revealed that in both acids, the inhibition efficiency increased with an increase in the inhibitor concentration. At the same time, IE was found to increase with rise in temperature up to 333 K, affording a maximum of 77.7% in H_2SO_4 and 65.6% in HCl. This suggest that the inhibitor species are adsorbed on the mild steel/solution interface where the adsorbed species mechanically screen the coated part of the metal surface from the action of the corrosive medium. An increase or decrease in the inhibition efficiency, depending on its concentration, was indicated with the increase of temperature indicating that adsorption of inhibitor species on mild steel surface at these conditions is not merely physical or chemical adsorption but obey a 'mixed' adsorption (Physical and Chemical adsorption).

Analysis of the effect of temperature on mild steel acid corrosion in the presence of investigated inhibitors may be interpreted as follows: This may be ascribed to the following reason: The adsorption and desorption of inhibitive molecules continuously occur at the metal surface and an equilibrium exists between these two molecules processed at particular temperature. With increase in temperature the equilibrium between adsorption and desorption process are shifted leading to higher desorption. The desorption at elevated temperature thus exposing the metal surface for further attack. This also explains low IE at higher temperature. (Rawat et al, 1987)

TABLE - 13 Variation of Inhibition efficiency of PNP2I on mild steel corrosion as a function of temperature in 0.5M H_2SO_4 and in 1M HCl

ACID MEDIA	Conc. in ppm	303K		313K		323K		333K		343K	
		C.R	I.E	C.R	I.E	C.R	I.E	C.R	I.E	C.R	I.E
		mpy	%	mpy	%	mpy	%	mpy	%	mpy	%
H_2SO_4	Blank	1430	---	1657	---	3794	---	7404	---	11321	
	40	1125	21.3	1193	28.0	2448	35.5	4631	37.4	9707	14.3
	50	1026	28.2	1045	36.9	2192	42.2	4049	45.3	8897	21.4
	60	990	30.8	956	42.3	1991	47.5	3739	49.5	8014	29.2
	70	965	32.5	937	43.5	1822	52.0	3471	53.1	7216	36.3
	80	903	36.8	897	45.8	1599	57.8	3213	56.6	6882	39.2
	100	855	40.2	828	50.0	1518	60.0	2716	63.3	6600	41.7
	120	794	44.4	736	55.6	1479	61.0	2381	67.8	6522	42.4
	140	782	45.3	670	59.5	1392	63.3	2233	69.8	5808	48.7
	160	745	47.9	634	61.7	1237	67.4	1993	73.1	5648	50.1
	200	733	48.7	572	65.5	1077	71.6	1649	77.7	5311	53.1
HCl	Blank	776		1334		1133		6585		15995	
	40	843	10.3	2429	12.7	6884	14.1	7473	29.4	13056	23.5
	50	806	14.3	2355	15.3	6527	18.6	7119	32.8	12271	28.1
	60	772	17.9	2279	18.1	6279	21.7	6789	35.9	11942	30.0
	70	762	19.0	2198	21.0	5958	25.7	6355	40.0	10698	37.3
	80	725	22.9	2064	25.8	5777	27.9	5894	44.3	9838	42.3
	100	723	23.1	1990	28.4	5665	29.3	5340	49.6	9070	46.8
	120	700	25.5	1973	29.1	5377	32.9	5038	52.4	8702	49.0
	140	678	27.9	1928	30.7	5138	35.9	4587	56.7	8267	51.5
	160	668	29.0	1899	31.7	4678	41.6	4307	59.3	7199	57.8
	200	647	31.2	1870	32.8	4618	42.4	3647	65.6	6525	61.8

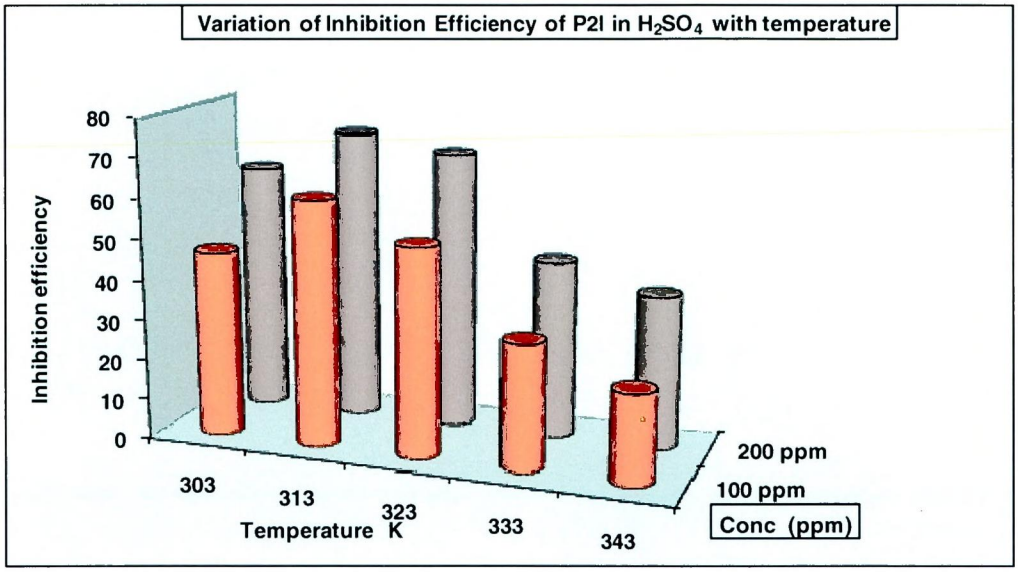

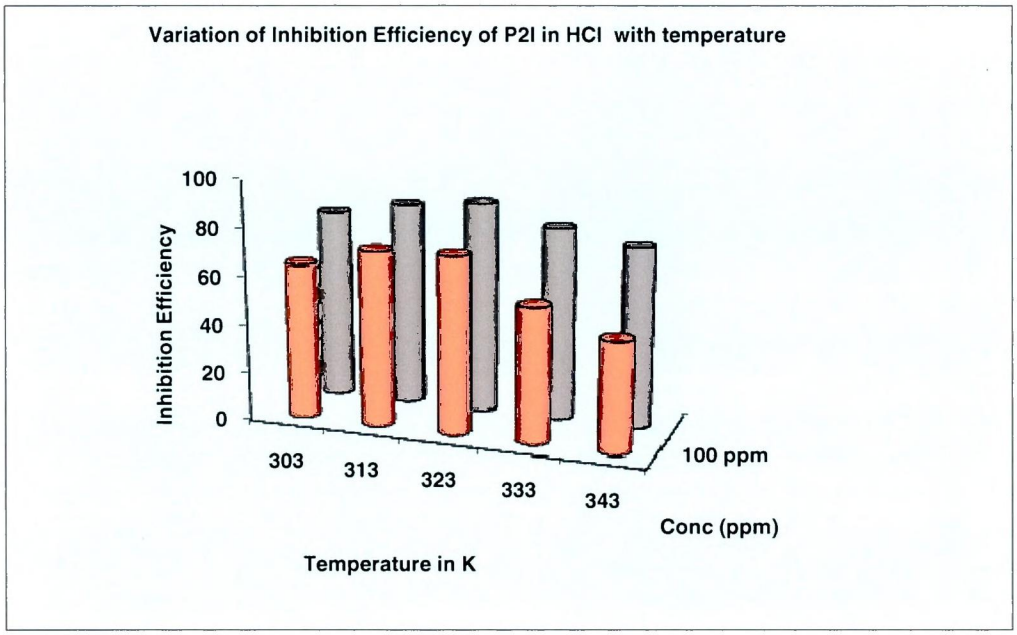

Figure - 33 Variation of inhibition efficiency of PNP2I with temperature

All the imidazoline derivatives furnished slightly high IE in Hydrochloric acid compared to sulphric acid medium. The higher inhibition efficiency of the compouns under investigation in HCl compared with the values in the case of H_2SO_4 can be explained as follows, in acidic solutions, the compounds exist either as neutral molecules or in the form of cations. If the neutral molecules are adsorbed on the metal surface, the water molecules from the metal surface will be displaced and sharing of electrons between the nitrogen atoms and the metal surface. Heterocyclic nitrogen compounds may also adsorb through electrostatic interaction between the positively charged nitrogen atoms and the negatively charged metal surface. It has been observed that the adsorption of the inhibitor can be influenced by the nature of anions in acidic solution. The specific adsorption of anions having a smaller degree of hydration, such as chloride ions, is expected to be more pronounced, while they create an excess negative charge towards the solution and favour more adsorption of the cations.

(Abd El-Maksoud *et al.*, 2008).

Table – 14 highlights the reason for lower/higer Inhibition Efficiency of Imidazoline derivatives in both investigated acid media.

Table – 14 Reason for higher/lower Inhibition Efficiency

Structure & Name of the compound	H_2SO_4	HCl	Reason for higher/lower Inhibition Efficiency
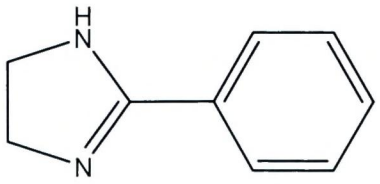 **Phenyl-2-imidazoline - P2I**	**88.8**	**91.4**	**-two hetero atoms, phenyl ring**
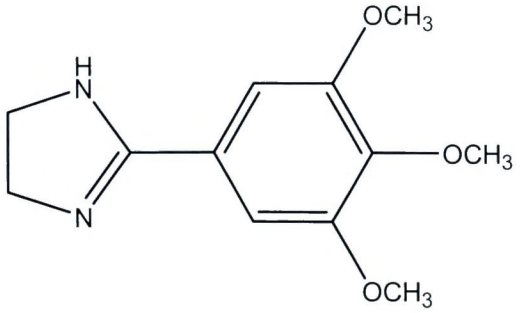 **2-(3',4',5'-Trimethoxyphenyl)-imidazoline - TMP2I**	**98.2**	**98.2**	**Electron releasing – OCH_3 group, phenyl ring**
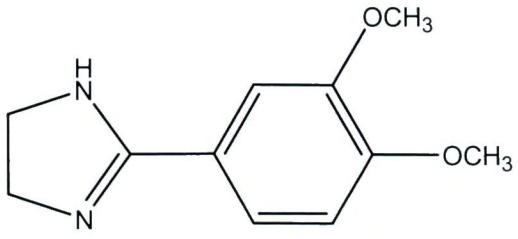 **2-(3',4'-Dimethoxyphenyl)-imidazoline - DMP2I**	**93.4**	**94.6**	**Electron releasing – OCH_3 Group, phenyl ring**

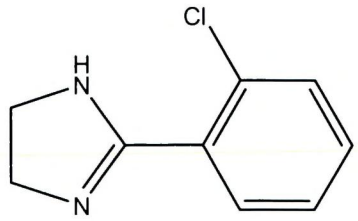 **2-(2'-Chlorophenyl)-imidazoline -OCP2I**	**90.6**	**93.6**	**-chloro group greater dipole moment**
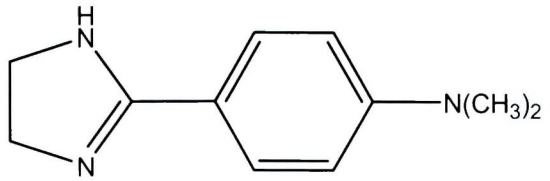 **2-(4'-N,N-Dimethylphenyl)-imidazoline - PNDMP2I**	**85.5**	**90.1**	**Steric hindarance- two methyl groups**
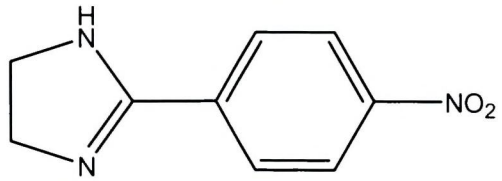 **2-(4'-Nitrophenyl)-imidazoline - PNP2I**	**81.7**	**83.6**	**Electron withdrawing nitro group**

Performance Evaluation of Imidazoline derivatives at Studied Temperatures (At 200 ppm Concentration)

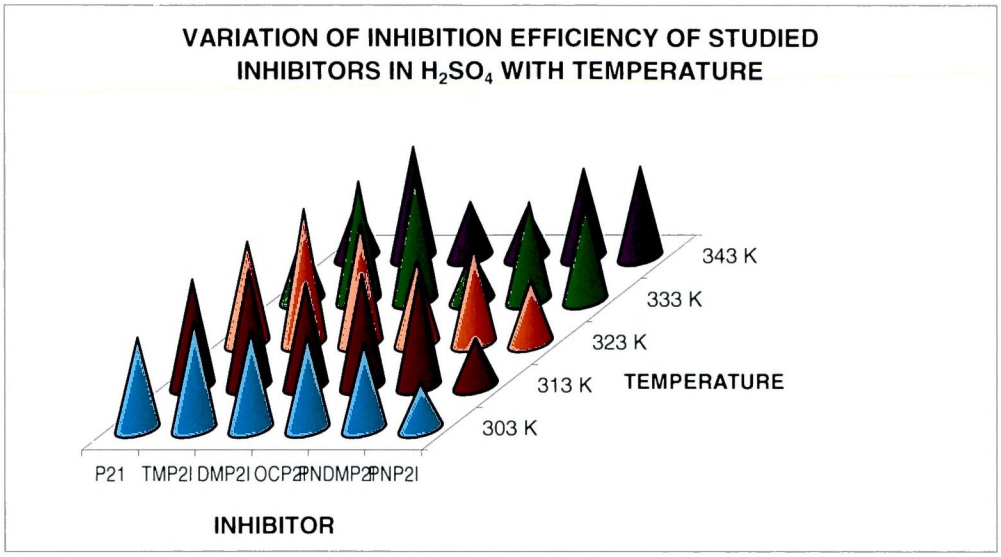

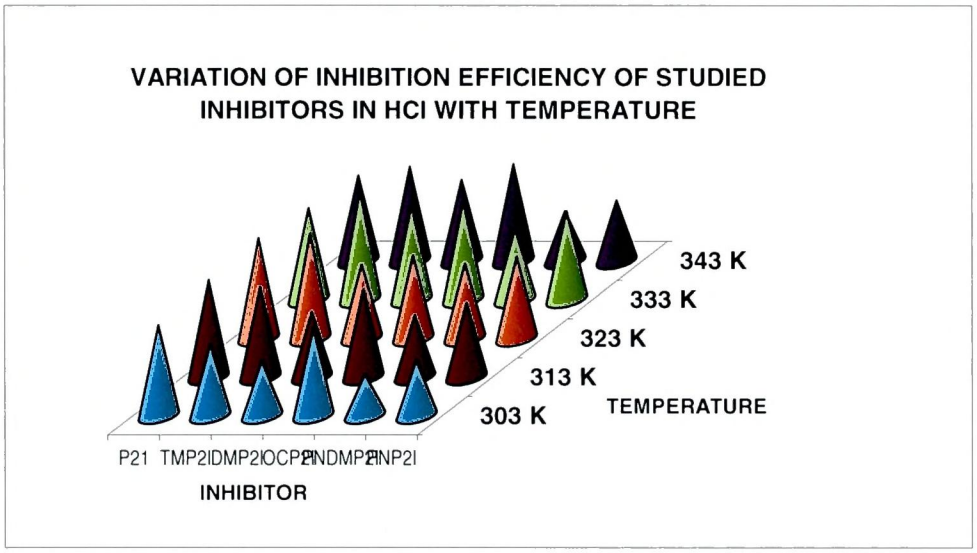

Figure – 34

The corrosiveness of acid is hugely limited in the presence of inhibitor concentration. **Bouklah *et al.*, 2006** considers the increase of IE(%) with temperature increases as the change in the nature of the adsorption mode, the inhibitor is being physically adsorbed at lower temperatures, while chemisorption is favoured as temperature increases. This is due to increase in the surface coverage by an inhibitor. Thus, at a high degree of coverage, the diffusion through the surface layer containing the inhibitor and corrosion products becomes the rate-determining step of the metal dissolution process.

4.2.4 Adsorption Isotherms

In acid corrosion, generally, it is assumed that inhibitors act through a process of adsorption on the metal surface. The adsorption of the inhibitor may determine a structural change of the double layer, thus reducing the rate of electrochemical- partial reactions. Moreover, adsorption that particularly takes place at the active sites of the metal surface, may hinder the reactivity of the metal in the process of dissolution. On the otherhand, if the adsorption is followed by reaction of hydration or reduction or polymerization of the inhibitor itself, thick layers may form that behave as a true physical barrier. In any case, the knowledge of the adsorption behaviour of the inhibitors is important for the definition of its action mechanism.

For an inhibitor to have a high surface coverage on the surface, a chemical bond between the inhibitor and the metal atom stronger than the one for water molecule should be formed. The adsorption of corrosion inhibitors at the metal/solution interface, may be due to the formation of either electrostatic or covalent bonding between the adsorbates and the metal surface atoms.

An adsorption isotherm gives the relation between the coverage of an interface with the adsorbed species and the concentration of the species in solution. Intrepretation of the performance of the adsorbent type of inhibitor can be enhanced by fitting the data in one of known adsorption isotherms using the **Statistical Software Package SPSS 17.**

According to Awady et al

$$S + Y1 \longleftrightarrow SI_Y \qquad \text{---------- (1)}$$

where S is the substrate and K' is a constant. This leads to the relationship

$$\frac{\theta}{1-\theta} = K'[I]^y \qquad \text{--------- (2)}$$

where θ is the surface coverage

$$\frac{\theta}{1-\theta} = K'[I]^y \qquad \text{--------- (3)}$$

The plot of log (θ/1-θ) Vs log C gives a straight line with a slope Y and intercept of K' if relation 3 is applicable.

Values of Y>1 imply the formation of multilayers of the inhibitor on the surface of the metal.Values of Y<1 mean inhibitor molecule will occupy more than one active sites.

The observed corrosion data in the presence of inhibitors, linear dependence of weight loss on immersion time (c), suggest that the corrosion inhibition of mild steel occurs through surface adsorption of inhibitors and /or their complexes.

For this reason, an attempt was also made to understand the nature of the interaction of these compounds on mild surface by adsorption characteristics.

The degree of surface coverage θ for different concentration of inhibited in both acids has been evaluated from weight loss values using the relation $\theta = \rho_o - \rho_i / \rho_o$ where ρ_o and ρ_i are the corrosion rate in the absence and presence of the inhibitor respectively.

Goodness of Fit:

Data were tested graphically by fitting to various isotherms. Statistical estimation of correlation for the curve fitting of isotherms have been used to investigate the goodness of fit of the isotherms **(Schulthess et al., 1996)**

A measure of the goodness of fit is the square of correlation coefficient . R^2 which shows the % of the total variation of the dependent variables that can be explained by the independent variable X. Symbiolically

$$R^2 = \frac{\Sigma Y_1^2}{\Sigma Y_1} = \frac{\text{explained variation}}{\text{Total variation}} \quad ----(4)$$

The value of R^2 generally lies between 0 and 1 ($0 \leq R^2 \leq 1$). The closer the value of R^2 lines to 1, the better is the regression line to data and vice versa.

To test the overall significance of regression model, the technology of ANOVA is used,which is defined by the F value.

$$F = \frac{\text{explained sum of square/degrees of freedom}}{\text{Residual sum of squares/ degrees of freedom}} \quad ----(5)$$

A large F value will be evidenced against the null hypothesis the explanatory variable have no effect of Y.

Adsorption isotherms are often shown to demonstrate the performance of organic adsorbent-type inhibitors.Corrosion inhibitors are found to protect steel corrosion in acid solutions by adsorbing themselves on steel surface. Adsorption is a separation process involving two phases between which certain components can

become differentially distributed. Adsorption can be described by two main types of interaction:

• **Physisorption,** involves electrostatic forces between ionic charges or dipoles on the adsorbed species and the electric charge at the metal/solution interface. The heat of adsorption is low and therefore this type of adsorption is stable only at relatively low temperatures.

• **Chemisorption,** involves charge sharing or charge transfer from the inhibitor molecules to the metal surface to form a coordinate type bond. In fact, electron transfer is typically for transition metals having vacant low-energy electron orbital. Chemisorption is signified by a much stronger adsorption energy than physical adsorption. Such a bond is therefore more stable at higher temperatures.

It is well recognized that the first step in inhibition of metallic corrosion is the adsorption of organic inhibitor molecules at the metal/solution interface. Furthermore, the adsorption depends on the molecule's chemical composition, the temperature and the electrochemical potential at the metal/solution interface. So the adsorption of organic inhibitor molecules from the aqueous solution can be regarded as a quasi-substitution process between the organic compounds in the aqueous phase [$Org_{(sol)}$] and water molecules at the electrode surface [$H_2O_{(ads)}$]

$$Org_{(sol)} + x\ H_2O_{(ads)} \longleftrightarrow Org_{(ads)} + x\ H_2O_{(sol)}$$

where x is the size ratio, that is, the number of water molecules replaced by one organic inhibitor. Basic information on the interaction between the inhibitor of the mild steel surface can be provided by the adsorption isotherm. In order to obtain the isotherm, the linear relation between degree of surface coverage (θ) values (θ = %IE/100) and inhibitor concentration (C)must be found. Attempts were made to fit the θ values to various isotherms including Langmuir, El Awady Isotherm, Temkin, Freundlich, Frumkin and Flory-Huggins.

In this section of study the changes in the surface coverage and thereby the change in the inhibition efficiency is measured using different models at the same level of temperature. These models include Langmuir adsorption, El-Awady isotherm, El-Awady isotherm, Freundlich adsorption isotherm, Frumkin isotherm and Flory-Huggins isotherm

Langmuir adsorption equation relates degree of surface coverage to concentration of inhibitor according to equation (1)

$$\text{Log } (C/\theta) = \log K + \log C \quad \text{---------} \quad (1)$$

El-Awady isotherm is the extended form of Langmuir adsorption isotherm

$$\text{Log } (\theta/1-\theta) = \log K + y\log C \quad \text{---------} \quad (2)$$

Temkin isotherm is formulated as in equation (3)

$$\text{Exp } (-2a\theta) = k\, C \quad \text{---------} \quad (3)$$

Freundlich adsorption isotherm obeys the equation (4)

$$\theta = K\, C^{1/n} \quad \text{----------} \quad (4)$$

Frumkin isotherm is given by equation (5)

$$\ln \left[\frac{\theta}{C(1-\theta)} \right] = \ln k + 2a\,\theta \quad \text{---------} \quad (5)$$

Flory-Huggins isotherm follows the following equation (6)

$$\log (\theta/C) = \log K + x \log (1-\theta) \quad \text{---------} \quad (6)$$

A particular model which has highest value of R^2 can be considered as the best model to explain the changes in performance of organic adsorbent-type inhibitors. Similarly, the effect of the level of concentration on the IE can be estimated by coefficienct of the equation and can be tested against the hypothesis.

The model used takes the following form $\ln y = \alpha + \beta x$, where 'y' is the surface coverage and 'x' is the concentration . The same model has applied for the six adsorption isotherms to identify the most suitable model for the problem understudy using **Statistical Software Package SPSS 17.**

Adsorption isotherm behaviour of investigated inhibitors in both acidic media :

Values of adsorption parameters deduced from various adsorption isotherm and the estimated coefficients of studied inhibitors in both acidic media are presented in Table-(15-26).

Table - 15 Adsorption parameters deduced from various adsorption isotherms - P2I in 0.5M H_2SO_4

ADSORPTION ISOTHERM MODELS	TEMP (K)	SLOPE	T	INTERCEPT	R^2	F
LANGMIUR	303	0.996	15.619** (0.000)	3.249	0.967	243.966** [0.000]
	313	1.097	24.569** (0.000)	3.715	0.99	603.621** [0.000]
	323	1.146	19.17** (0.000)	3.918	0.98	367.473** [0.000]
	333	1.087	13.05** (0.000)	3.455	0.952	170.302** [0.000]
	343	1.372	12.683** (0.000)	4.142	0.954	160.853** [0.000]
TEMKIN	303	0.523	14.419** (0.000)	2.208	0.963	207.907** [0.000]
	313	0.512	30.455** (0.000)	2.248	0.992	927.52** [0.000]
	323	0.499	33.415** (0.000)	2.236	0.985	517.662** [0.000]
	333	0.574	15.427** (0.000)	2.323	0.967	237.977** [0.000]
	343	0.74	12.012** (0.000)	2.733	0.95	144.289** [0.000]
FREUNDLICH	303	0.362	11.91** (0.000)	-0.432	0.943	141.852** [0.000]
	313	0.33	20.172** (0.000)	-0.35	0.982	406.894** [0.000]
	323	0.309	15.562** (0.000)	-0.312	0.969	242.164** [0.000]
	333	0.439	17.015** (0.000)	-0.532	0.972	289.514** [0.000]
	343	0.683	17.475** (0.000)	-0.724	0.977	305.374** [0.000]
FLORY-HUGGINS	303	0.958	9.236** (0.000)	-0.268	0.914	85.296** [0.000]
	313	2.635	19.362** (0.000)	-0.924	0.979	374.870** [0.000]
	323	1.205	14.028** (0.000)	-0.461	0.961	196.791** [0.000]
	333	1.116	7.087** (0.000)	-0.165	0.863	50.220** [0.000]
	343	1.829	4.426* (0.002)	-0.240	0.710	19.592* [0.002]
FRUMKIN	303	1.002	0.467 (0.653)	-2.443	0.852	0.218 [0.653]
	313	0.917	2.634 (0.030)	-2.370	0.826	6.939 [0.030]
	323	1.543	2.872 (0.021)	-4.219	0.879	8.247 [0.021]
	333	0.575	2.634 (0.030)	-1.374	0.950	6.433 [0.022]
	343	0.963	2.547 (0.056)	-2.465	0.835	7.599 [0.043]

** - 1% level of significane: * - 5% level of significance

Table - 16 Adsorption parameters deduced from various adsorption isotherms - P2I in 1M HCl

Adsorption Isotherm Models	TEMP (K)	Slope	t	Intercept	R^2	F
Langmuir	303	1.108	22.509** (0.000)	3.258	0.984	506.654** [0.000]
	313	0.997	29.183** (0.000)	3.159	0.991	851.63** [0.000]
	323	1.251	22.216** (0.000)	3.744	0.985	493.557** [0.000]
	333	1.31	10.475** (0.000)	3.512	0.937	109.73** [0.000]
	343	1.303	15.899** (0.000)	3.358	0.973	252.764** [0.000]
Temkin	303	0.594	35.069** (0.000)	2.249	0.993	1229.843 [0.000]**
	313	0.546	24.705** (0.000)	2.228	0.986	610.343 [0.000]**
	323	0.678	20.782** (0.000)	2.532	0.983	431.891 [0.000]**
	333	0.546	11.348** (0.000)	1.931	0.946	128.787 [0.000]**
	343	0.482	11.859** (0.000)	1.684	0.949	140.642 [0.000]**
Freundlich	303	0.639	12.243** (0.000)	-0.805	0.949	149.882** [0.000]
	313	0.441	13.723** (0.000)	-0.546	0.956	188.319** [0.000]
	323	0.676	15.16** (0.000)	-0.75	0.966	229.81** [0.000]
	333	0.981	9.684** (0.000)	-1.328	0.924	93.78** [0.000]
	343	1.028	16.374** (0.000)	-1.551	0.973	268.099** [0.000]
Flory-huggins	303	1.122	7.243** (0.000)	0.110	0.868	52.465** [0.000]
	313	2.228	16.169** (0.000)	-0.403	0.970	261.434** [0.000]
	323	1.540	6.695** (0.000)	0.189	0.849	44.818** [0.000]
	333	-0.108	-2.560 (0.804)	-0.205	0.008	0.066 [0.804]
	343	-0.491	-0.883 (0.403)	-0.442	0.089	0.780 [0.403]
Frumkin	303	0.351	2.542* (0.035)	-0.516	0.110	6.549 [0.035]
	313	-1.310	1.713 (0.125)	4.921	0.500	2.936 [0.125]
	323	1.603	17.382* (0.000)	-3.909	0.920	302.121** [0.000]
	333	0.42	3.953** (0.004)	-0.409	0.270	15.629* [0.004]
	343	1.697	5.970* (0.000)	-3.596	0.560	35.642** [0.000]

** - 1% level of significane: * - 5% level of significance

Table - 17 Adsorption parameters deduced from various adsorption isotherms - TMP2I in 0.5M H_2SO_4

Adsorption Isotherm Models	TEMP (K)	Slope	t	Intercept	R^2	F
Langmuir	303	1.582	30.005** (0.000)	4.867	0.992	900.271** [0.000]
	313	1.058	16.800** (0.000)	3.543	0.972	282.241** [0.000]
	323	1.215	18.264** (0.000)	4.236	0.976	333.585** [0.000]
	333	1.456	8.886** (0.000)	4.632	0.909	78.965** [0.000]
	343	2.508	9.185** (0.000)	7.743	0.915	84.359** [0.000]
Temkin	303	0.827	33.067** (0.000)	3.043	0.995	1093.433** [0.000]
	313	0.596	15.898** (0.000)	2.497	0.971	252.757** [0.000]
	323	0.474	24.207** (0.000)	2.202	0.981	585.966** [0.000]
	333	0.757	7.642** (0.000)	2.909	0.886	58.393** [0.000]
	343	0.945	10.569** (0.000)	3.312	0.935	111.704** [0.000]
Freundlich	303	0.704	10.842** (0.000)	-0.658	0.935	117.556** [0.000]
	313	0.323	7.629** (0.000)	-0.400	0.871	58.197** [0.000]
	323	1.010	9.338** (0.000)	-0.516	0.914	87.205** [0.000]
	333	0.280	14.366** (0.000)	-0.259	0.961	206.379** [0.000]
	343	1.007	16.353** (0.000)	-0.853	0.970	267.419** [0.000]
Flory-huggins	303	0.410	4.309* (0.003)	-0.134	0.699	18.571** [0.003]
	313	1.104	8.438** (0.000)	0.392	0.899	71.196** [0.000]
	323	0.001	0.15 (0.988)	-0.224	0.004	0.000* [0.988]
	333	0.741	13.901** (0.000)	0.409	0.960	193.233* [0.000]
	343	-0.036	0.518 (0.618)	-0.381	0.033	0.269 [0.618]
Frumkin	303	0.3509	0.95 (0.370)	-0.516	0.108	0.902 [0.370]
	313	-1.3096	2.753 (0.0250)	4.921	0.497	7.579 [0.0250]
	323	1.6031	9.911 (0.000)	-3.909	0.918	98.233* [0.000]
	333	0.4214	1.696 (0.128)	-0.409	0.267	2.878 [0.128]
	343	1.6973	1.789 (0.134)	-3.596	0.564	10.434 [0.012]

** - 1% level of significane: * - 5% level of significance

Table - 18 Adsorption parameters deduced from various adsorption isotherms - TMP2I in 1M HCl

Adsorption Isotherm Models	TEMP (K)	Slope	t	Intercept	R^2	F
Langmuir	303	1.644	12.209** (0.000)	4.808	0.948	149.069** [0.000]
	313	1.574	6.401** (0.000)	4.987	0.837	40.972** [0.000]
	323	1.888	9.129** (0.000)	5.864	0.913	83.335** [0.000]
	333	1.215	18.180** (0.000)	4.236	0.976	330.514** [0.000]
	343	1.609	7.644** (0.000)	4.957	0.881	58.438** [0.000]
Temkin	303	0.803	16.328** (0.000)	2.852	0.969	266.597** [0.000]
	313	0.820	5.841** (0.000)	3.096	0.810	34.115** [0.000]
	323	0.752	17.966** (0.000)	2.801	0.920	322.792** [0.000]
	333	0.806	9.661** (0.000)	3.222	0.920	93.326** [0.000]
	343	0.838	7.647** (0.000)	3.076	0.877	58.482** [0.000]
Freundlich	303	1.047	8.233** (0.000)	-0.918	0.894	67.784** [0.000]
	313	0.712	5.148** (0.000)	0.137	0.768	26.502** [0.000]
	323	0.704	10.752** (0.000)	-0.251	0.935	115.608** [0.000]
	333	0.497	8.090** (0.000)	0.222	0.891	65.452** [0.000]
	343	0.693	8.737** (0.000)	-0.364	0.905	76.330** [0.000]
Flory-huggins	303	-0.265	0.456 (0.660)	-0.354	0.025	0.208 [0.660]
	313	0.563	0.882 (0.404)	-0.330	0.089	0.778 [0.404]
	323	1.706	4.309 (0.003)	0.127	0.699	18.571* [0.003]
	333	0.711	5.739* (0.000)	-0.539	0.805	32.940** [0.000]
	343	1.432	1.850* (0.102)	0.012	0.300	3.421 [0.102]
Frumkin	303	1.002	6.886** (0.000)	-2.443	0.852	47.417** [0.000]
	313	0.917	6.125** (0.000)	-2.370	0.826	37.518** [0.000]
	323	1.543	7.613** (0.000)	-4.219	0.879	57.952** [0.000]
	333	0.575	12.291** (0.000)	-1.374	0.950	151.061* [0.000]
	343	0.963	6.380** (0.000)	-2.465	0.835	40.705** [0.000]

** - 1% level of significane: * - 5% level of significance

Table - 19 Adsorption parameters deduced from various adsorption isotherms - DMP2I in 0.5M H_2SO_4

Adsorption Isotherm Models	TEMP (K)	Slope	t	Intercept	R^2	F
Langmuir	303	1.858	15.457** (0.000)	5.446	0.967	238.909** [0.000]
	313	0.981	11.199** (0.000)	2.999	0.943	125.425** [0.000]
	323	0.914	8.643** (0.000)	2.995	0.907	74.697** [0.000]
	333	0.921	19.135** (0.000)	2.682	0.978	366.151** [0.000]
	343	1.226	10.637** (0.000)	3.195	0.934	113.141** [0.000]
Temkin	303	0.896	16.896** (0.000)	3.130	0.973	285.476** [0.000]
	313	0.543	11.547** (0.000)	2.160	0.944	133.341** [0.000]
	323	0.470	9.849** (0.000)	2.044	0.925	97.008** [0.000]
	333	0.379	0.983** (0.000)	1.910	0.965	233.232** [0.000]
	343	0.462	14.214** (0.000)	1.650	0.962	202.035** [0.000]
Freundlich	303	1.174	10.097** (0.000)	-0.945	0.923	101.958** [0.000]
	313	0.469	14.025** (0.000)	-0.662	0.962	196.692** [0.000]
	323	0.327	11.347** (0.000)	-0.471	0.946	128.753** [0.000]
	333	0.222	12.053** (0.000)	-0.261	0.948	145.264** [0.000]
	343	0.961	9.278** (0.000)	-1.428	0.915	86.081** [0.000]
Flory-huggins	303	-1.225	0.074 (0.943)	-0.910	0.435	0.006* [0.943]
	313	-2.274	6.259** (0.000)	-1.639	0.347	39.176* [0.000]
	323	-0.435	0.678 (0.517)	-0.435	0.093	0.459* [0.517]
	333	1.496	0.324 (0.754)	-1.078	0.841	0.105* [0.754]
	343	1.298	1.368 (0.208)	0.022	0.919	1.872* [0.208]
Frumkin	303	0.366	0.896 (0.396)	-0.681	0.502	0.803* [0.396]
	313	-1.023	2.049 (0.075)	3.818	0.355	4.199* [0.075]
	323	0.621	6.805* (0.000)	-1.137	0.856	46.309** [0.000]
	333	0.338	1.695 (0.129)	-0.179	0.266	2.872 [0.129]
	343	0.900	3.23* (0.003)	-1.894	0.681	10.434* [0.003]

** - 1% level of significane: * - 5% level of significance

Table - 20 Adsorption parameters deduced from various adsorption isotherms - DMP2I in 1M HCl

Adsorption Isotherm Models	TEMP (K)	Slope	t	Intercept	R^2	F
Langmuir	303	1.473	16.518** (0.000)	3.929	0.973	272.831** [0.000]
	313	1.675	20.092** (0.000)	4.671	0.980	403.678** [0.000]
	323	1.756	9.758** (0.000)	5.182	0.923	95.217** [0.000]
	333	0.755	8.612** (0.000)	2.682	0.901	74.161** [0.000]
	343	1.162	21.311** (0.000)	3.550	0.986	454.166** [0.000]
Temkin	303	0.581	9.351** (0.000)	2.012	0.920	87.439** [0.000]
	313	0.727	13.770** (0.000)	2.513	0.960	189.616** [0.000]
	323	0.852	12.412** (0.000)	3.023	0.951	154.053** [0.000]
	333	0.356	7.615** (0.000)	1.785	0.876	57.984** [0.000]
	343	0.638	21.443** (0.000)	2.450	0.984	459.812** [0.000]
Freundlich	303	1.120	18.948** (0.000)	-1.457	0.979	359.021** [0.000]
	313	1.194	15.140** (0.000)	-1.247	0.965	229.233** [0.000]
	323	1.106	7.000** (0.000)	-0.878	0.859	49.005** [0.000]
	333	0.228	6.333** (0.000)	-0.339	0.834	40.111** [0.000]
	343	0.576	15.349** (0.000)	-0.661	0.967	235.580** [0.000]
Flory-huggins	303	0.022	13.765* (0.208)	-0.283	0.001	189.483 [0.208]
	313	1.502	1.340* (0.59)	-0.689	0.830	2.407 [0.59]
	323	-0.724	1.157* (0.280)	-0.542	0.054	1.340 [0.280]
	333	0.093	8.845** (0.000)	-0.164	0.013	78.230* [0.000]
	343	-0.398	3.703 (0.006)	-0.386	0.190	13.714* [0.006]
Frumkin	303	0.572	2.858 (0.021)	-1.385	0.443	8.165* [0.021]
	313	0.438	1.771 (0.134)	-1.118	0.192	3.137* [0.134]
	323	1.665	5.109* (0.001)	-4.674	0.736	26.101* [0.001]
	333	0.224	4.394 (0.002)	-0.133	0.670	19.309* [0.002]
	343	0.536	2.837 (0.022)	-1.155	0.439	8.051 [0.022]

** - 1% level of significane: * - 5% level of significance

Table - 21 Adsorption parameters deduced from various adsorption isotherms - OCP2I in 0.5M H_2SO_4

Adsorption Isotherm Models	TEMP (K)	Slope	t	Intercept	R^2	F
Langmuir	303	1.264	4.947* (0.001)	3.77	0.918	24.475** [0.000]
	313	0.769	9.138** (0.000)	2.535	0.749	83.506** [0.000]
	323	1.703	24.497** (0.000)	4.959	0.967	600.097** [0.000]
	333	1.253	6.773** (0.000)	3.54	0.848	45.875** [0.000]
	343	1.352	15.158** (0.000)	3.448	0.988	229.76** [0.000]
Temkin	303	0.625	5.76** (0.000)	2.373	0.803	33.174** [0.000]
	313	0.406	10.049** (0.000)	1.84	0.936	100.983** [0.000]
	323	0.842	19.359** (0.000)	2.955	0.981	374.772** [0.000]
	333	0.574	10.006** (0.000)	2.11	0.925	100.123** [0.000]
	343	0.437	14.33** (0.000)	1.527	0.97	205.347** [0.000]
Freundlich	303	0.6388	3.98** (0.004)	-0.805	0.9486	15.839** [0.004]
	313	0.4408	12.932** (0.001)	-0.546	0.9562	167.236** [0.001]
	323	0.6758	15.122** (0.000)	-0.75	0.9656	12.927** [0.000]
	333	0.9805	5.37** (0.000)	-1.328	0.9239	28.841** [0.000]
	343	1.0284	13.004** (0.000)	-1.55	0.9734	169.103** [0.000]
Flory-huggins	303	0.0222	0.074 (0.943)	-0.283	0.0007	0.006 [0.943]
	313	1.5017	6.259** (0.000)	-0.688	0.8304	39.176** [0.000]
	323	-0.7237	0.678 (0.517)	-0.542	0.0543	0.459 [0.517]
	333	0.0934	0.324 (0.754)	-0.164	0.0129	0.105 [0.754]
	343	-0.3978	1.368 (0.208)	-0.386	0.1896	1.872 [0.208]
Frumkin	303	0.551	3.889** (0.000)	0.618	0.655	15.124** [0.000]
	313	-0.654	1.629* (0.142)	2.721	0.258	2.654 [0.142]
	323	1.148	15.497** (0.000)	-2.842	0.968	240.16* [0.000]
	333	0.661	2.458 (0.039)	-1.466	0.424	6.044 [0.039]
	343	0.872	5.492** (0.000)	-1.875	0.723	30.163** [0.000]

** - 1% level of significane: * - 5% level of significance

Table - 22 Adsorption parameters deduced from various adsorption isotherms - OCP2I in 1M HCl

Adsorption Isotherm Models	TEMP (K)	Slope	t	Intercept	R^2	F
Langmuir	303	0.953	22.011** (0.000)	3.066	0.985	484.474** [0.000]
	313	1.52	10.72** (0.000)	4.66	0.934	114.919** [0.000]
	323	1.36	7.282** (0.000)	4.045	0.871	53.033** [0.000]
	333	0.892	12.058** (0.000)	3.224	0.943	145.395** [0.000]
	343	1.059	6.513** (0.000)	3.665	0.838	42.42** [0.000]
Temkin	303	0.513	21.492** (0.000)	2.152	0.983	461.917** [0.000]
	313	0.791	11.433** (0.000)	2.929	0.941	130.712** [0.000]
	323	0.694	8.189** (0.000)	2.565	0.895	67.054** [0.000]
	333	0.385	8.113** (0.000)	1.924	0.888	65.824** [0.000]
	343	0.5	5.195** (0.000)	2.243	0.766	26.984** [0.000]
Freundlich	303	0.3831	16.356** (0.000)	-0.465	267.511	0.943** [0.000]
	313	0.3296	6.615** (0.000)	-0.349	43.754	0.9819** [0.000]
	323	0.3088	5.84** (0.000)	-0.311	34.108	0.9691** [0.000]
	333	0.4394	6.689** (0.000)	-0.532	44.746	0.9715** [0.000]
	343	0.6828	4.154** (0.000)	-0.72	17.254	0.977** [0.003]
Flory-huggins	303	0.908	13.765** (0.000)	-0.227	0.9595	189.483** [0.000]
	313	2.0633	1.551* (0.159)	-0.244	0.2313	2.407* [0.159]
	323	0.5596	1.157* (0.280)	-0.096	0.1434	1.34* [0.280]
	333	0.8262	8.845** (0.000)	-0.565	0.9072	78.23** [0.000]
	343	0.8619	3.7003* (0.006)	-0.5	0.6316	13.714* [0.006]
Frumkin	303	-1.037	5.379** (0.000)	3.919	0.065	28.937** [0.000]
	313	1.13	6.811** (0.000)	-2.958	0.835	46.395** [0.000]
	323	0.919	5.324** (0.000)	-2.259	0.633	28.344** [0.000]
	333	-0.202	10.736** (0.000)	1.47	0.015	115.259** [0.000]
	343	0.714	10.043** (0.000)	-1.766	0.345	100.857** [0.000]

** - 1% level of significane: * - 5% level of significance

Table - 23 Adsorption parameters deduced from various adsorption isotherms - PNDMP2I in 0.5M H_2SO_4

Adsorption Isotherm Models	TEMP K	Slope	t	Intercept	R^2	F
Langmuir	303	1.18	6.473** (0.000)	3.462	0.837	41.899** [0.000]
	313	1.388	11.072** (0.000)	4.342	0.938	122.588** [0.000]
	323	1.012	13.111** (0.000)	3.325	0.954	171.899** [0.000]
	333	0.819	6.318** (0.000)	2.648	0.83	39.914** [0.000]
	343	0.927	10.174** (0.000)	2.772	0.928	103.508** [0.000]
Temkin	303	0.595	8.091** (0.000)	2.25	0.889	65.471** [0.000]
	313	0.738	10.446** (0.000)	2.809	0.931	109.114** [0.000]
	323	0.527	11.291** (0.000)	2.234	0.939	127.485** [0.000]
	333	0.451	6.234** (0.000)	1.96	0.826	38.863** [0.000]
	343	0.512	10.538** (0.000)	2.034	0.932	111.045** [0.000]
Freundlich	303	-0.015	5.084** (0.000)	5.873	0.76	25.848** [0.000]
	313	-0.089	6.846** (0.000)	39.229	0.852	46.866** [0.000]
	323	-0.051	8.03** (0.000)	19.771	0.887	64.476** [0.000]
	333	-0.001	5.126** (0.000)	1.388	0.762	26.273** [0.000]
	343	-1.782	8.252** (0.000)	689.1	0.894	68.096** [0.000]
Flory-huggins	303	0.298	0.960* (0.365)	-0.158	0.103	0.923* [0.365]
	313	2.721	2.799* (0.023)	-0.272	0.495	7.836* [0.023]
	323	0.947	7.635** (0.023)	-0.296	0.879	58.291** [0.000]
	333	0.566	3.559* (0.007)	-0.285	0.613	12.665** [0.007]
	343	0.701	4.701* (0.002)	-0.084	0.734	22.103** [0.002]
Frumkin	303	0.707	5.228** (0.000)	-1.623	0.3809	27.333** [0.000]
	313	1.285	7.569** (0.000)	-3.498	0.7869	57.291** [0.000]
	323	0.718	7.476** (0.000)	-1.730	0.0861	55.889** [0.000]
	333	-0.443	3.547** (0.002)	0.477	0.0901	12.584** [0.002]
	343	-0.028	4.548** (0.001)	0.558	0.0002	20.682** [0.001]

** - 1% level of significane: * - 5% level of significance

Table - 24 Adsorption parameters deduced from various adsorption isotherms - PNDMP2I in 1M HCl

Adsorption Isotherm Models	TEMP (K)	Slope	t	Intercept	R^2	F
LANGMUIR	303	1.321	7.831** (0.000)	3.478	0.884	61.33** [0.000]
	313	1.041	27.781** (0.000)	2.875	0.989	771.809** [0.000]
	323	0.925	15.837** (0.000)	2.739	0.969	250.811** [0.000]
	333	1.054	18.733** (0.000)	3.078	0.976	350.917** [0.000]
	343	0.805	10.044** (0.000)	2.124	0.924	100.886** [0.000]
TEMKIN	303	0.471	12.139** (0.000)	1.679	0.9322	108.033** [0.000]
	313	0.52	20.377** (0.000)	1.928	0.9809	415.23** [0.000]
	323	0.508	16.75** (0.000)	2.005	0.9727	280.565** [0.000]
	333	0.565	22.427** (0.000)	2.15	0.9828	502.955** [0.000]
	343	0.381	14.534** (0.000)	1.487	0.9617	211.242** [0.000]
FREUNDLICH	303	1.054	7.048** (0.000)	-1.433	0.86	49.671** [0.000]
	313	0.684	23.693** (0.000)	-1.049	0.984	561.367** [0.000]
	323	0.504	13.104** (0.000)	-0.761	0.954	171.705** [0.000]
	333	0.613	12.314** (0.000)	-0.825	0.947	151.628** [0.000]
	343	0.562	8.175** (0.000)	-1.099	0.89	66.833** [0.000]
FLORY-HUGGINS	303	-0.199	0.925 (0.000)	-0.251	0.097	0.856** [0.000]
	313	1.057	(0.382)	0.275	0.898	70.072* [0.382]
	323	1.836	7.682** (0.000)	-0.068	0.881	59.015** [0.000]
	333	0.993	2.253 (0.037)	0.083	0.846	5.075 [0.037]
	343	0.432	0.422 (0.678)	0.022	0.717	0.178 [0.678]
FRUMKIN	303	0.624	6.481** (0.000)	-1.316	0.543	42.007** [0.000]
	313	1.997	4.474** (0.000)	-5.146	0.203	20.013** [0.000]
	323	-0.736	4.279** (0.000)	2.641	0.067	18.309** [0.000]
	333	1.377	0.666** (0.000)	-3.582	0.179	20.677** [0.000]
	343	-0.622	3.938* (0.001)	2.019	0.235	15.508* [0.001]

** - 1% level of significane: * - 5% level of significance

Table - 25 Adsorption parameters deduced from various adsorption isotherms - PNP2I in 0.5M H_2SO_4

Adsorption Isotherm Models	TEMP (K)	Slope	T	Intercept	R^2	F
LANGMUIR	303	0.791	10.906** (0.000)	1.840	0.935	118.945** [0.000]
	313	0.781	9.938** (0.000)	1.871	0.922	98.764** [0.000]
	323	0.909	17.631** (0.000)	2.359	0.973	310.869** [0.000]
	333	0.950	40.471** (0.000)	2.829	0.996	1637.887** [0.000]
	343	1.039	20.179** (0.000)	3.027	0.982	407.209** [0.000]
TEMKIN	303	0.289	18.102** (0.000)	1.102	0.976	327.689** [0.000]
	313	0.309	11.942** (0.000)	1.185	0.948	142.611** [0.000]
	323	0.408	20.641** (0.000)	1.532	0.983	426.038** [0.000]
	333	0.527	36.356** (0.000)	2.069	0.995	1321.726** [0.000]
	343	0.559	21.342** (0.000)	2.131	0.985	455.461** [0.000]
FREUNDLICH	303	0.630	9.516** (0.000)	-1.494	0.9156	90.554** [0.000]
	313	0.605	8.94** (0.000)	-1.389	0.9085	79.919** [0.000]
	323	0.657	13.765** (0.000)	-1.223	0.9581	189.485** [0.000]
	333	0.507	28.354** (0.000)	-0.743	0.9907	803.922** [0.000]
	343	0.604	14.714** (0.000)	-0.832	0.9631	216.504** [0.000]
FLORY- HUGGINS	303	0.323	4.241** (0.000)	0.094	0.6922	17.990** [0.000]
	313	0.751	3.734** (0.000)	0.154	0.6355	13.946** [0.000]
	323	0.623	5.997** (0.000)	0.169	0.818	35.962** [0.000]
	333	0.895	21.422** (0.000)	-0.013	0.9829	458.916** [0.000]
	343	1.003	8.099* (0.069)	0.092	0.8913	65.588* [0.069]
FRUMKIN	303	-0.591	5.879** (0.003)	1.686	0.356	334.559** [0.003]
	313	-0.522	5.303** (0.006)	1.570	0.269	28.122** [0.006]
	323	-0.993	4.71** (0.000)	2.907	0.181	21.182** [0.000]
	333	-3.964	4.391** (0.000)	12.286	0.344	19.284** [0.000]
	343	1.480	1.932** (0.000)	-3.878	0.144	3.732** [0.000]

** - 1% level of significane: * - 5% level of significance

Table - 26 Adsorption parameters deduced from various adsorption isotherms - PNP2I in 1M HCl

Adsorption Isotherm Models	TEMP (K)	Slope	t	Intercept	R^2	F
LANGMUIR	303	0.769	13.901** (0.000)	2.112	0.960	193.231** [0.000]
	313	0.926	21.282** (0.000)	2.796	0.980	452.916** [0.000]
	323	0.885	17.051** (0.000)	2.799	0.967	290.750** [0.000]
	333	1.068	49.653** (0.000)	3.428	0.997	2465.466** [0.000]
	343	1.097	8.422** (0.000)	3.100	0.899	70.923** [0.000]
TEMKIN	303	0.398	17.572** (0.000)	1.589	0.975	308.758** [0.000]
	313	0.513	24.042** (0.000)	2.051	0.985	578.030** [0.000]
	323	0.489	14.285** (0.000)	2.046	0.963	204.071** [0.000]
	333	0.570	36.605** (0.000)	2.330	0.994	1339.916** [0.000]
	343	0.536	11.550** (0.000)	2.009	0.942	133.395** [0.000]
FREUNDLICH	303	0.493	10.820** (0.000)	-0.958	0.9358	117.083** [0.000]
	313	0.483	12.579 (0.000)	-0.696	0.9471	158.220** [0.000]
	323	0.402	10.049** (0.000)	-0.562	0.9265	100.978** [0.000]
	333	0.436	16.856** (0.000)	-0.500	0.9697	284.134** [0.000]
	343	0.730	6.748** (0.000)	-0.9705	0.8473	45.541** [0.000]
FLORY- HUGGINS	303	0.498	7.66** (0.000)	-0.012	0.8803	58.812** [0.000]
	313	0.812	10.701** (0.000)	-0.074	0.9347	114.511** [0.000]
	323	1.76	9.272** (0.000)	-0.462	0.9149	85.974** [0.000]
	333	1.109	28.352** (0.000)	-0.198	0.9901	803.857** [0.000]
	343	0.485	1.789* (0.111)	-0.013	0.2857	3.201* [0.111]
FRUMKIN	303	-1.054	0.016** (0.988)	3.344	0.532	0.000* [0.988]
	313	-1.317	0.981** (0.340)	4.470	0.148	0.963** [0.340]
	323	-1.007	2.196** (0.041)	3.731	0.165	4.822** [0.041]
	333	5.230	3.414** (0.003)	-16.24	0.658	11.656** [0.003]
	343	0.694	2.089** (0.051)	-1.570	0.228	4.363** [0.051]

** - 1% level of significane: * - 5% level of significance

Analysing the values of F, the following table were arrived at and the adsorption models which were followed by studied inhibitors are presented in the table- 27 The highest values of F were highlighted in the Tables - 27.

Table -27 The results of Statistical SPSS 17 package on adsorption isotherms and the various adsorption models obeyed by the investigated inhibitors and their highest F values and corresponding R^2 values

INHIBITOR	MODELS (Highest F value)	Highest value of F		R^2	
		H_2SO_4	HCl	H_2SO_4	HCl
P2I	Temkin	1229.843	927.522	0.993	0.992
TMP2I	Temkin	1093.433	-	0.995	-
	Langmuir	-	330.514	-	0.976
DMP2I	Temkin	285.476	459.892	0.973	0.984
OCP2I	Langmuir	600.97	484.475	0.967	0.985
PNDMP2I	Langmuir	171.899	771.809	0.954	0.989
PNP2I	Langmuir	1637.887	2465.46	0.996	0.997

From the tables - 27 it could be noticed that Langmuir, Temkin and Freundlich models were found to have highest R^2 when compared to the other models . The highest R^2 indicates best fit of the model. This was supported by significant F value at 1% level of significance. From statistical analysis P2I obeys Temkin model, TMP2I obeys Langmuir and Temkin models, DMP2I obeys Temkin Model, OCP2I, PNDMP2I, PNP2I obeys Langmuir models. The obeyed adsorption isotherms for the investigated inhibitors are further explained

Temkin Adsorption Model for P2I , DMP2I and TMP2I:

From the statistical analysis it has been found that P2I and DMP2I obey **Temkin adsorption** model in both acidic media, TMP2I obeys Temkin adsorption in H_2SO_4. Straight lines were obtained indicating that the adsorption of the additives onto mild steel surface can be approximated using Temkin adsorption isotherm given as in equation (7)

$$\theta = (1/f \ \ln K_{ads} C) \text{ -------- } (7)$$

'f ' can be calculated from the slope, (f =2a) where 'a' is the slope.

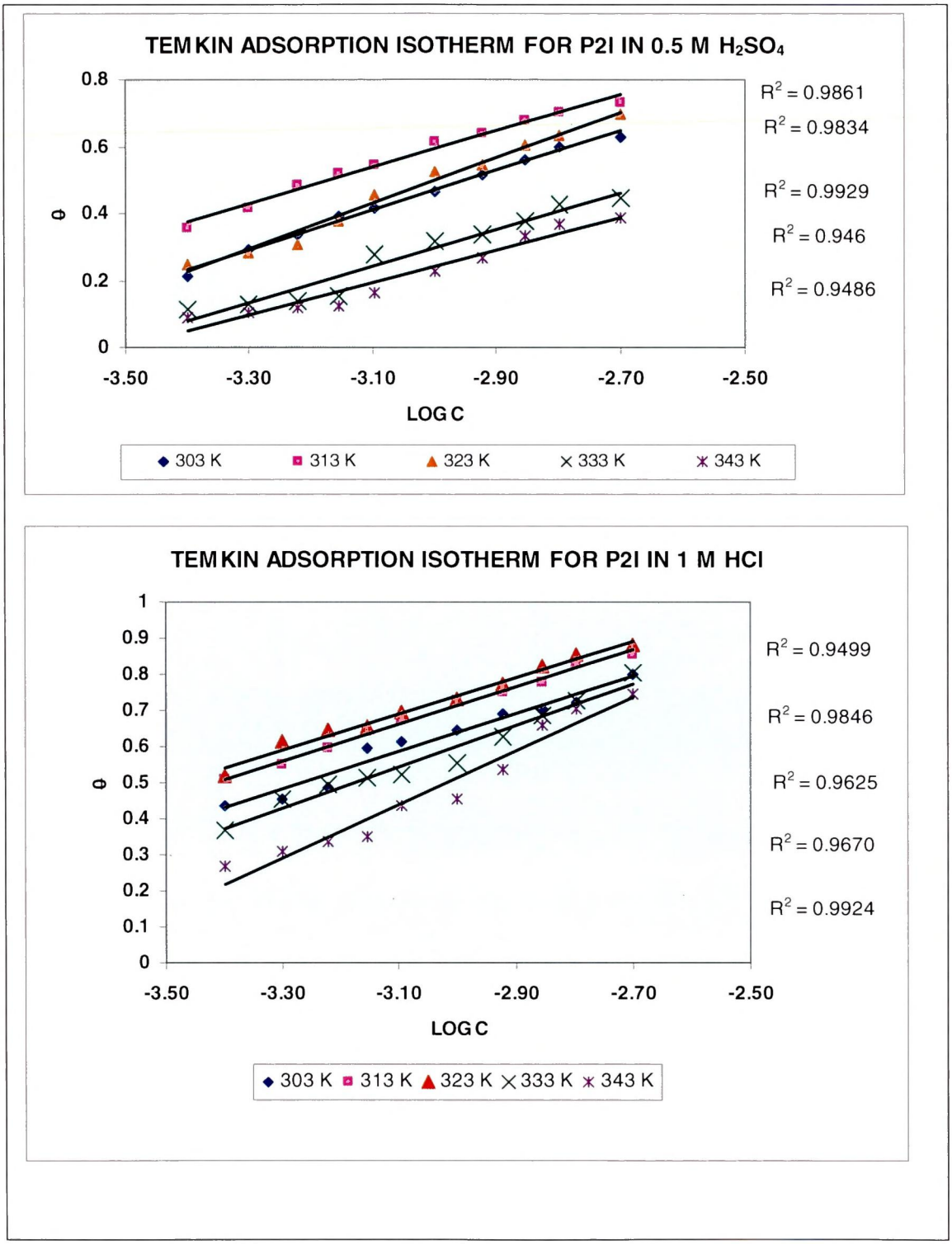
TEMKIN ADSORPTION ISOTHERM FOR P2I IN 0.5 M H_2SO_4
0.8
0.6
0.4
0.2
0
θ
-3.50
-3.30
-3.10
-2.90
-2.70
-2.50
LOG C
R^2 = 0.9861
R^2 = 0.9834
R^2 = 0.9929
R^2 = 0.946
R^2 = 0.9486
303 K
313 K
323 K
333 K
343 K
TEMKIN ADSORPTION ISOTHERM FOR P2I IN 1 M HCl
1
0.9
0.8
0.7
0.6
0.5
0.4
0.3
0.2
0.1
0
θ
-3.50
-3.30
-3.10
-2.90
-2.70
-2.50
LOG C
R^2 = 0.9499
R^2 = 0.9846
R^2 = 0.9625
R^2 = 0.9670
R^2 = 0.9924
303 K
313 K
323 K
333 K
343 K

Figure – 35

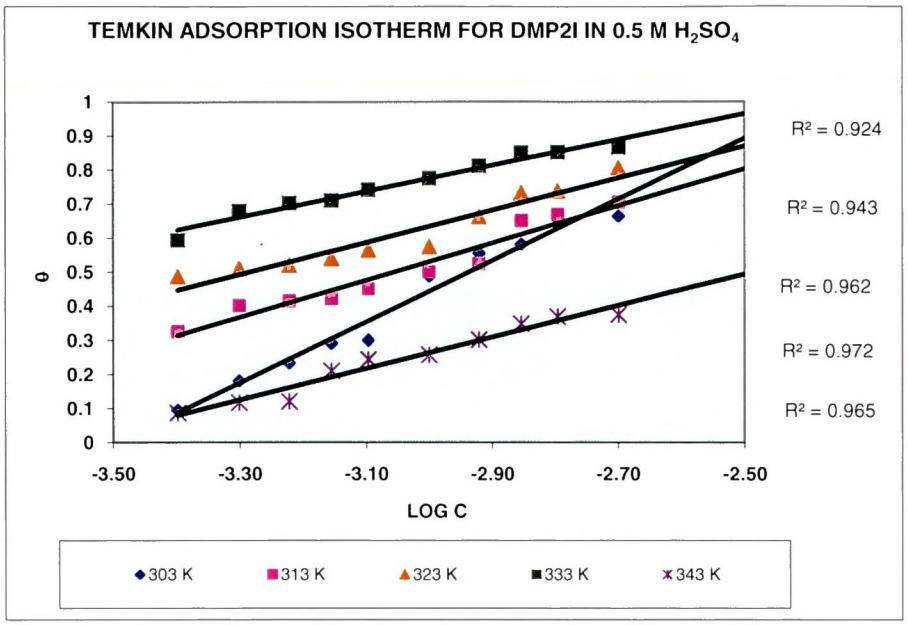
TEMKIN ADSORPTION ISOTHERM FOR DMP2I IN 0.5 M H_2SO_4
θ
LOG C
1
0.9
0.8
0.7
0.6
0.5
0.4
0.3
0.2
0.1
0
-3.50
-3.30
-3.10
-2.90
-2.70
-2.50
R² = 0.924
R² = 0.943
R² = 0.962
R² = 0.972
R² = 0.965
303 K
313 K
323 K
333 K
343 K

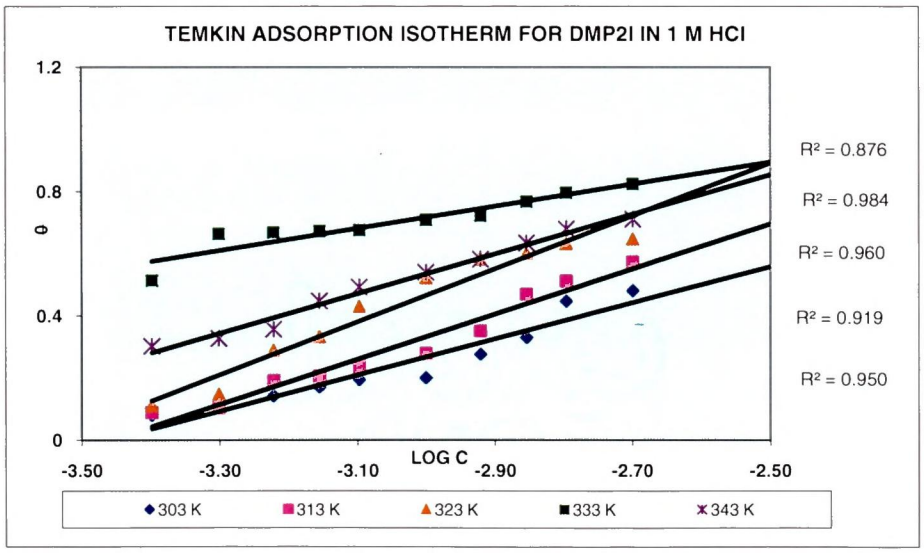
TEMKIN ADSORPTION ISOTHERM FOR DMP2I IN 1 M HCl
θ
LOG C
1.2
0.8
0.4
0
-3.50
-3.30
-3.10
-2.90
-2.70
-2.50
R² = 0.876
R² = 0.984
R² = 0.960
R² = 0.919
R² = 0.950
303 K
313 K
323 K
333 K
343 K

Figure – 36

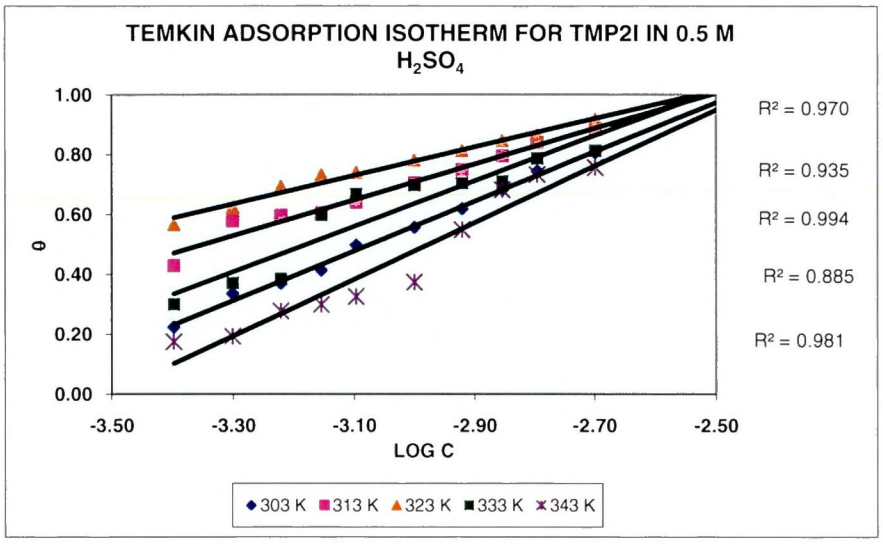

Figure – 37

Temkin adsorption isotherm fitted well to the experimental data for P2I, DMP2I in both acidic media and TMP2I in sulphuric acid medium.

The molecular interaction constant *f* were calculated and listed in Table – 28

Table - 28 Deduced adsorption parameters of mild steel in P2I, TMP2I, DMP2I using Temkin Adsorption Isotherm

Temkin Adsopriton	Medium	Molecular constant - f				
		303	313	323	333	343
P2I	H_2SO_4	1.18	1.09	1.35	1.09	0.96
	HCl	1.04	1.02	0.99	1.14	1.48
DMP2I	H_2SO_4	1.79	1.08	0.94	0.75	0.92
	HCl	1.16	1.45	1.70	0.71	1.27
TMP2I	H_2SO_4	1.65	1.19	0.94	1.51	1.88

It was reported that the constant *f* depends on the intermolecular interaction in the adsorbed layer and on the heterogeneity of the surface. If *f* is positive, mutual attraction of molecules occur and if *f* is negative repulsion takes place. The positive and rather high values of molecular interaction constant indicate the existence of a strong attractive interaction between adsorbed inhibitor in the adsorbed layer. The highest value of f reflects the high mutual attraction of the inhibitor on the iron surface and this results in strong adsorption. (**Morad 2008).**

Langmuir Adsorption model for OCP2I, PNDMP2I, PNP2I and TMP2I:

Analysis of the results of statistical data it has been found that OCP2I, PNDMP2I and PNP2I were best decribed by Langmuir adsorption isotherm model in both acidic media. TMP2I can also be ascribed by Langmuir adsorption isotherm model in H_2SO_4 medium.

4.2.4.1 Langmuir Adsorption Isotherm:

Langmuir adsorption equation relates degree of surface coverage to concentration of inhibitor according to equation (1)

$$\text{Log } (C/\theta) = \log K + \log C \quad \text{--------- (1)}$$

A plot of log $(\theta/1-\theta)$ versus log C from weight loss data obtained for imidazoline derivatives yielded straight lines as represented in Figure – (38, 39,40) .

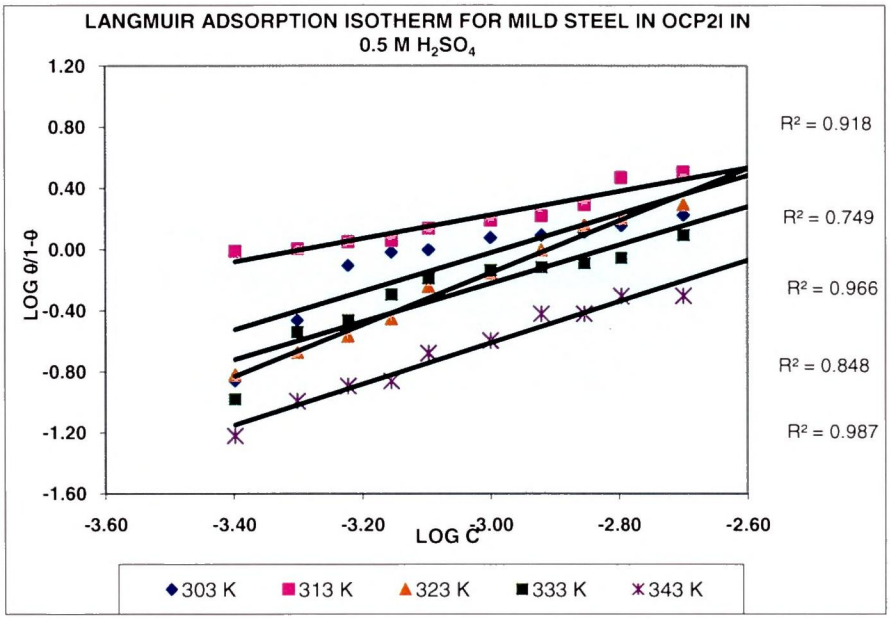

Figure-38

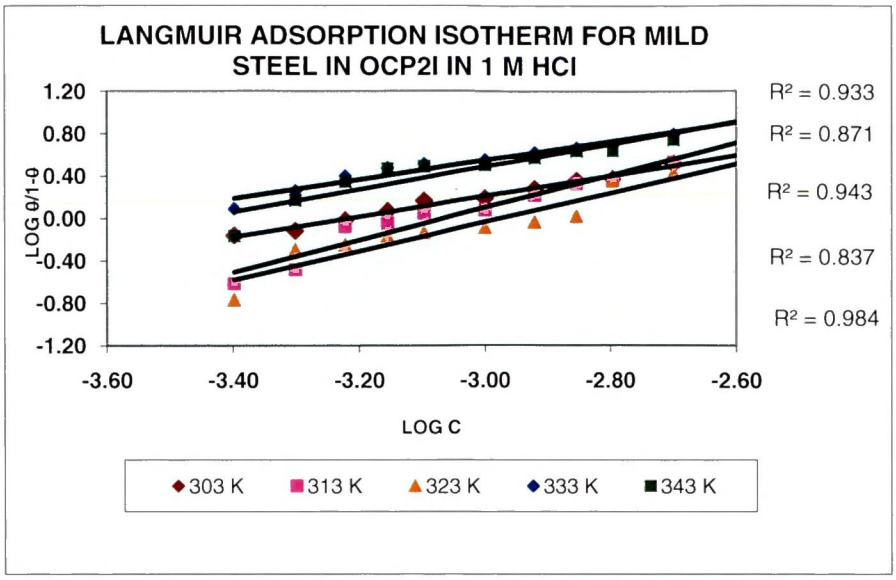

Figure – 39

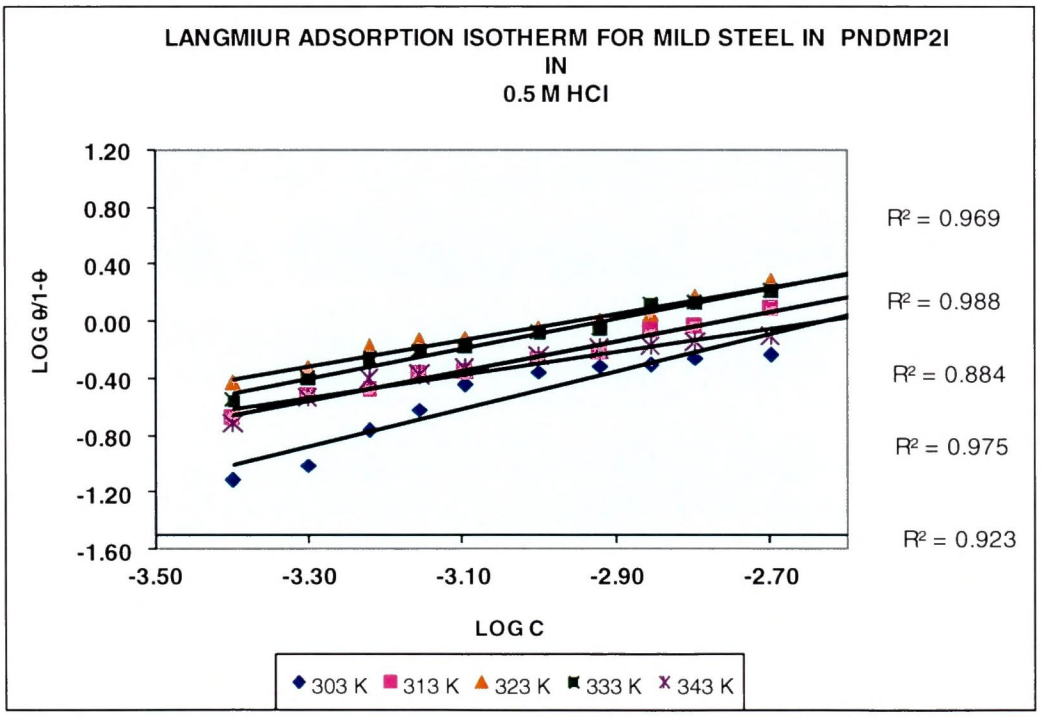

Figure - 40

The slope deviates from unity. This deviation may be explained on the basis of the interaction among adsorbed species on the metal surface. It has been postulated in the derivation of Langmuir adsorption isotherm equation that adsorbed molecules do not interact with one another, but this is not the case of large organic molecules

having polar atoms (or) groups which can adsorbed on the cathodic and anodic sites of the metal surface Such adsorbed species interact by mutual repulsion or attraction **(Eddy *et al.*, 2010 , Solomon *et al.*, 2010).**

4.2.4.2 El – awady et al., Thermodynamic – Kinetic isotherm model :

The adsorption isotherm relationship of El awady et al.., a thermodynamic-kinetic model which is given by the following equation:

$$\log [\theta/(1-\theta)] = \log K' + y \log C.$$

Where θ is the degree of coverage, x is the number of active sites.

Surface coverage (θ) data are very useful while discussing adsorption characteristics. For an inhibitor to have a high surface coverage on the surface, a chemical bond between the inhibitor and the metal atom stronger than the one for water molecules should be formed. The adsorption therefore of corrosion inhibitors at the metal/solution interface may be due to the formation of either electrostatic or covalent bonding between the adsorbates and the metal surface atoms.

'x' is the number of inhibitor molecules occupying one active site (or the number of water molecules replaced by one molecule (1/y = x). The calculated values of 'x' for all the studied inhibitors are given in Table-29 . Inspection of the data shows that the values 'x' are less than one and are approximately equal to one mean that a given inhibitor molecule will occupy more than one active site. Values indicate that the imidazoline molecules occupy more than one active site.

Table – 29 Deduced adsorption parameter using El Awady tthermodynamic-kinetic model

El Awady		x=1/y				
Inhibitor	Medium	303 K	313 K	323 K	333 K	343 K
P2I	H_2SO_4	0.9	1.0	0.8	0.8	0.8
	HCl	1.0	0.9	0.9	0.9	0.7
TMP2I	H_2SO_4	0.6	0.9	0.8	0.7	0.4
	HCl	1.0	0.9	0.9	0.9	0.7
DMP2I	H_2SO_4	0.5	1.0	1.1	1.1	0.8
	HCl	0.7	0.6	0.6	1.3	0.9
OCP2I	H_2SO_4	0.8	1.3	0.6	0.8	0.7
	HCl	1.1	0.7	0.7	1.1	0.9
PNDMP2I	H_2SO_4	0.9	0.7	1.0	1.2	1.1
	HCl	0.8	1.0	1.1	1.0	1.2
PNP2I	H_2SO_4	1.3	1.3	1.1	1.1	1.0
	HCl	1.3	1.1	1.1	0.9	0.9

4.2.4.3 Freundlich isotherm

To ascertain the nature of the adsorption values for imidazoline derivatives are fitted into Freundlich isotherm which is plot of ln θ Vs ln C.

Freundlich isotherm can be written as $\theta = K C^{1/n}$

Where 'n' is the adsorption intensity, 'C' is the inhibitor concentration and 'K' is the equilibrium constant of adsorption reaction

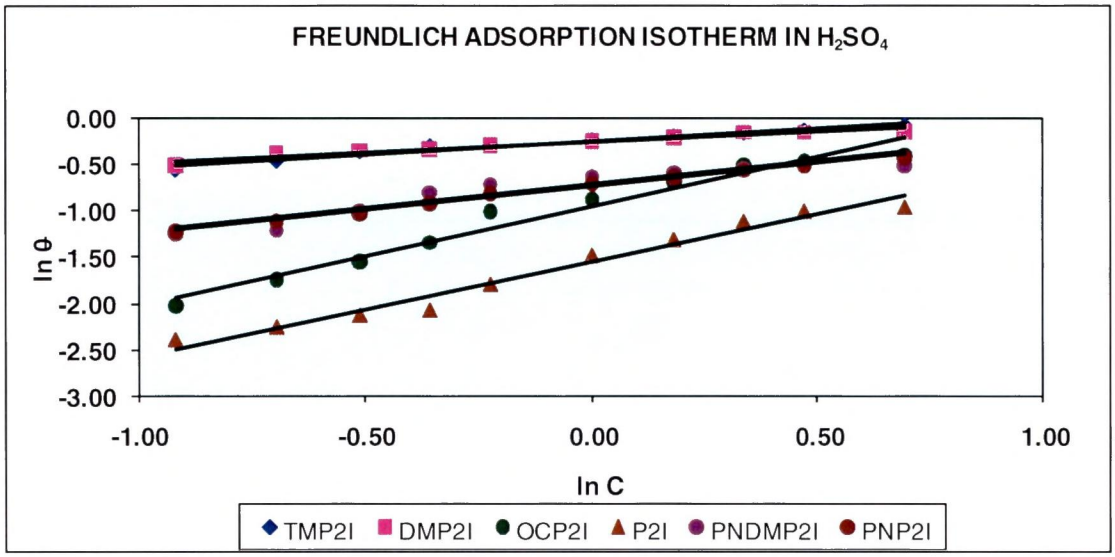

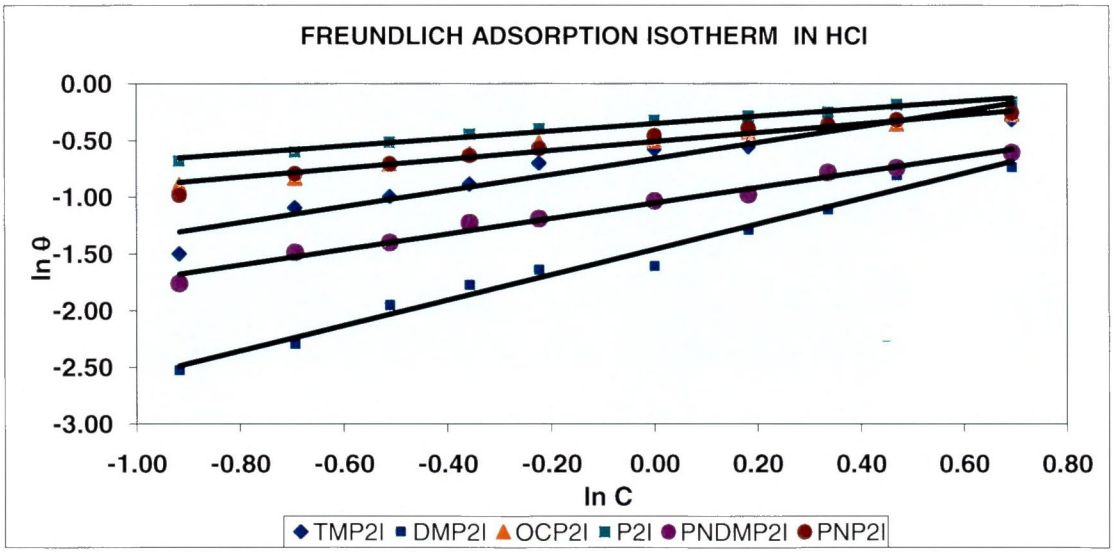

Figure - 42

The observed changes in θ are shown in Figure-41-42. The linear plots obtained (R^2 = 1) suggest that the experimental data fit the Freundlich adsorption isotherm. Though a straight line was obtained for the studied inhibitors for Freundlich adsorption isotherm, the statistical 'F' value for Freundlich adsorption isotherm is

low compared to Langmuir and Temkin adsorption isotherm. Therefore the best obeyed model for all the investigated models are Langmuir and Temkin adsorption isotherms.

4.2.4.4 Flory- Huggins Isotherm & Frumkin Adsorption Isotherm:

Surface coverage data are quite useful in determining inhibitor adsorption characteristics. Flory –Huggins isotherm was also tested for its fit to the experimental data obtained from the weight loss measurement. The characteristic of Flory-Huggins adsorption isotherm is given by equation (4).

$$\log (\theta/C) = \log K + x \log (1-\theta) \text{ --------- (4)}$$

Where 'θ' is the degree of surface coverage, 'C' is the concentration of the system studied, 'x' is the number of water molecule replaced by one inhibitor molecules and 'K' is the equilibrium constant for the adsorption process.

The number of acitive sites x is approximately constant and equal to one under all conditions studied. This means that the inhibitor molecule adsorbs displacing one water molecule.

Since the R^2 values and Fvalues are very less and in the case of the investigated inhibitors it can be concluded that they donot obey Flroy-Huggins and Frumkin adsorption isotherms.

4.2.5 Corrosion Kinetic Parameters

The apparent acitivation for the corrosion process is calculated from Arrhenius type plot according to the following equation:

$$\log CR = k \exp(-E_a/RT) \quad \text{- - - - - - - (5)}$$

where E_a is the apparent activation corrosion energy, R is the universal gas constant

($R = 8.314\ Jmol^{-1}K^{-1}$) , k is the Arrhenius pre-exponential constant and T is the absolute temperature.

Values of E_a for mild steel with the absence and presence of various concentrations of imidazolie derivatives were determined from the slope of log CR Vs 1/T plots and presented in tables – 30 a and 30 b.

Table – 30 a Apparent activation energy for the corrosion of mild steel in H_2SO_4 in the absence and presence of different concentration of imidazoline derivatives

Conc	Ea kJ/mol H_2SO_4					
in ppm	OCP2I	TMP2I	PNDM2I	DMP2I	P2I	PNP2I
Blank	62.12	62.12	62.12	62.12	62.12	62.12
40	65.71	64.49	57.64	57.32	67.21	48.58
50	66.8	68.41	59.2	57.41	69.58	48.62
60	71.52	67.58	60.48	58.02	71.29	47.49
70	72.1	64.66	59.68	57.47	73.06	45.65
80	71.38	65.81	61.49	56.38	71.94	45.65
100	74.29	67.88	60.99	61.22	73.17	45.07
120	71.42	63.03	60.98	61.4	74.1	45.99
140	72.41	63.5	61.09	61.75	74.83	44.5
160	74.16	59.62	61.83	64.97	76.64	44.28
200	74.75	58.98	63.7	65.13	76.64	42.64
Average	71.45	64.4	60.71	60.11	72.85	45.85

Table – 30 b Apparent activation energy for the corrosion of mild steel in HCl in the absence and presence of different concentration of imidazoline derivatives

Conc	Ea kJ/mol HCl					
in ppm	OCP2I	TMP2I	PNDM2I	DMP2I	P2I	PNP2I
Blank	48.55	48.55	48.55	48.55	48.55	48.55
40	43.76	41.79	46.19	38.32	54.96	57.56
50	36.31	41.26	44.98	34.94	53.87	57.12
60	34.64	40.2	44.05	59.5	55.64	57.26
70	32.14	47.1	44.78	33.72	59.21	55.34
80	34.19	45.87	45.92	32.95	58.08	54.66
100	33.99	39.23	45.64	30.88	59.91	52.77
120	34.64	28.5	45.33	31.47	58.52	52.18
140	35.43	29.06	44.54	30.66	53.77	51.22
160	35.45	24.76	44.8	31.28	53.31	48.69
200	37.06	21.31	44.53	30.54	54.49	46.25
Average	43.76	35.91	45.08	45.43	52.17	53.3

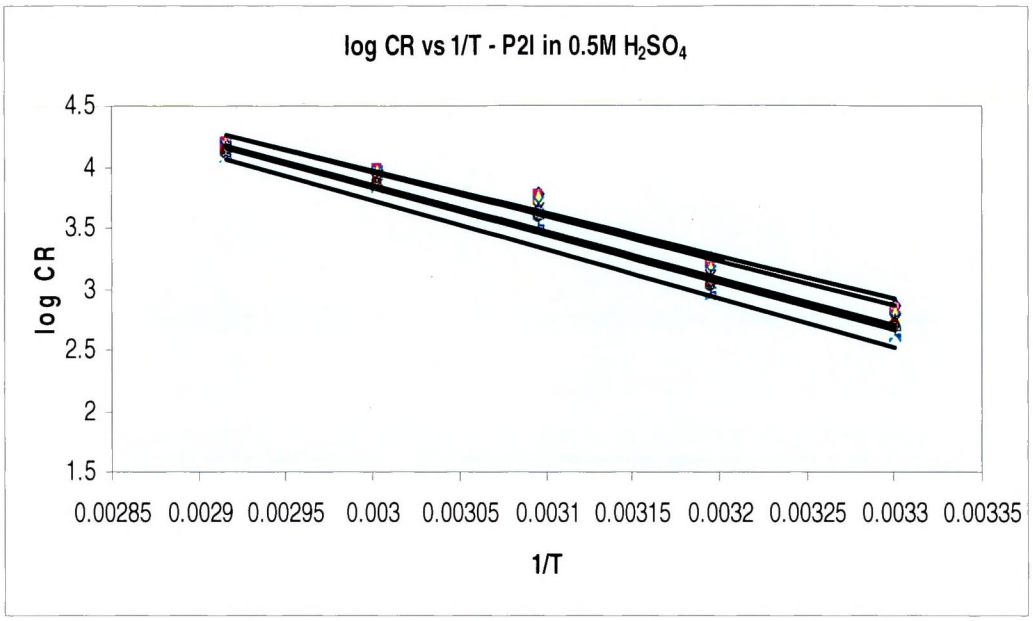
log CR vs 1/T - P2I in 0.5M H_2SO_4
log CR
4.5
4
3.5
3
2.5
2
1.5
0.00285 0.0029 0.00295 0.003 0.00305 0.0031 0.00315 0.0032 0.00325 0.0033 0.00335
1/T

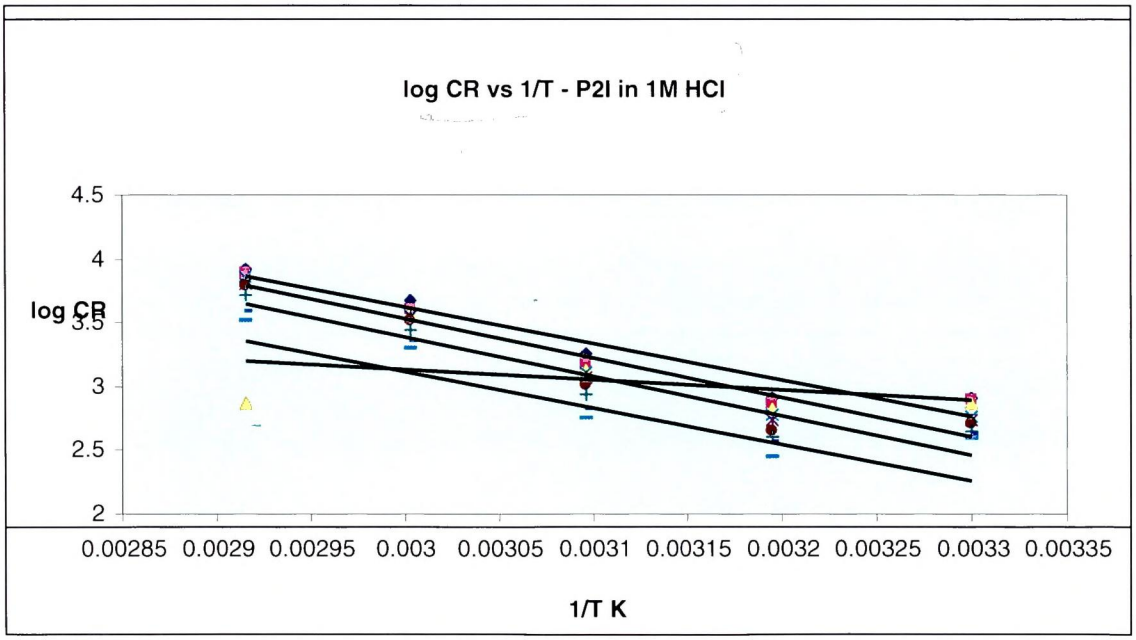
log CR vs 1/T - P2I in 1M HCl
log CR
4.5
4
3.5
3
2.5
2
0.00285 0.0029 0.00295 0.003 0.00305 0.0031 0.00315 0.0032 0.00325 0.0033 0.00335
1/T K

Figure - 43

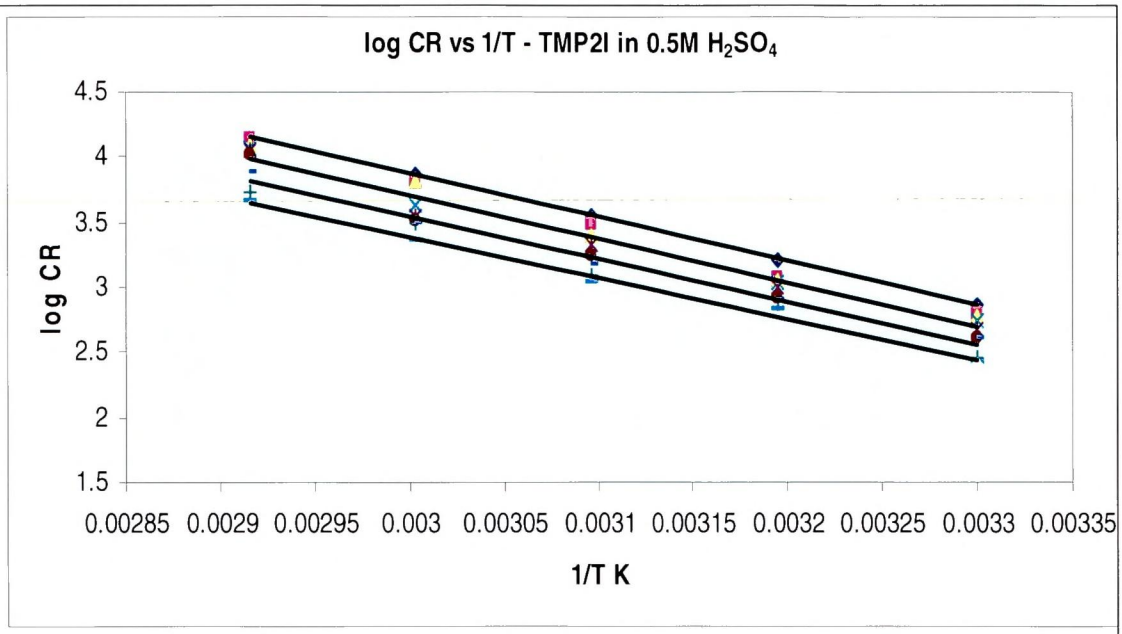
log CR vs 1/T - TMP2I in 0.5M H_2SO_4
log CR
4.5
4
3.5
3
2.5
2
1.5
0.00285 0.0029 0.00295 0.003 0.00305 0.0031 0.00315 0.0032 0.00325 0.0033 0.00335
1/T K

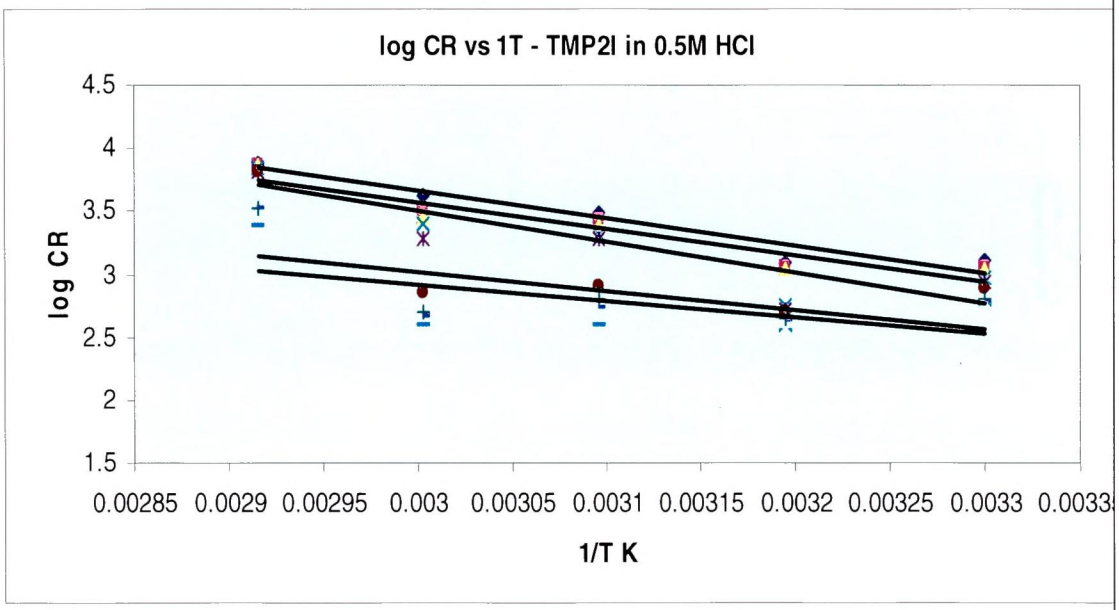
log CR vs 1T - TMP2I in 0.5M HCl
log CR
4.5
4
3.5
3
2.5
2
1.5
0.00285 0.0029 0.00295 0.003 0.00305 0.0031 0.00315 0.0032 0.00325 0.0033
1/T K

Figure - 44

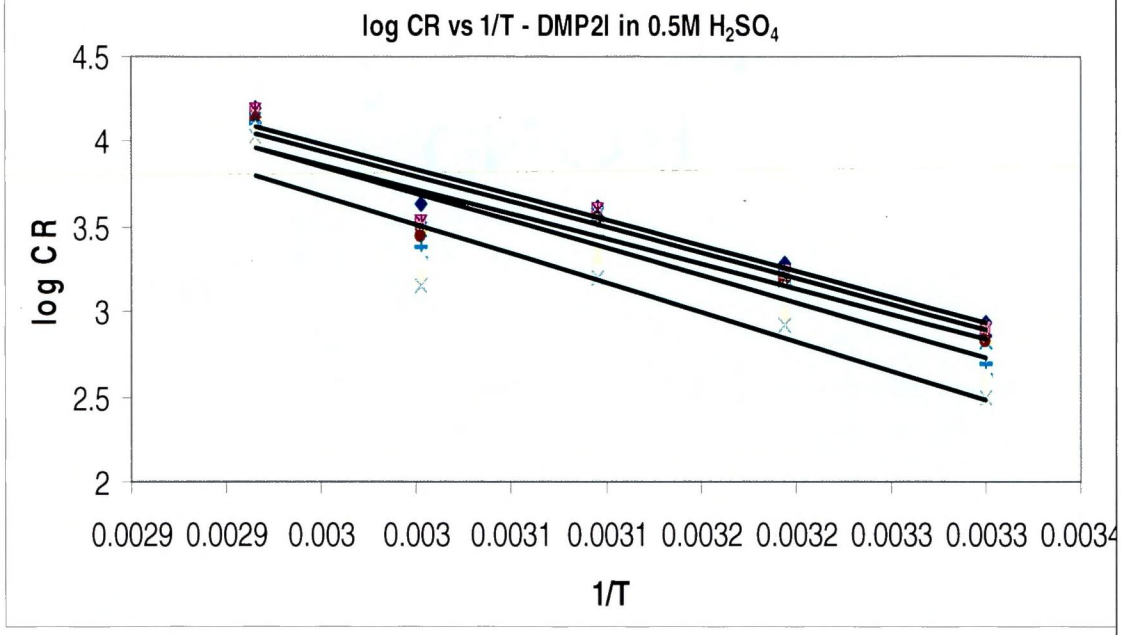
log CR vs 1/T - DMP2I in 0.5M H_2SO_4
log CR
4.5
4
3.5
3
2.5
2
0.0029 0.0029 0.003 0.003 0.0031 0.0031 0.0032 0.0032 0.0033 0.0033 0.0034
1/T

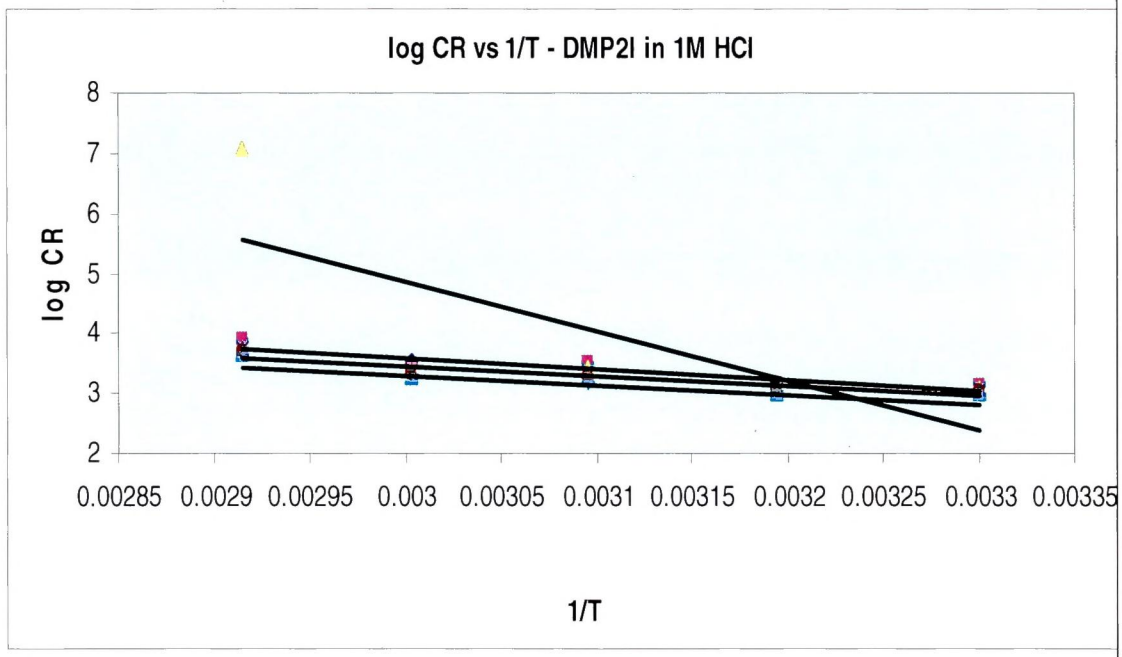
log CR vs 1/T - DMP2I in 1M HCl
log CR
8
7
6
5
4
3
2
0.00285 0.0029 0.00295 0.003 0.00305 0.0031 0.00315 0.0032 0.00325 0.0033 0.00335
1/T

Figure - 45

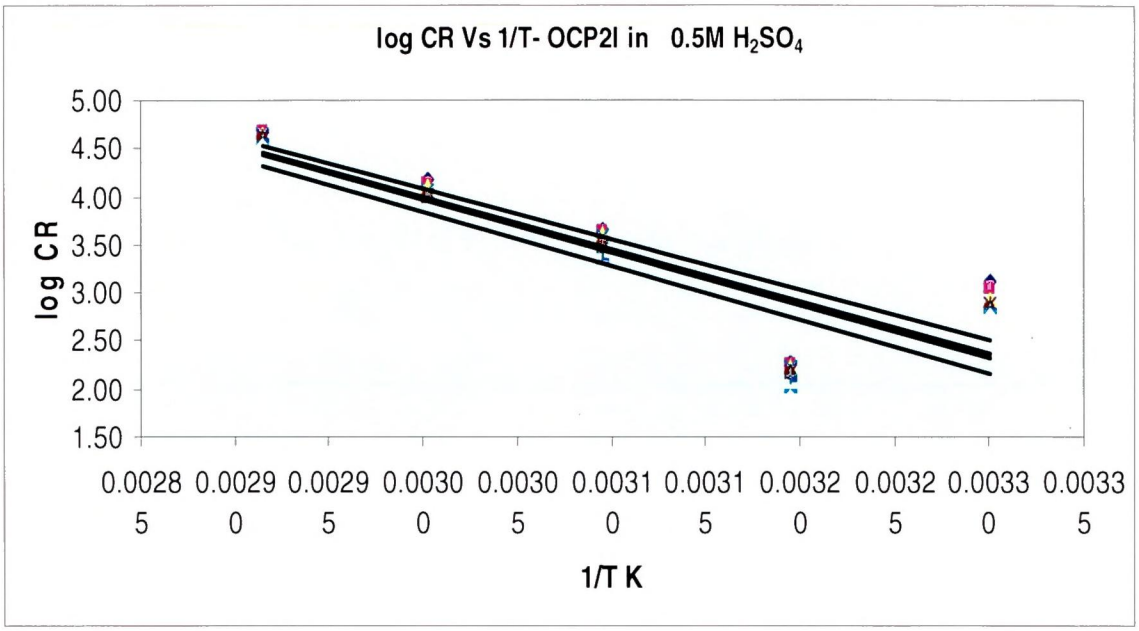
log CR Vs 1/T- OCP2l in 0.5M H_2SO_4
log CR
5.00
4.50
4.00
3.50
3.00
2.50
2.00
1.50
0.00285 0.00290 0.00295 0.00300 0.00305 0.00310 0.00315 0.00320 0.00325 0.00330 0.00335
1/T K

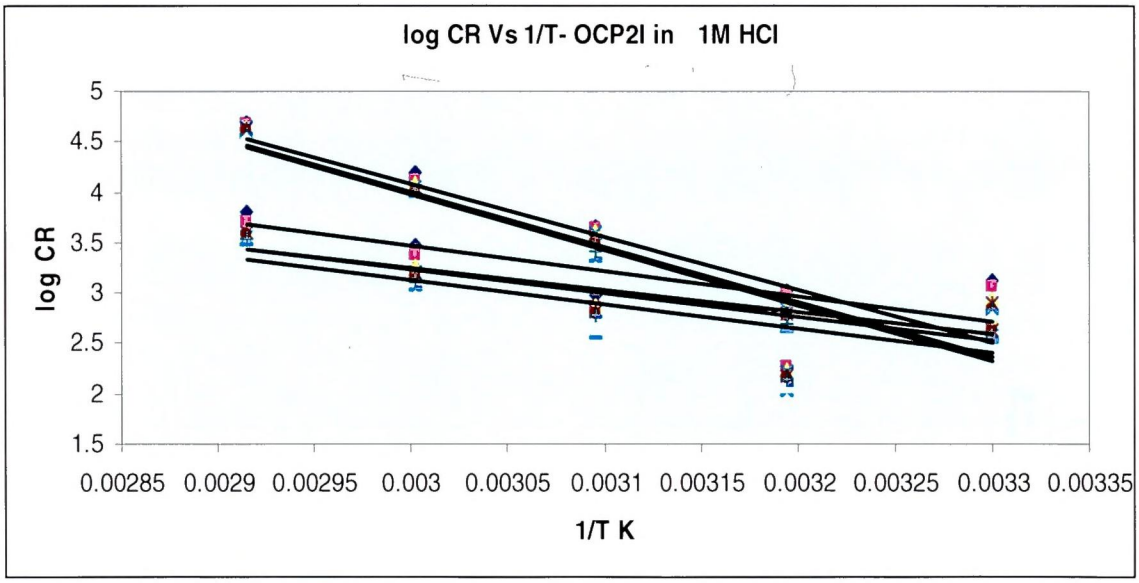
log CR Vs 1/T- OCP2l in 1M HCl
log CR
5
4.5
4
3.5
3
2.5
2
1.5
0.00285 0.0029 0.00295 0.003 0.00305 0.0031 0.00315 0.0032 0.00325 0.0033 0.00335
1/T K

Figure - 46

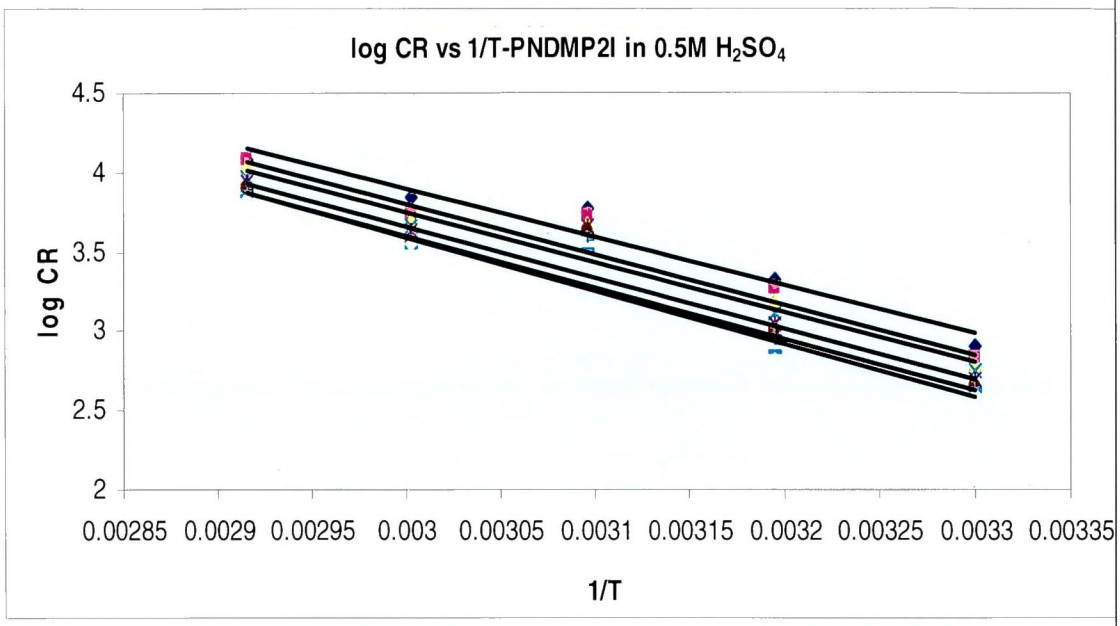
log CR vs 1/T-PNDMP2I in 0.5M H_2SO_4
4.5
4
3.5
3
2.5
2
log CR
0.00285 0.0029 0.00295 0.003 0.00305 0.0031 0.00315 0.0032 0.00325 0.0033 0.00335
1/T

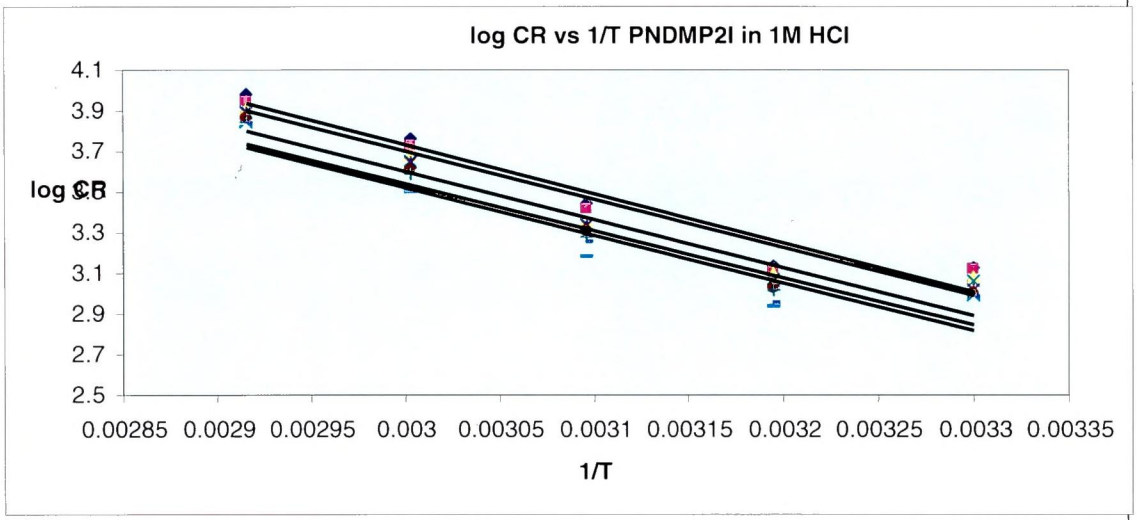
log CR vs 1/T PNDMP2I in 1M HCl
4.1
3.9
3.7
3.5
3.3
3.1
2.9
2.7
2.5
log CR
0.00285 0.0029 0.00295 0.003 0.00305 0.0031 0.00315 0.0032 0.00325 0.0033 0.00335
1/T

Figure - 47

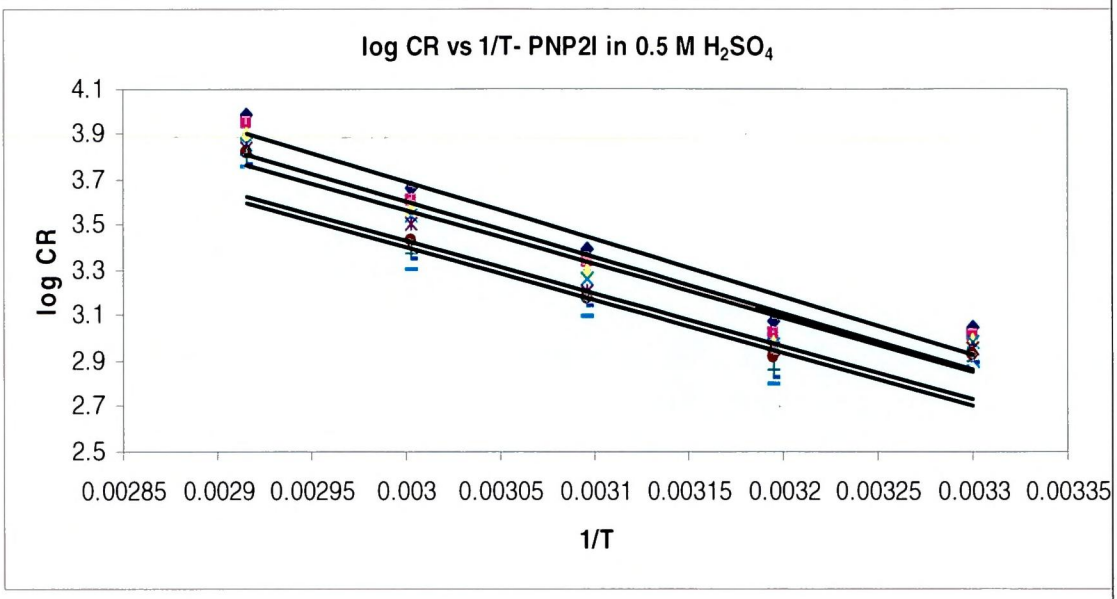
log CR vs 1/T- PNP2I in 0.5 M H_2SO_4
log CR
4.1
3.9
3.7
3.5
3.3
3.1
2.9
2.7
2.5
0.00285 0.0029 0.00295 0.003 0.00305 0.0031 0.00315 0.0032 0.00325 0.0033 0.00335
1/T

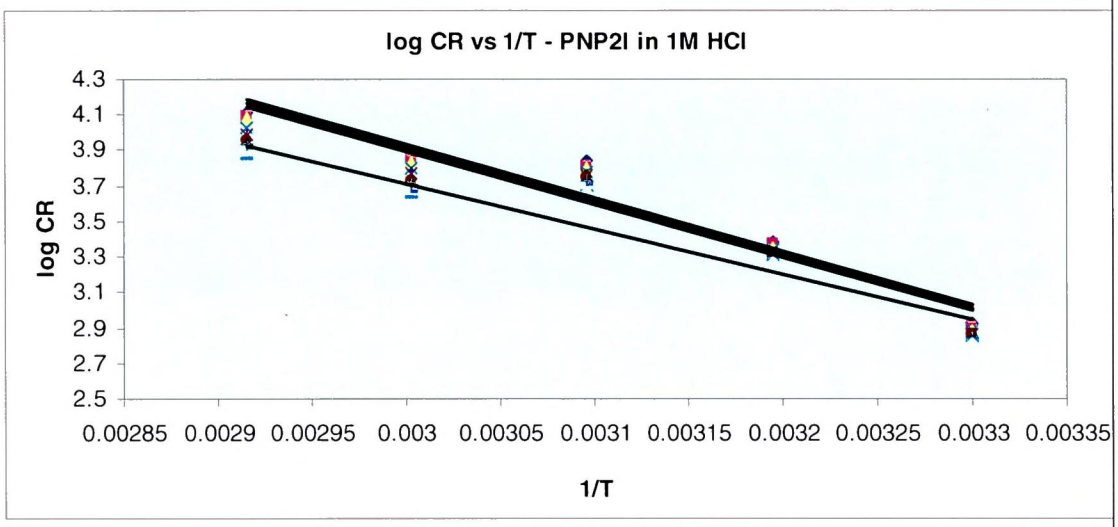
log CR vs 1/T - PNP2I in 1M HCl
log CR
4.3
4.1
3.9
3.7
3.5
3.3
3.1
2.9
2.7
2.5
0.00285 0.0029 0.00295 0.003 0.00305 0.0031 0.00315 0.0032 0.00325 0.0033 0.00335
1/T

Figure – 48

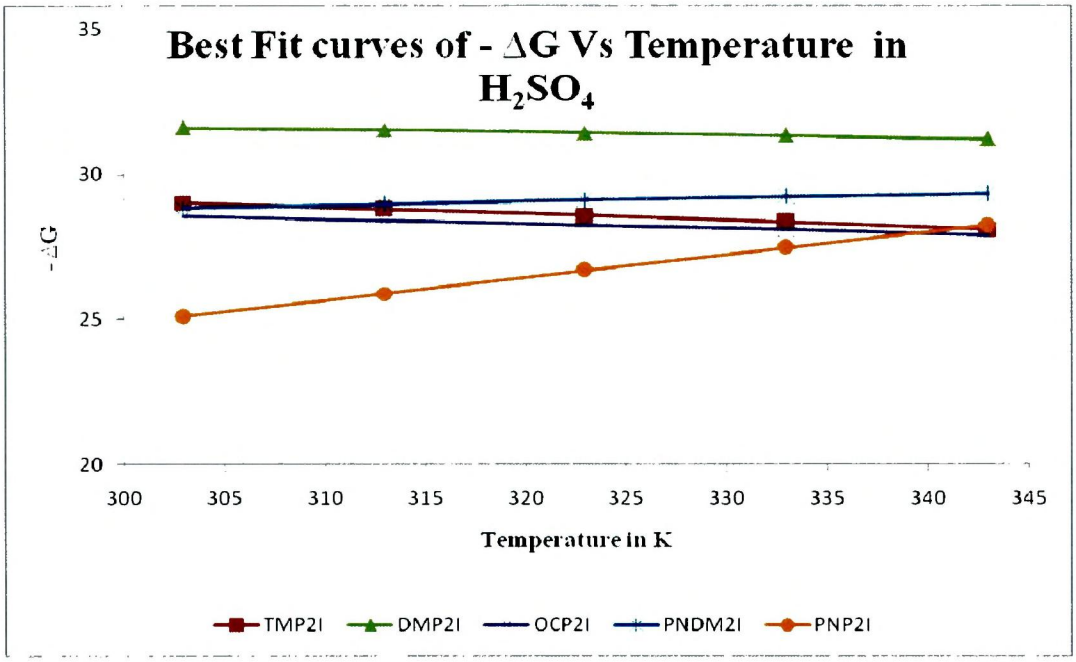

Figure -49

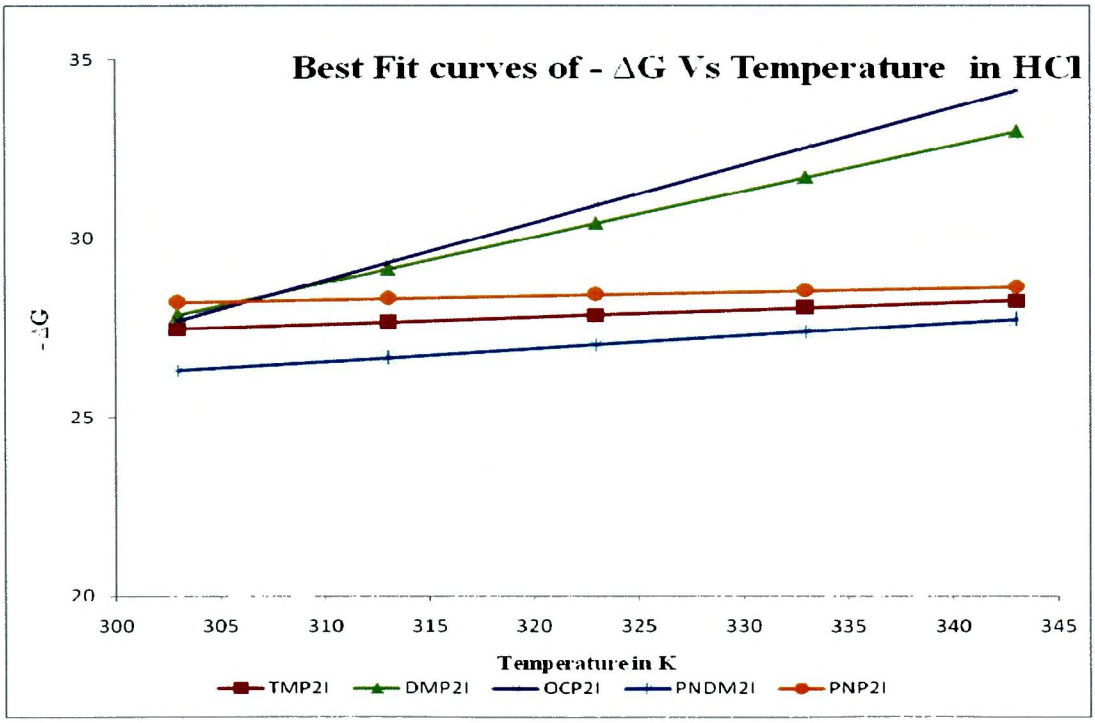

Figure - 50

- Linear plots were obtained, from the slope ($-E_a/2.303R$), activation energy (E_a) values are deduced and listed in Table 30 a, 30 b. The temperature dependence of the inhibiting effect and the comparison of the values of the apparent activation energy of the corrosion process in the absence and presence of inhibitors can provide further evidence concerning the mechanism of the inhibiting action.
- The decrease of the inhibitor efficiency with temperature rise, which refers to a higher value of E_a, when compared to that in an acid with no inhibitor, is interpreted as an indication for an electrostatic character of the inhibitor's adsorption.

  Unchanged or lower values of E_a in inhibited systems compared to the blank have been reported to be indicative of chemisorption mechanism, whereas higher values of E_a suggest a physical adsorption mechanism.
- Investigation of the results presented in the Table infer that the H_2SO_4 medium, OCP2I, TMP2I and P2I inhibitor systems furnish high E_a values compared to the blank. PNDMP2I, DMP2I and PNP2I inhibitor systems could give low E_a values compared to the blank.

  The results of E_a for the inhibitor system studies in HCl revealed a low E_a values for OCP2I, TMP2I, PNDMP2I and DMP2I and high E_a values for P2I and PNP2I systems.

  Experiments conducted by Bag *et al.,* (1996) also reflected lower E_a values for the inhibited systems. Studies carried out by Taha *et al.,* (1995) revealed the presence of inhibitors decreased the Ea of the reaction to an extent depending on the nature of inhibitor.
- The lower value of E_a in an inhibited solution when compared to that of an uninhibited one shows that strong chemisorption bond between the inhibitor and the metal is highly probable. Ea values were higher than that in its absence (blank).

  The higher values of E_a in the inhibited solution can be correlated with the increased thickness of the double layer, which enhances the activation energy of the corrosion process. The increase in activation

medium. All the estimated values of ΔG^{o}_{ads}, ΔH^{o}_{ads} and ΔS^{o}_{ads} were recorded and interpreted as follows:

ΔG^{o}_{ads}:

Figures 43-44 clearly shows the dependence of ΔG^{o}_{ads} on T, indicating the good correlation among thermodynamic parameters. The large and negative values **of** ΔG^{o}_{ads} ensure the spontaneity of the adsorption process and stability of the adsorbed layer on the steel surface.

The calculated value of ΔG^{o}_{ads} presented in table -31, are negative which indicate that the adsorption of inhibitor's molecules on the metal surface is a spontaneous process. As, observed, the studies inhibitors obey the general rule that the effectiveness of corrosion inhibition increases with increasing the negative value of ΔG^{o}_{ads}.

❖ Generally, values of ΔG^{o}_{ads} around -20 $kJmol^{-1}$ or lower are consistent with the electrostatic interaction between the charged molecules and the charged metal (physisorption); those around -40 $kJmol^{-1}$ or higher involve charge sharing or transfer from organic molecules to the metal surface to form a coordinate type of bond (chemisorption). In the present work, the calculated ΔG^{o}_{ads} values are almost slightly less negative than -40 $kJmol^{-1}$ ranging from -25 to 34 $kJmol^{-1}$ indicating that the adsorption of the inhibitor molecules is not merely physical or chemisorption but obeying a comprehensive adsorption (physical and chemical adsorption). **(Obi-Egbedi *et al.*, 2010).**

Table - 31 Thermodynamic adsorption parameters for mild steel/ inhibitors in H_2SO_4 and HCl systems at different temperatures – ($-\Delta G$)

INHIBITOR	- ΔG kJ/mol									
	H_2SO_4					HCl				
	303	313	323	333	343	303	313	323	333	343
P2I	27.98	29.41	28.28	25.81	25.02	29.96	30.91	31.29	29.53	28.46
TMP2I	27.87	29.47	29.47	28.91	27.01	26.6	28.88	27.87	27.87	28.09
DMP2I	30.02	31.5	32.81	34.82	27.88	27.77	28.61	30.34	33.94	31.5
OCP2I	27.3	29.82	28.19	28.74	27.02	28.71	28.87	29	33.73	34.31
PNDM2I	27.89	29.36	30.12	29.6	28.38	25.42	26.9	28.21	27.89	26.71
PNP2I	25.27	25.63	26.22	28.29	27.86	27.29	28.54	29.3	29.72	27.22

Table - 32 Enthalpy and entropy of adsorption for mild steel corrosion in H_2SO_4 and HCl in the absence and presence of inhibitors.

INHIBITOR	- ΔH kJ/mol		ΔS J/mol K	
	H_2SO_4	HCl	H_2SO_4	HCl
P2I	58.07	44.19	95.25	43.84
TMP2I	35.93	21.51	22.85	19.67
DMP2I	34.5	10.87	-9.58	127.91
OCP2I	33.52	20.97	16.43	160.69
PNDM2I	25.15	15.48	12.14	35.75
PNP2I	31.36	25.06	78.3	10.39

ΔH^{o}_{ads} and ΔS^{o}_{ads} :

The ΔH^{o}_{ads} values are negative for all studied inhibitors (Table – 32), suggests that the inhibitor molecules adsorption onto the metal surface are an exothermic process **(Noor *et al.*, 2007).**

The average values of ΔS^{o}_{ads} for the investigated inhibitors are positive and the positive sign of ΔS^{o}_{ads} arises from substitutional process, which can be attributed to the increase in the solvent entropy and more positive water desorption entropy. This leads to an increase in disorder due to the fact that more water molecules can be desorbed from the metal surface by one inhibitor molecule. **(Obi-egbedi *et al.*, 2010).**

4.3 Electrochemical Measurements

Evaluation of inhibition efficiency (%) can also be performed through electrochemical experiments. Electrochemical measurements were carried out using Electrochemical Analyser Solartron -1284 B. Linear Polarisation measurements, Tafel intercept and Electrochemical impedance measurements are carried out for mild steel acid corrosion in the presence of imidazoline derivatives to predict the nature of the inhibitor- anodic, cathodic or mixed type and to predict a suitable mechanism for inhibition process.

4.3.1. Potentiodynamic Polarization Studies

P2I:

Polarisation curves for mild steel at various concentrations of P2I are shown in Figure- 51 . The extrapolation of the Tafel straight line allows the calculation of the corrosion current density (I_{corr}). The values of I_{corr} , the corrosion potential (E_{corr}) and the Tafel slopes (b_a &b_c), IE(%) as function of P2I concentrations are recorded in Table-33.

Table – 33 Electrochemical parameters of mild steel at various concentrations of P2I in 0.5 M H_2SO_4 and 1 M HCl and corresponding inhibition efficiency values

ACID MEDIUM	Conc ppm	- E_{corr} mV/SCE	I_{corr} µA/cm^2	b_a mV/dec	b_c mV/dec	IE %	Rp ohm/cm^2	IE %
H_2SO_4	Blank	512	836.7	182	136	-	3.1	-
	40	523	753.7	213	164	9.9	3.5	10.1
	60	530	574.2	252	155	31.3	4.5	31.3
	80	527	538.5	245	150	35.6	5.2	39.8
	120	529	476.0	212	148	43.1	5.5	43.4
	160	530	446.3	187	135	46.6	6.2	49.7
	200	531	388.5	181	126	53.5	6.7	53.6
HCl	Blank	510	645.4	210	138	-	4.0	-
	40	514	385.9	153	133	40.2	6.8	40.1
	60	514	352.6	152	139	45.3	7.4	45.3
	80	515	345.9	148	138	46.4	8.7	53.6
	120	509	264.1	157	119	59.0	14.2	71.5
	160	502	168.8	149	110	73.8	15.6	74.1
	200	503	159.6	166	98	75.2	16.3	75.2

The analysis of these data shows that

the values of I_{corr} of mild steel in the inhibited solutions were smaller than those for the P2I-free solutions in both medium i.e. the addition of P2I decreases markedly by the corrosion current density. This behaviour reflects its ability to inhibit the corrosion of mild steel in both examined medium.

It has been found that the inhibition efficiency increased with inhibitor concentration and the corresponding efficiency values are 53.5% and 75.2% respectively in 0.5 M H_2SO_4 and 1 M HCl

The addition of P2I on acid corrosion of mild steel in both investigated acid medium, do not show any appreciable shift in E_{corr} values which imply that the analysed inhibitor acts as mixed type inhibitor and influences both metal dissolution and hydrogen evolution.

The polarization curves show that the P2I has an effect on both cathodic and anodic processes. This indicated a modification of the mechanism of cathodic hydrogen evolution and as well as anodic dissolution of iron, which suggest that P2I powerfully inhibits the corrosion process of mild steel and its ability as corrosion inhibitor is enhanced as its concentration is increased.

The values of the Tafel slopes b_a and b_c clearly indicate that both the cathodic and anodic reactions are inhibited thus reducing the corrosion on mild steel surface.

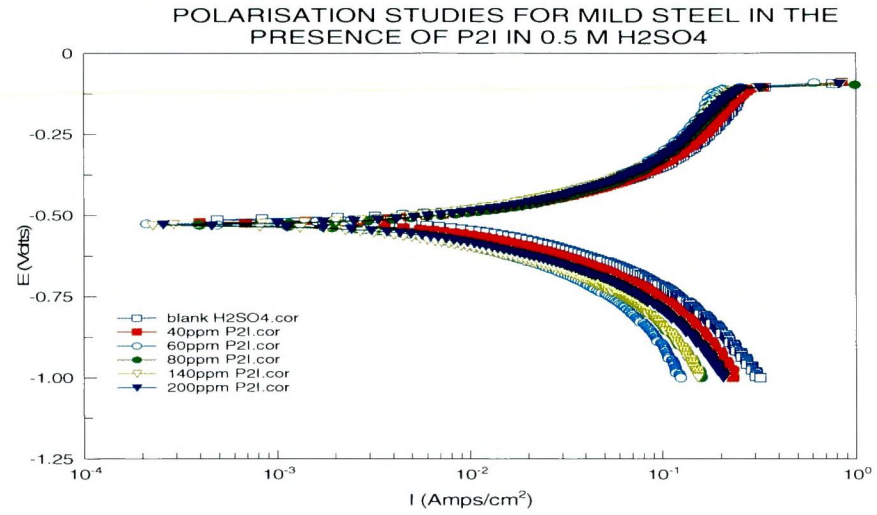

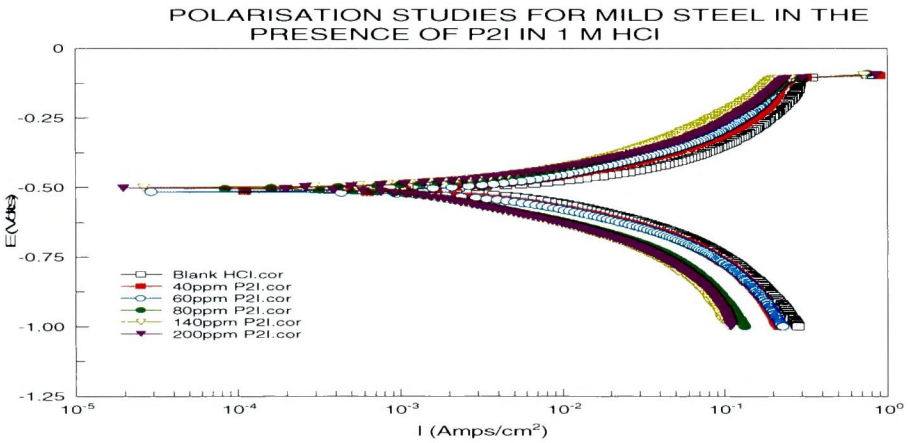

Figure – 51 Potentiodynamic curves for mild steel in 0.5 M H_2SO_4 and 1 M HCl in the presence of P2I

TMP2I :

The effect of concentration of TMP2I on the anodic and cathodic polarization behaviour of mild steel in both studied acidic media has been carried out by polarization measurements and the recorded Tafel plots are shown in Figure - 52 . The respective kinetic parameters deirived from the above plots are listed in Table- 34

The examination of Figure – 52 and Table - 34 show that

- the addition of the studied inhibitor decreases the corrosion current density (I_{corr}) values of mild steel .The decrease is more pronounced with the increase of the inhibitor concentration furnishing maximum inhibition efficiency of 89.7% in 0.5M H_2SO_4 and 91.7% in 1M HCl.
- E_{corr} values do not remarkably shift in the present system and hence, can be said to be a mixed-type inhibitor.
- The anodic Tafel slopes changes slightly whereas the change in cathodic Tafel slopes are larger which means the TMP2I molecules are adsorbed on both sites but under predominently cathodic control resulting in inhibition of anodic dissolution and as well as cathodic reduction reaction.

Table - 34 Electrochemical parameters of mild steel at various concentrations of TMP2I in 0.5 M H_2SO_4 and 1 M HCl and corresponding inhibition efficiencyvalues

ACID MEDIUM	Conc ppm	$-E_{corr}$ mV/SCE	I_{corr} mA/cm^2	ba mV/dec	bc mV/dec	IE %	Rp ohm/cm^2	IE %
H_2SO_4	Blank	475	101.9	73	159	-	25.5	
	40	450	33.3	53	110	67.3	78.1	67.9
	60	453	31.6	46	70	68.9	82.4	68.9
	100	469	29.3	49	116	71.2	88.8	71.1
	120	454	28.5	52	105	72.0	91.2	71.9
	160	442	14.8	40	74	85.4	175.9	85.4
	200	442	10.4	44	95	89.7	249.4	89.7
HCl	Blank	465	879.9	79	122	-	29.6	
	40	459	333.1	78	221	62.1	78.2	62.1
	60	454	224.8	71	218	74.4	116.0	74.4
	100	443	185.3	65	140	78.9	140.7	78.9
	120	450	137.9	68	131	84.3	189.0	84.2
	160	451	90.3	62	140	89.7	288.6	89.7
	200	450	72.5	64	132	IE %	359.4	91.7

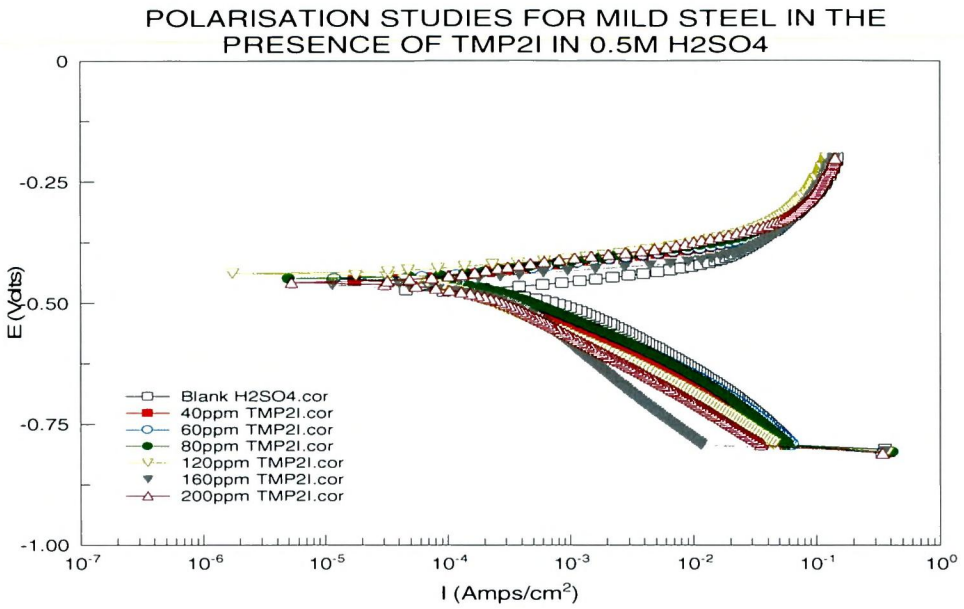

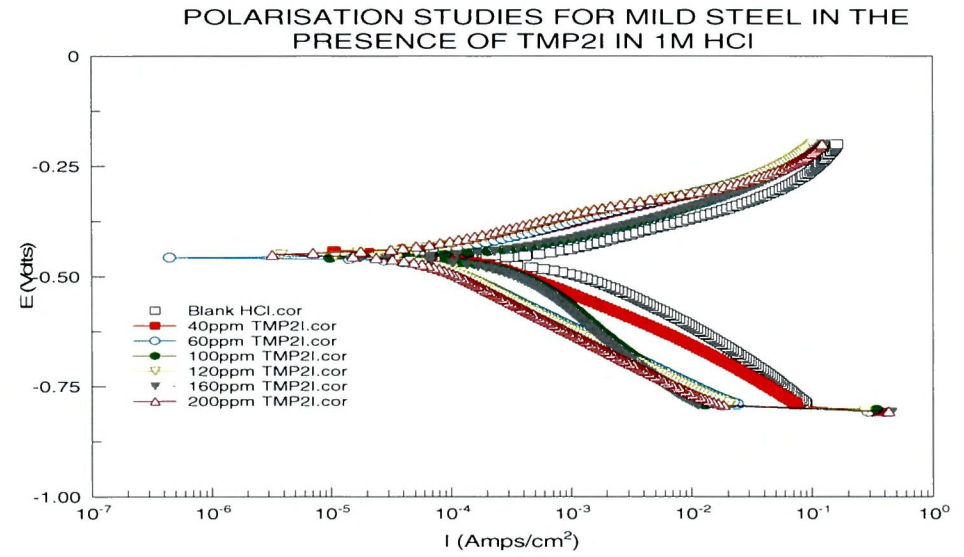

Figure - 52 Potentiodynamic curves for mild steel in 0.5 M H_2SO_4 and 1 M HCl in the presence of TMP2I

1.3 DMP2I:

The polarization curves are used to find the interaction between the organic inhibitor and the electrode surface. The potentiodynamic polarization curves of mild steel in 0.5M H_2SO_4 and 1M HCl with the addition of various concentrations of DMP2I is depicted in Figure - 53. Corresponding electrochemical parameters anlaysed using traditional Tafel method are computed and listed in Table - 35

Investigation of the data revealed that

the corrosion current density values I_{corr} decreases from 430.5 mA/cm^2 of the blank acid to 119.4 mA/ cm^2 in H_2SO_4 and from 555.8 mA/cm^2 to 157.2 mA/cm^2 for the addition of DMP2I resulting in 71.1% and 71.7% of inhibition efficiencies respectively.The decrease in corrosion current densities in the presence of DMP2I might be due to the adsorption of the inhibitor molecule on the mild steel surface.

E_{corr}, b_a and b_c values do not change appreciably with the addition of DMP2I indicating that the inhibitor is interfering the anodic dissolution and cathodic hydrogen evolution reactions and acts as mixed type inhibitor.

Review of literature reveals that, if the displacement in corrosion potential is more than 85 mV with respect to corrosion potential of uninhibited solution, the inhibitor can be seen as anodic or cathodic type. In the present study, maximum displacement was 25mV, indicating that DMP2I belonged to mixed type. These results suggests that studied inhibitor was first adsorbed onto the metal surface and impeded by merely blocking the metal surface without affecting the anodic and cathodic reaction mechanism.

Table - 35 Electrochemical parameters of mild steel at various concentrations of DMP2I in 0.5 M H_2SO_4 and 1 M HCl and corresponding inhibition efficiency values

ACID MEDIUM	Conc ppm	- E_{corr} mV/sec	I_{corr} mA/cm^2	ba mV/dec	bc mV/dec	IE %	Rp ohm/cm^2	IE %
H_2SO_4	Blank	541	430.5	302	207	-	6.0	-
	40	550	369.9	186	135	14.0	7.0	14.1
	60	550	356.3	156	120	17.2	7.3	17.3
	80	548	338.0	224	153	21.4	7.7	21.5
	120	540	171.4	157	107	60.1	15.2	60.2
	160	530	123.3	175	102	71.3	21.1	71.3
	200	534	119.4	140	91	71.1	21.8	72.2
HCl	Blank	517	555.8	202	145	-	4.6	-
	40	532	406.5	247	140	26.8	6.4	26.8
	60	527	347.7	168	106	37.4	7.5	37.4
	80	534	290.6	159	101	47.7	9.0	48.1
	120	529	285.8	199	115	49.0	9.5	50.7
	160	524	179.8	194	106	67.6	14.5	67.6
	200	524	157.2	192	106	71.7	16.5	71.7

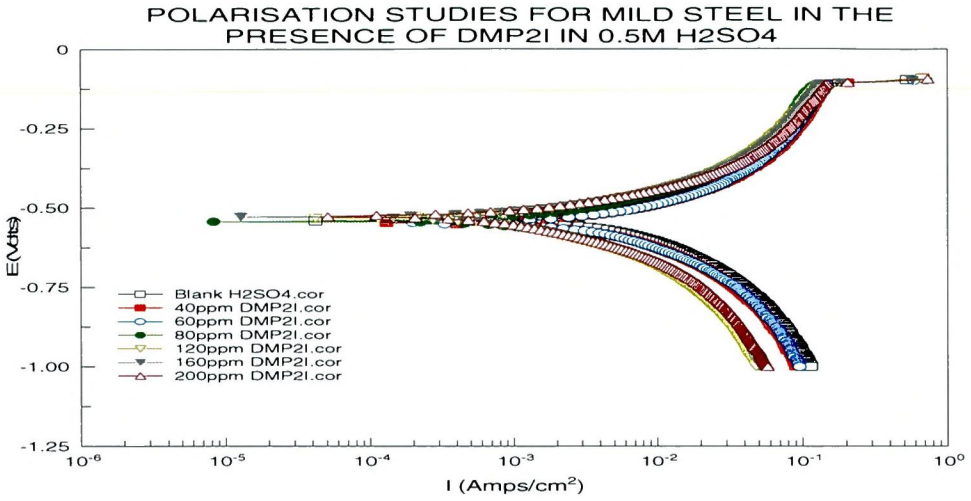

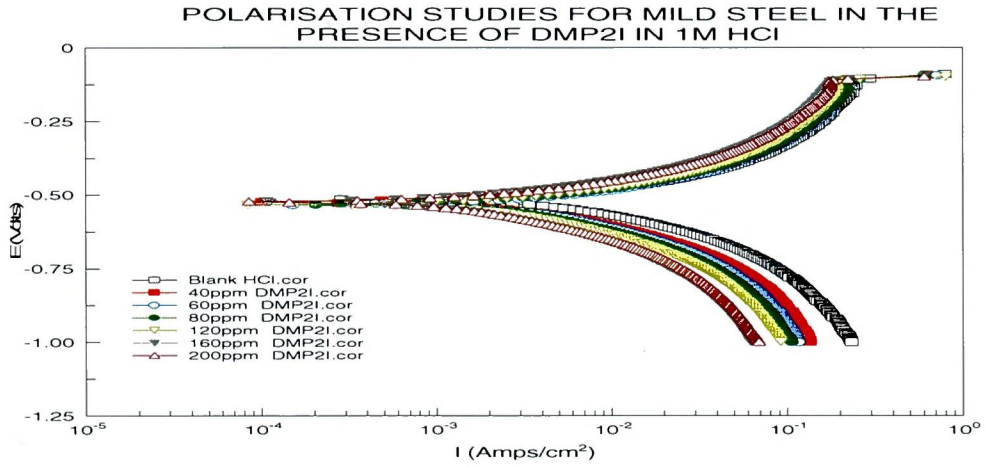

Fig- 53 Potentiodynamic curves for mild steel in 0.5 M H_2SO_4 and 1 M HCl in the presence of DMP2I

OCP2I

Representative Tafel polarization curves for mild steel in H_2SO_4 and HCl with different concentrations of OCP2I are given in Figure - 54. Values of associated electrochemical parameters such as corrosion potential (E_{corr}), corrosion current density (I_{corr}), cathodic and anodic Tafel slopes (b_a and b_c) obtained by extrapolation of the Tafel lines and the calculated inhibition efficiency are presented in Table - 36

Inspection of the data in the Table – 36 infer that

- the corrosion current I_{corr} decreases from the blank value accordingly, IE enhances with increase in each inhibitor concentration. The maximum decrease in the corrosion current density was observed for the OCP2I derivative, corresponding to a maximum efficiency of about 71.5% (H_2SO_4) and 89.4% (HCl) at 200 ppm.

  Further inspection of Table – 36 reveals that the presence of the studied inhibitor does not remarkably shift the corrosion potential E_{corr}, therefore OCP2I can be described as a mixed-type inhibitor for mild steel corrosion.

  Both the anodic and cathodic Tafel slopes slightly change upon addition of OCP2I. These findings infer that the inhibitor molecules are adsorbed on both anodic and cathodic sites, retarding both anodic dissolution and cathodic reduction reactions.

Table – 36 Electrochemical parameters of mild steel at various concentrations of OCP2I in 0.5 M H_2SO_4 and 1 M HCl and corresponding inhibition efficiency values

ACID MEDIUM	Conc ppm	$-E_{corr}$ mV/sec	I_{corr} mA/cm^2	ba mV/dec	bc mV/dec	IE (%)	Rp ohm/cm^2	IE %
H_2SO_4	Blank	462	133.4	55	98	--	19.5	
	40	462	129.9	55	98	2.6	20	2.6
	60	465	115.0	62	150	13.7	22.6	13.8
	80	461	109.7	62	168	17.7	23.7	17.7
	120	462	56.7	52	146	57.4	45.9	57.4
	160	459	53.6	47	109	59.7	57.2	59.7
	200	466	37.9	54	146	71.5	68.8	71.5
HCl	Blank	521	108	99	150	-	23.9	
	40	503	47.2	159	142	56.2	55.1	56.5
	60	506	44.4	162	136	58.8	56.3	57.5
	80	513	38.0	175	123	64.8	58.6	64.8
	120	458	11.6	62	119	78.2	58.9	78.2
	160	456	11.4	60	120	89.4	109.6	89.4
	200	458	11.4	65	121	89.4	223.6	89.4

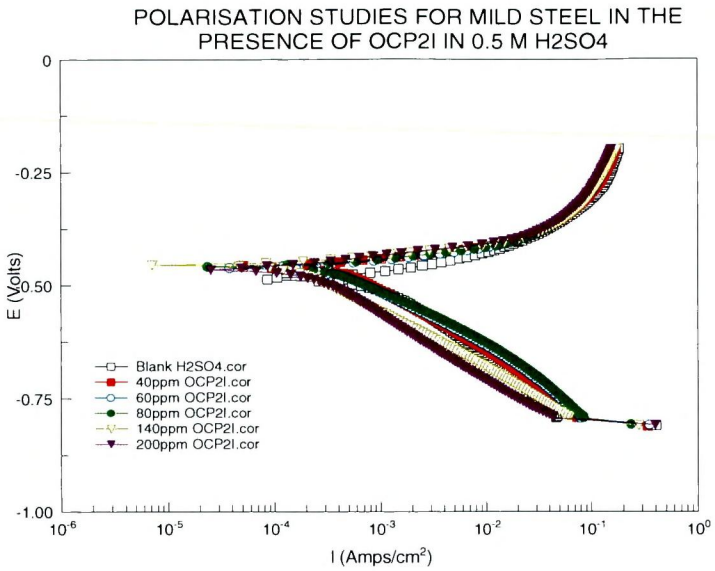

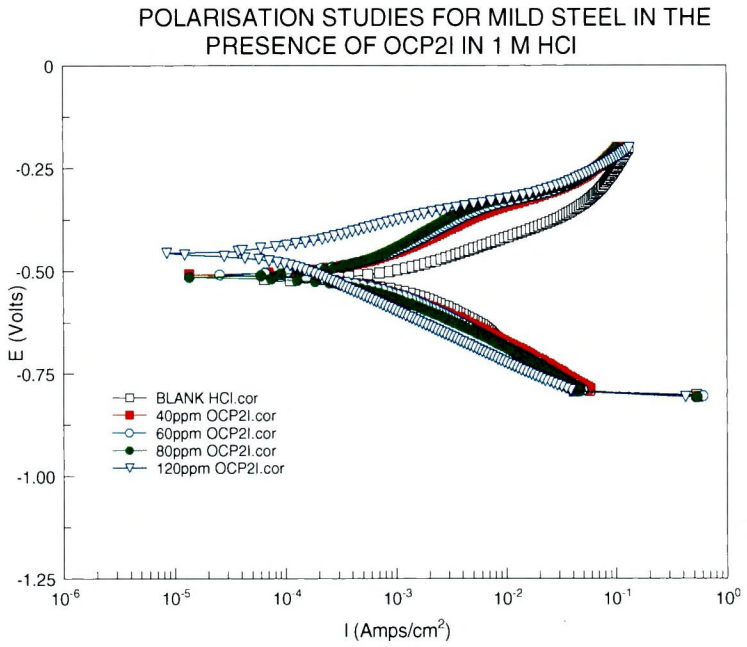

Fig- 54 Potentiodynamic curves for mild steel in 0.5 M H_2SO_4 and 1 M HCl in the presence of OCP2I

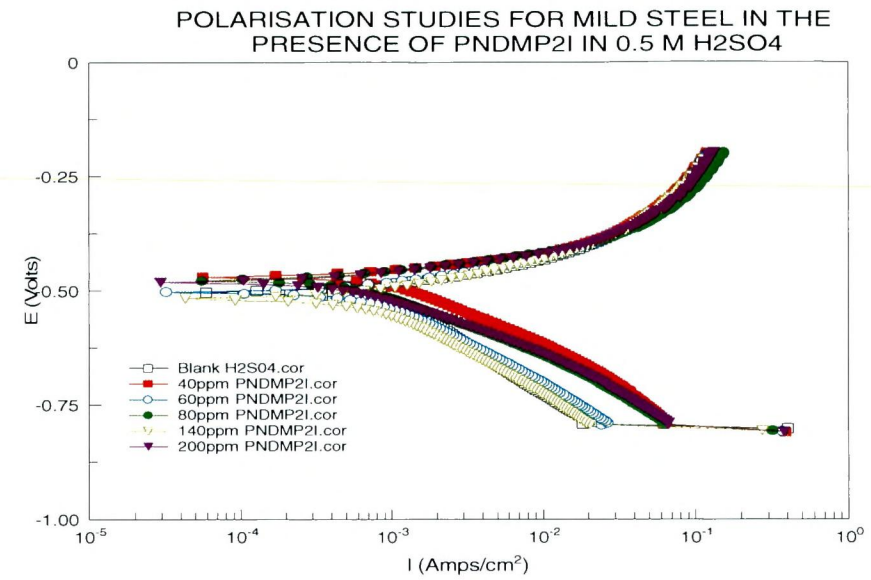

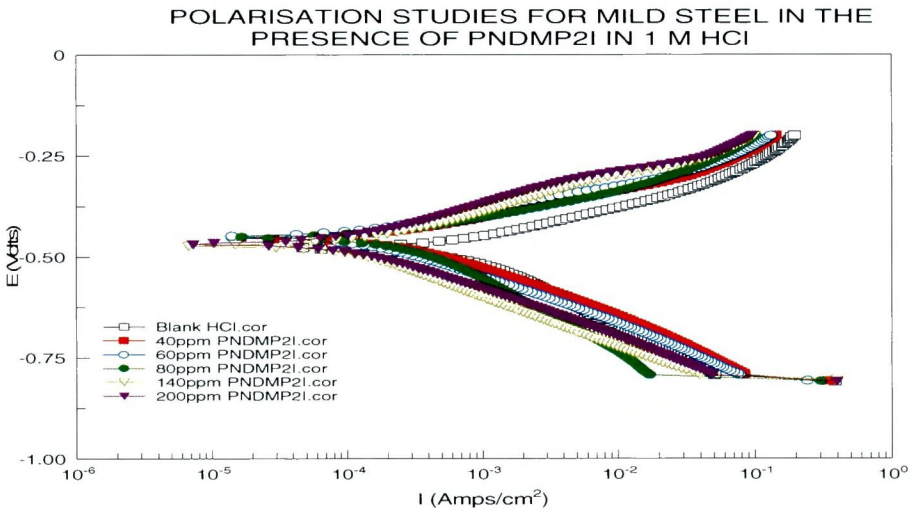

Fig – 55 Potentiodynamic curves for mild steel in 0.5 M H_2SO_4 and 1 M HCl in the presence of

PNDMP2I

PNP2I:

The effect of PNP2I concentration on the anodic and cathodic polarization behaviour of mild steel in 0.5 M H_2SO_4 and 1M HCl solution has been studied by polrisation measurements and the recorded Tafel plots are shown in Figure - 55. The respective kinetic parameters derived from the above plots are given in Table-38

Inspection of the Table - 38 reveals that

An increase in inhibitor concentration resulted in increased inhibition efficiency. It is evident from the results that the I_{corr} values decrease considerably in the presence of PNP2I. Thus, inhibition efficiency increases with inhibitor concentration, reaching the maximum values of 57.4% in H_2SO_4 and 51.7% in HCl at 200 ppm.

The trend in variation in E_{corr} on addition of inhibitor is not regular in both investigated acid media. This infers the mixed type behaviour of PNP2I.

The potentiodynamic curves show that there is a clear reduction of both the anodic and cathodic currents in the presence of PNP2I compared with those for the blank solution. Hence the cathodic reaction (hydrogen evolution) and the anodic reaction (dissolution metal) were inhibited. As can be seen, addition of PNP2I affects both anodic dissolution and cathodic reduction reactions indicating that the PNP2I could be classified as mixed type inhibitor.

Table - 38 Electrochemical parameters of mild steel at various concentrations of PNP2I in 0.5 M H_2SO_4 and 1 M HCl and corresponding inhibition efficiency values

ACID MEDIUM	Conc ppm	$-E_{corr}$ mV/sec	I_{corr} mA/cm^2	ba mV/dec	bc mV/dec	IE %	Rp ohm/cm^2	IE %
H_2SO_4	Blank	520	952.0	167	138	-	2.74	-
	40	523	869.9	261	168	8.6	2.99	8.3
	60	511	671.7	237	191	29.4	4.13	33.6
	80	508	630.2	183	142	33.8	4.72	41.9
	140	529	485.5	167	118	49.0	6.84	59.9
	200	537	404.9	254	158	57.4	9.63	71.5
HCl	Blank	519	668.8	201	137	-	3.9	-
	40	517	575.0	192	144	14.0	4.53	13.9
	60	517	498.4	191	134	25.4	5.23	25.4
	80	514	451.9	177	115	32.4	5.77	32.4
	140	512	355.0	194	118	46.9	6.66	41.4
	200	507	323.0	193	115	51.7	8.07	51.6

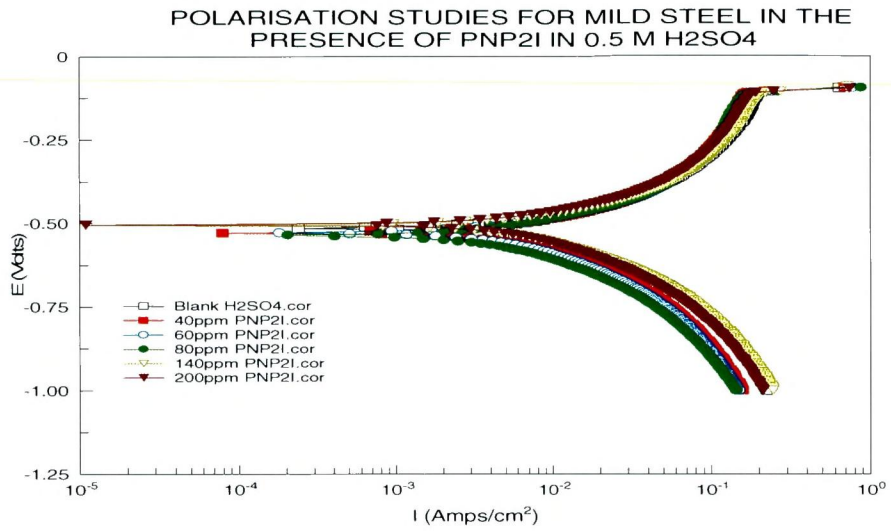

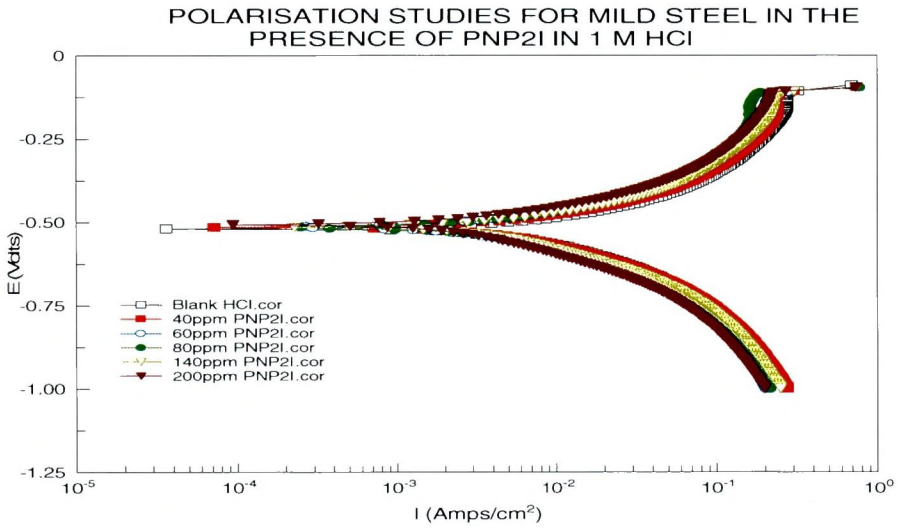

Fig – 56 Potentiodynamic curves for mild steel in 0.5 M H_2SO_4 and 1 M HCl in the presence of PNP2I

From the results obtained, the system under study ie the imidazoline derivatives can be classified as mixed type inhibitors.

Decrease in Values of Icorr and Increase in values of Rp of Mild Steel in the presence of studied inhibitors in both acidic media are pictorially represented in the Figure – 57 and Figure – 58.

Figure – 57 The values of I_{corr} and R_p of mild steel in the presence of studied inhibitors in sulphuric acid medium

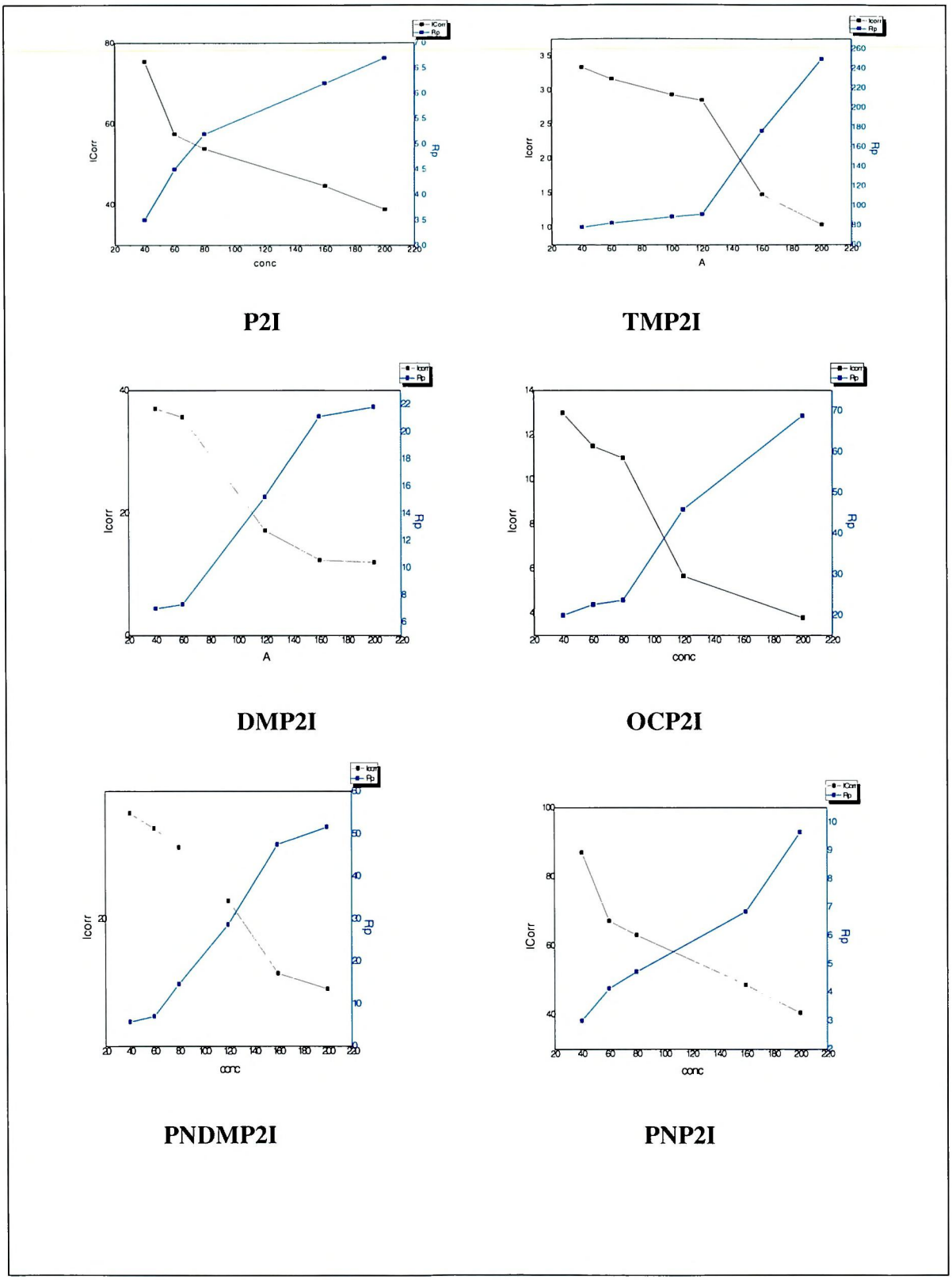

Figure – 58 The values of I_{corr} and R_p of mild steel in the presence of studied inhibitors in hydrochloric acid meidum

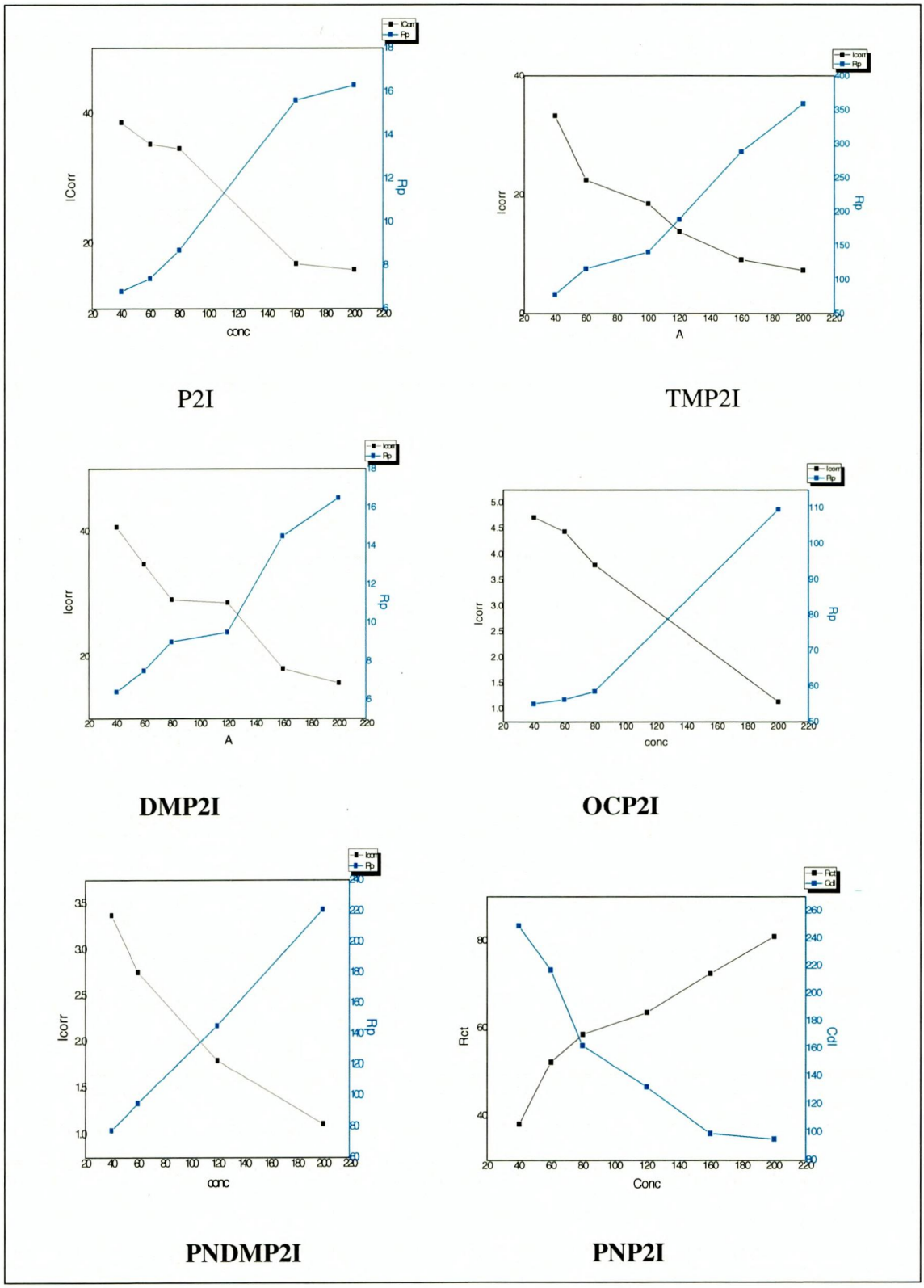

4.3.2 Linear Polarisation Resistance: (R_p)

R_p can be used as an index of corrosion inhibition. Polarisation resistance of mild steel in both acidic media in the presence of imidazoline derivatives are presented in the tables – 35-38 and discussed.

P2I:

Examination of the performance of P2I revealed an increase in the R_p value from 3.1 Ohm/cm^2 to 6.7 Ohm/cm^2 in H_2SO_4 and from 4.0 Ohm/cm^2 to 16.3 Ohm/cm^2 in HCl furnishing IE 53.6% and 75.2 % in H_2SO_4 and HCl medium respectively.

TMP2I:

The results of TMP2I addition on mild steel corrosion show an increase in R_p values and IE with increasing additive concentration which is evident from the R_p values ranging from 78.1 Ohm/cm^2 to 249.4 Ohm/cm^2 in H_2SO_4 and 78.2 Ohm/cm^2 to 359.4 Ohm/cm^2 in HCl . The protection efficiency increases from 67.3 % to 89.7 % in H_2SO_4 and from 62.1% to 91.7% in HCl medium.

DMP2I:

Polarisation resistance of mild steel in the presence of DMP2I in sulphuric acid and hydrochloric acid increases from 7.0 Ohm/cm^2 to 21.8 Ohm/cm^2 and 6.4 Ohm/cm^2 to 16.5 Ohm/cm^2 respectively with increase in the concentration. The IE values were found to be 71.1 % and 71.7% at 200 ppm in H_2SO_4 and HCl medium respectively.

OCP2I:

Polarization resistance of mild steel in the presence of OCP2I increases with increase in inhibitor concentration. The R_p values ranges from 20.0 Ohm/cm^2 to 68.8 Ohm/cm^2 in H_2SO_4 and from 55.1 Ohm/cm^2 to 223.6 Ohm/cm^2 in HCl. The IE increases from 2.6 % to 71.6 % in H_2SO_4 and from 56.5 % to 89.3 % in HCl.

PNDMP2I:

The R_p values for PNDM2I showed only a slight variation with increase in concentration of the inhibitor attaining an efficiency of about 51.6 % at 200 ppm in H_2SO_4. The R_p values ranges from 28.2 Ohm/cm^2 to 14.5 Ohm/cm^2 . In the case of hydrochloric acid medium the R_p value showed considerable change with increase in inhibitor concentration. Polaristion resistance increases from 77.3 Ohm/cm^2 to 220.9 Ohm/cm^2. The IE increases from 50.9 % and reaches 82.8 % at 200 ppm.

PNP2I:

There is a slight variation in the R_p values of PNP2I in H_2SO_4 ranging from 2.9 Ohm/cm^2 to 9.6 Ohm/cm^2 and in HCl ranging from 4.5 Ohm/cm^2 to 8.0 Ohm/cm^2 . the IE increases and attains a maximum of 71.5 % at 200 ppm in H_2SO_4 and 51.6 % at 200 ppm in HCl medium.

The increase in R_p values suggests that the inhibition efficiency increases with the increase in the inhibitor concentrations. All the inhibitors are effective inhibitors at 200ppm and they inhibit corrosion by blocking the active sites **(Sudhish Kumar Shukla *et al.*, 2009).**

In general, the R_p values increases with increase in inhibitor concentration thereby increases the protective efficiency of the imidazoline derivatives under study.

The results of the study indicated that the addition of inhibitor increased the slope of the curve and hence the polarization resistance R_p that the values of R_p distinctly increased when M.S was exposed to the studied inhibitors. This supports that the imidazoline derivatives have excellent inhibitive action on the surface of the mild steel. Inhibitor efficiency increases with increase in concentration of the inhibitor could clearly confirmed that the coverage of the mild steel surface by the inhibitor gradually increased with increase in concentration of the inhibitor.

4.3.3 Electrochemical Impedance Spectroscopy:

In order to obtain information about the kinetics of iron corrosion in presence of imidazoline derivatives, the electrochemical process taking place at the open circuit potential was examined by Electrochemical Impedance Spectroscopy. Results pertaining to Electrochemical Impedance Spectroscopy studies are tabulated and discussed.

P2I

The corrosion behaviour of mild steel in acidic solutions 0.5 M H_2SO_4 and 1 M HCl in the presence of P2I was investigated by EIS method. The Nyquist plots of mild steel in inhibited and uninhibited acidic solution containing various concentrations of P2I are depicted in Figure – 59. . The impedance parameters derived from these investigations are listed in Table-.39.

Table -39 Impedance parameters of Mild steel in the presence of P2I in 0.5M H_2SO_4 and 1M HCl

Conc in ppm	H_2SO_4				HCl			
	R_{ct} ohm/cm^2	IE %	C_{dl} µF/cm^2	θ	R_{ct} ohm/cm^2	IE %	C_{dl} µF/cm^2	θ
Blank	2.7	-	403	-	30.9	-	262	-
40	5.4	50.0	309	0.23	38.1	18.9	249	0.05
60	11.7	77.0	286	0.29	52.2	40.8	217	0.17
80	14.4	81.4	199	0.51	58.5	47.2	162	0.38
120	19.7	86.3	164	0.59	63.5	51.3	132	0.49
160	27.5	90.2	89	0.73	72.4	41.5	99	0.62
200	42.0	93.6	90	0.78	80.9	61.8	95	0.64

It can be seen that the obtained impedance diagram show almost a semicircle for the free acid and in the presence of P2I. The differences have been attributed to the frequency dispersion. The semicircle appearance indicates that the corrosion of steel is mainly controlled by the charge transfer process and the presence of P2I does not alter the mechanism of dissolution of steel surface.

Analysis of the Table - 39 reveal that, the R_{ct} values increase from the value of 2.7 Ohmcm^2 for the blank acid to 42.0 Ohmcm^2 for the highest concentration of P2I thereby increasing the IE calculated from R_{ct} value from 50.0 % to 93.6 % in H_2SO_4. In HCl solution the R_{ct} increase from 30.9 Ohm/cm^2 for the blank acid to 80.9 Ohmcm^2 for the highest concentration and IE increases from 18.9 % to 61.8 % using R_{ct} values.

The interfacial double layer capacitance C_{dl} decreases from 403 µF/cm^2 for the blank H_2SO_4 solution to 90 µF/cm^2 and from 262 µF/cm^2 for the blank HCl solution to 95 µF/cm^2 for P2I at 200 ppm. The decrease in C_{dl} values increases the surface coverage (θ) from 0.23 to 0.78 in H_2SO_4 solution and from 0.05 to 0.64 in HCl solutions with the addition of various concentrations of P2I .

EIS data show that the R_{ct} values increases and the C_{dl} values decreases with increasing the inhibitor concentrations. This leads to an increase of θ and the inhibition efficiency. The decrease in C_{dl} can result from the decrease of the local dielectric constant and/or from the increase of thickness of the electrical double layer

(Hosseini *et al.*, 2007). Suggested that the inhibitor molecules function by adsorption at the metal/solution interface. Thus, the decrease in C_{dl} values and the increase in R_{ct} values and consequently of inhibition efficiency may be due to gradual replacement of water molecules by the adsorption of the inhibitor molecules on the metal surface, decreasing the extent of dissolution reaction **(Bentiss *et al.*, 2002, Ishtiaque Anamad *et al.*, 2010, Sathiyanarayana *et al.*, 2005).**

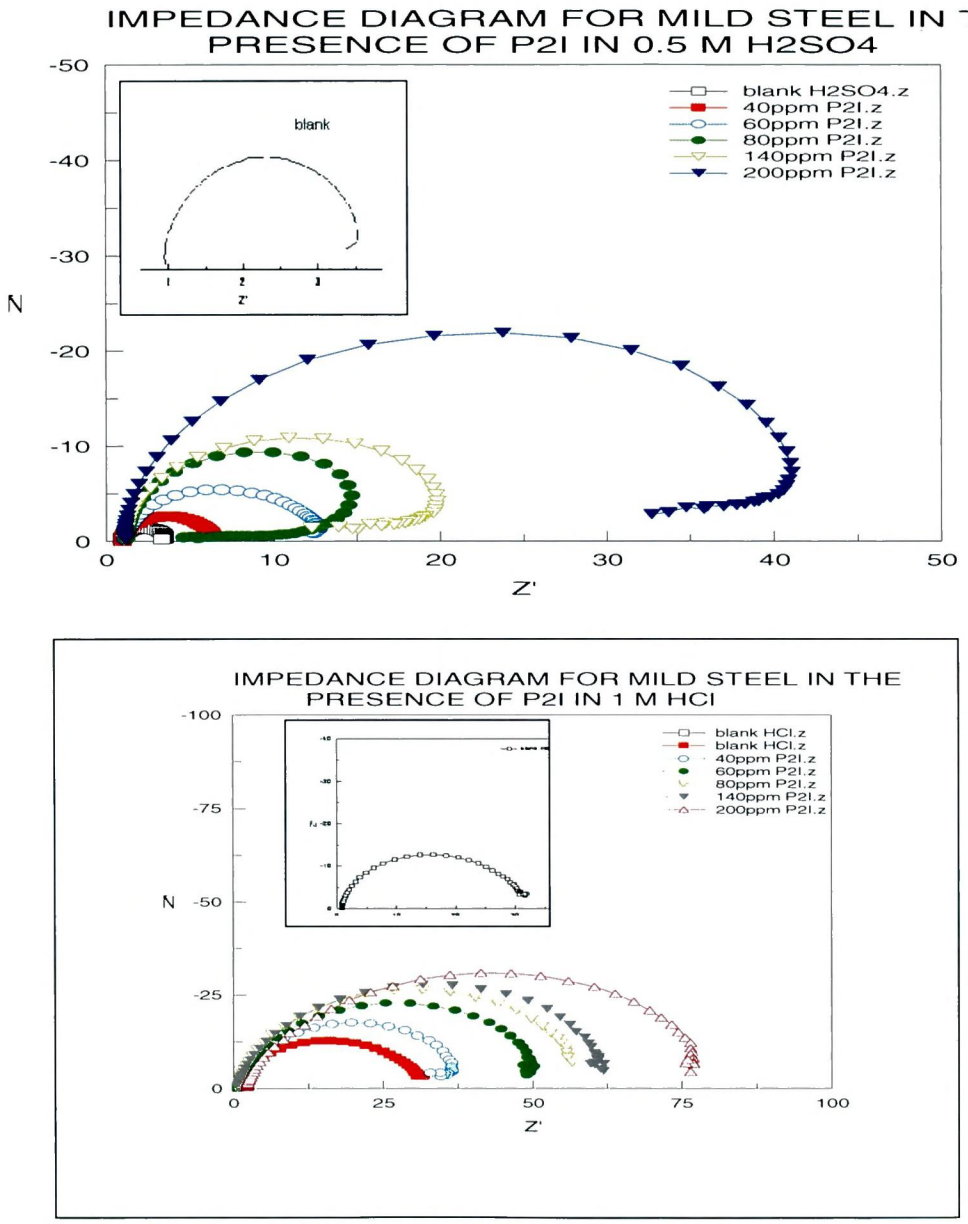

Figure –59 Impedance diagram for mild steel in the presence of P2I in 0.5M H_2SO_4 and 1M HCl

TMP2I

EIS were carried with frequency range from 20 KHz to 0.1Hz at open circuit potential. Impedance spectra for mild steel in 0.5 M H_2SO_4 and 1M HCl in absence and presence of TMP2I are shown in the form of Nyquist plots (Figure- 60). The impedance parameters derived from these investigations are mentioned in Table – 40.

Table – 40 Impedance parameters of Mild steel in the presence of TMP2I in 0.5M H_2SO_4 and 1M HCl

	H_2SO_4				HCl			
Conc in ppm	Rct ohmcm^2	IE %	Cdl µF/cm^2	θ	Rct ohmcm^2	IE %	Cdl µF/cm^2	θ
Blank	7.9	-	305	-	13.5	-	197	-
40	29.9	73.5	288	0.05	122.9	89	118	0.39
60	34.9	77.3	243	0.2	211.2	93.6	80	0.59
80	77.2	89.7	131	0.56	250.5	94.6	7.8	0.6
120	103.5	92.3	128	0.57	311.3	95.6	69	0.64
160	129.6	93.9	73	0.76	316.9	95.7	60	0.69
200	183.2	95.6	61	0.8	461.7	97	60	0.69

It is found from table – 40, that as the TMP2I concentration increases, the R_{ct} values increases, but C_{dl} tend to decrease. The R_{ct} value increases from 7.9 Ohmcm^2 for the blank H_2SO_4 solution to 183.2 Ohmcm^2 and the R_{ct} value increases from 13.5 Ohmcm^2 for the blank HCl solution to 461.7 Ohmcm^2 for the maximum concentration of the inhibitor (200 ppm). The increase in R_{ct} values with the concentration of the studied inhibitor increases the inhibition efficiency from 73.5 % to 95.6 % in H_2SO_4 solution and from 89.0% to 97.0% in HCl solution.

The interfacial double layer capacitance C_{dl} decreases from 305µF/cm^2 for the blank H_2SO_4 solution to 61 µF/cm^2 and from 1975 µF/cm^2 for the blank HCl solution to 60µF/cm^2 for TMP2I at 200 ppm. The decrease in C_{dl} values increases the surface coverage (θ) from 0.05 to 0.80 in H_2SO_4 solution and from 0.39 to 0.69 in HCl solutions with the addition of various concentrations of TMP2I .

The R_{ct} values increase as well, but the C_{dl} tend to decrease. The decrease in C_{dl} is due to the adsorption of TMP2I on the mild steel surface.This result indicated that the dissolution mechanism of mild steel was being controlled by the charge

transfer rate across the phase boundary in the presence and absence of the inhibitor. Moreover, the presence of TMP2I did not alter the mechanism of the dissolution of the mild steel.

It is worthy to note that, the presence of inhibitor does not alter the profile of impedance diagram which are almost semicircular (figure-60) indicating a charge transfer process mainly controls the corrosion of mild steel. Deviations of perfect circular shape are often referred to the frequency dispersion of interfacial impedance. This anomalous phenomenon is interpreted by the inhomogeneity of the electrode surface arising from surface roughness or interfacial phenomena.

Values of double layer capacitance are also brought down to the maximum extent in the presence of inhibitor and the decrease in C_{dl} means that the adsorption of this TMP2I takes place on the metal surface in acidic solution. **(Bentiss *et al.*, 2002, Ishtiaque Anamad *et al.*, 2010, Sathiyanarayana *et al.*, 2005,Mns).**

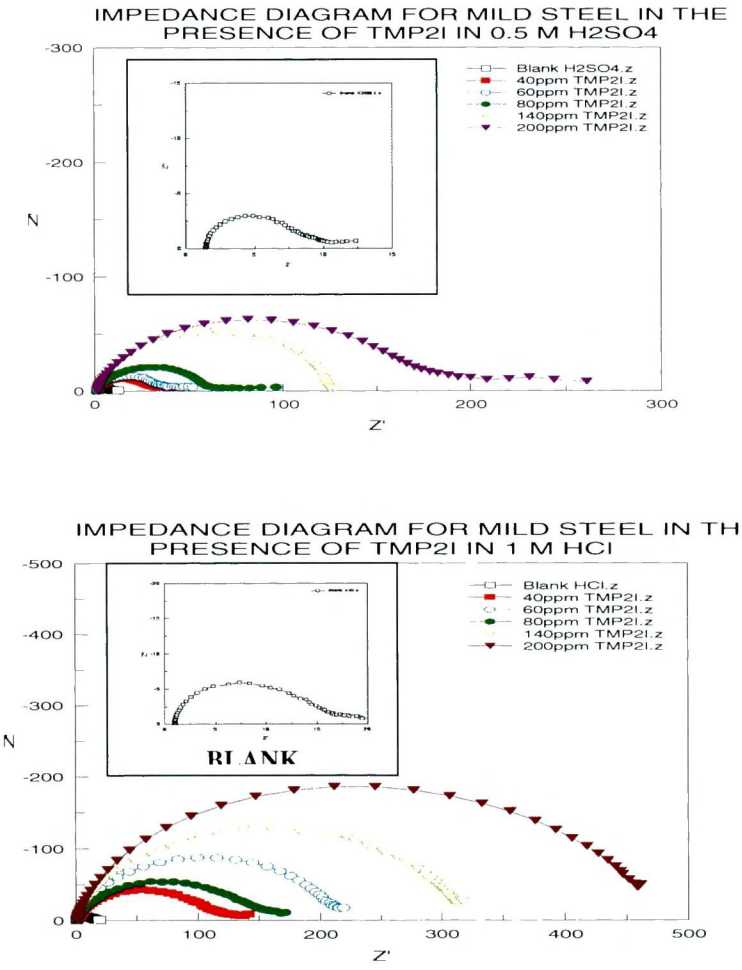

Figure – 60 Impedance diagram for mild steel in the presence of TMP2I in 0.5M H_2SO_4 and 1M HCl

DMP2I

Figure – 61 show a typical Nyquist plots for mild steel in 0.5 M H_2SO_4 and 1 M HCl in the absence and presence of various concentrations of DMP2I. The main parameters deduced from the analysis of of Nyquist diagram are the charge transfer resistance (R_{ct}), the double layer capacitance (C_{dl}). The characteristic parameters associated to the impedance diagram and inhibition efficiency are presented in Table-41.

Table - 41 Impedance parameters of Mild steel in the presence of DMP2I in 0.5M H_2SO_4 and 1M HCl

H_2SO_4					HCl			
Conc in ppm	Rct ohmcm^2	IE %	Cdl µF/cm^2	θ	Rct ohmcm^2	IE %	Cdl µF/cm^2	θ
Blank	13.5	-	222	-	27.6	-	229	-
40	22.7	40.4	185	0.16	58.2	52.6	203	0.11
60	34.7	60.9	125	0.43	90.6	69.5	161	0.29
80	51.7	73.7	116	0.47	109.1	74.7	156	0.31
120	64.6	79	93	0.58	115.2	76	111	0.51
160	88.1	84.5	73	0.66	180	84.6	96	0.57
200	144.5	90.6	73	0.66	205.9	86.5	93	0.59

As it can be seen from table-41 , the R_{ct} values increased with increase inhibitor concentration. The R_{ct} value increases from 13.5 Ohmcm^2 for the blank H_2SO_4 solution to 144.5 Ohmcm^2 and the R_{ct} value increases from 27.6 Ohmcm^2 for the blank HCl solution to 205.9 Ohmcm^2 for the maximum concentration of the inhibitor (200 ppm). The increase in R_{ct} values with the concentration of the inhibitor increases the inhibition efficiency from 40.4% to 90.6% in H_2SO_4 solution and from 52.6% to 86.5% in HCl solution.

The diameter of Nyquist plots increase on increasing the DMP2I concentration. this suggested the formed inhibitive film was strengthened by addition of DMP2I . The impedance diagram contains a depressed semicircle with the center under the real axis, such behaviour characteristic for solid electrode and often referred to frequency dispersion have been attributed to roughness and inhomogeneties of solid surface.

The analysis of the results presented in the table reveals that Cdl decrease with the increase of concentration. The interfacial double layer capacitance C_{dl} decreases from 222 $\mu F/cm^2$ for the blank H_2SO_4 solution to 73 $\mu F/cm^2$ and from 229 $\mu F/cm^2$ for the blank HCl solution to 93 $\mu F/cm^2$ for TMP2I at 200 ppm. The decrease in C_{dl} values increases the surface coverage (θ) from 0.16 to0.66 in H_2SO_4 solution and from 0.11 to 0.59 in HCl solutions with the addition of various concentrations of DMP2I.

The double layer between the charged metal surface and the solution is considered as an electrical capacitor. The adsorption of the DMP2I derivative on the electrode decreases its electrical capacity because they displace the water molecules and other ions originally adsorbed on the metal surface. The decrease in this capacity with increasing concentration of DMP2I may be attributed to the formation of a protective layer at electrode surface. **(Bentiss *et al.*, 2002, Ishtiaque Anamad *et al.*, 2010, Sathiyanarayana *et al.*, 2005).**

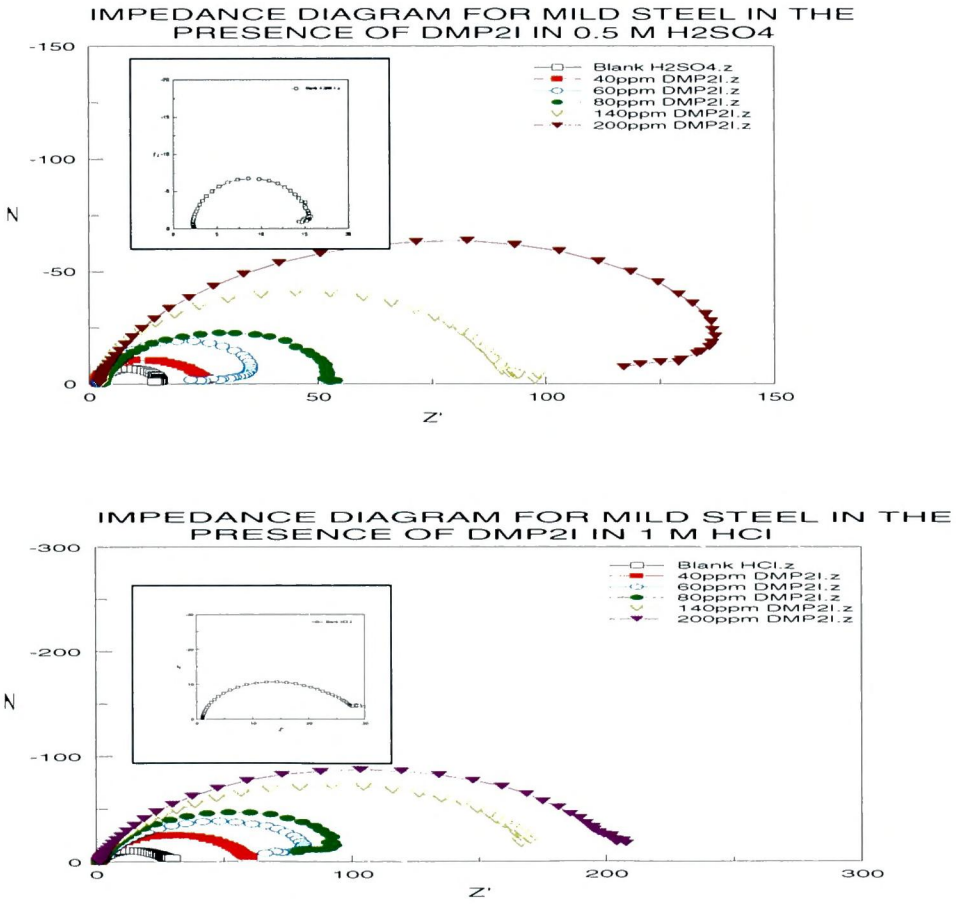

Figure – 61 Impedance diagram for mild steel in the presence of DMP2I in 0.5M H_2SO_4 and 1M HCl

OCP2I

Nyquist representations of mild steel in H_2SO4 and HCl containing various concentration of OCP2I are shown in figure - 62. Various parameters such as charge transfer resistance (R_{ct}), double layer capacitance (C_{dl}) and calculated percentage inhibition efficiency and surface coverage (θ) have been calculated and listed in Table- 42.

Table - 42 Impedance parameters of Mild steel in the presence of OCP2I in 0.5M H_2SO_4 and 1M HCl

Conc in ppm	H_2SO_4				HCl			
	Rct ohmcm^2	IE %	Cdl μF/cm^2	θ	Rct ohmcm^2	IE %	Cdl μF/cm^2	θ
Blank	5.6		414		19.2		481	
40	12.2	54.3	390	0.05	30.9	37.8	461	0.04
60	14.7	61.8	303	0.26	37.3	48.4	426	0.11
80	15.6	64	218	0.47	39.4	50	406	0.15
120	20.2	72.2	151	0.63	47.9	58.9	385	0.19
160	30	81.3	111	0.73	102.4	80.7	140	0.70
200	34.4	83.6	106	0.74	213.4	90.7	101	0.79

It is clear from the plots that impedance response of mild steel in test solution was significantly changed after addition of the inhibitors.

Examination of the table- 42, the R_{ct} values increased with increase inhibitor concentration. The R_{ct} value increases from 5.6 Ohmcm^2 for the blank H_2SO_4 solution to 34.4 Ohmcm^2 and the R_{ct} value increases from 19.2 Ohmcm^2 for the blank HCl solution to 213.4 Ohmcm^2 for the maximum concentration of the inhibitor (200 ppm). The decrease in double layer is attributed to increase in thickness of electronic double layer. The analysis of the results presented in the table - 42 reveals that C_{dl} decrease with the increase of concentration. The interfacial double layer capacitance C_{dl} decreases from 414 μF/cm^2 for the blank H_2SO_4 solution to 106 μF/cm^2 and from 481 μF/cm^2 for the blank HCl solution to 101 μF/cm^2 for OCP2I at 200 ppm. The decrease in C_{dl} values increases the surface coverage (θ) from 0.05 to

0.74 in H_2SO_4 solution and from 0.04 to 0.79 in HCl solutions with the addition of various concentrations of OCP2I.

Generally Figure-62 showed that the impedance spectra exhibit one single depressed semicircle, and the diameter of semicircle increases with the inhibitor concentration. The single semicircle can be attributed to the charge transfer that takes place at electrode/solution interface and the transfer process controls the corrosion reaction of steel and the presence of inhibitor does not change the mechanism of dissolution of steel. It is also clear that these impedance diagrams consists of one large capacitive loop and they are not perfect semicircles and this difference has been attributed to frequency dispersion and the heterogeneity of metal surface.

The increase of charge transfer resistance and decrease in double layer capacitance with increasing OCP2I concentration indicate this compound inhibit the corrosion rate of mild steel by an adsorption mechanism. The increase in charge transfer resistance value is attributed to the formation of metal/solution interface thereby increasing the surface coverage. **(Bentiss *et al.*, 2002, Ishtiaque Anamad *et al.*, 2010, Sathiyanarayana *et al.*, 2005).**

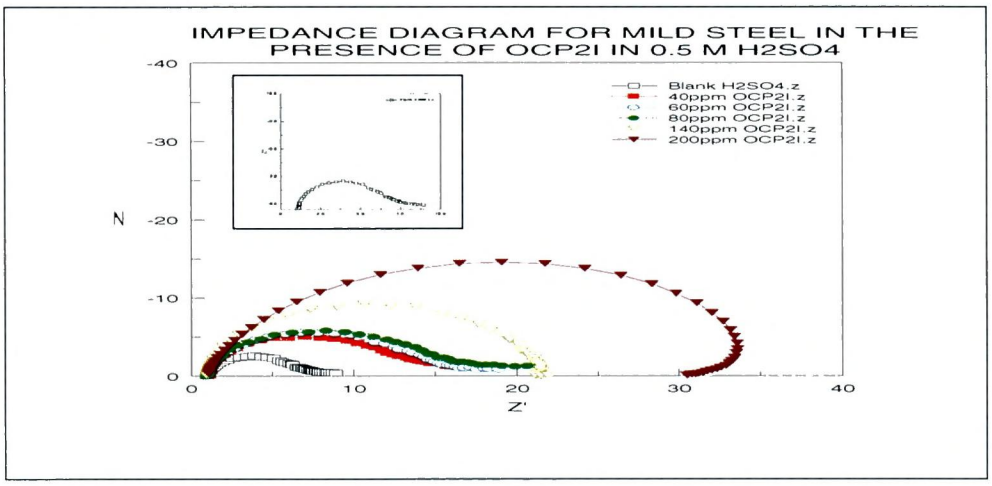

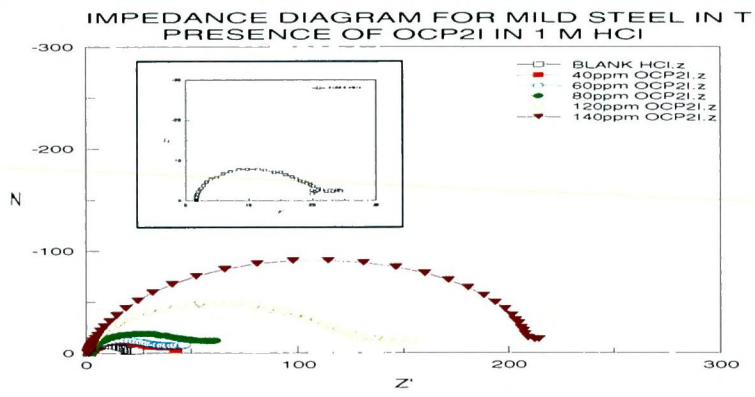

Figure- 62 Impedance diagram for mild steel in the presence of OCP2I in 0.5M H_2SO_4 and 1M HCl

PNDMP2I:

The corrosion behaviour of mild steel in 0.5 M H_2SO_4 and 1 M HCl in the absence and presence of PNDMP2I derivative was also investigated by the electrochemical impedance spectroscopy. Nyquist plots of mild steel in uninhibited and inhibited acidic solutions containing various concentrations of PNDMP2I are represented in Figure- 63.

The characteristic parameters associated to the impedance diagram (Rct and Cdl) and the calculated inhibition efficiency and surface coverage are listed in Table - 43.

Examination the table-43, infer that the Rct values increased with increase inhibitor concentration. The Rct value increases from 7.9 $Ohmcm^2$ for the blank H_2SO_4 solution to 31.2 $Ohmcm^2$ and the Rct value increases from 21.1 $Ohmcm^2$ for the blank HCl solution to 216.1 $Ohmcm^2$ for the maximum concentration of the inhibitor (200 ppm).

Analysing C_{dl} values reveal that C_{dl} decrease with the increase of concentration. The interfacial double layer capacitance C_{dl} decreases from 305 $\mu F/cm^2$ for the blank H_2SO_4 solution to 63 $\mu F/cm^2$ and from 244 $\mu F/cm^2$ for the blank HCl solution to 86 $\mu F/cm^2$ for PNDMP2I at 200 ppm. The decrease in Cdl values increases the surface coverage (θ) from 0.17 to 0.793 in H_2SO_4 solution and from 0.023 to 0.646 in HCl solutions with the addition of various concentrations of

PNDMP2I. The decrease in double layer is attributed to increase in thickness of electrical double layer.

Recorded EIS spectra infer that, the Nyquist plots contain depressed semi-circles, whose size increase with the inhibitor concentrations, indicating a charge transfer process mainly controlling the corrosion of mild steel. Such behaviour, is characteristic for solid electrodes and often referred to a frequency dispersion, has been attributed to roughness and inhomogeneities of the solid surface. This indicated that the impedance of the inhibited substrate had increased with increasing concentration of PNDMP2I.

In the case of impedance study inhibition efficiency calculated from R_{ct} increases with inhibitor concentration. On the other hand, the values of C_{dl} decreased with an increase in the inhibtor concentration. This situation was that result of an increase in surface coverage by the inhibitor which led to an increase in the inhibition efficiency. This decrease in C_{dl} values was caused by the gradual replacement of water molecules by the adsorption of organic molecules on the metal surface, decreasing the extent of the metal surface. **(Bentiss *et al.*, 2002, Ishtiaque Anamad *et al.*, 2010, Sathiyanarayana *et al.*, 2005).**

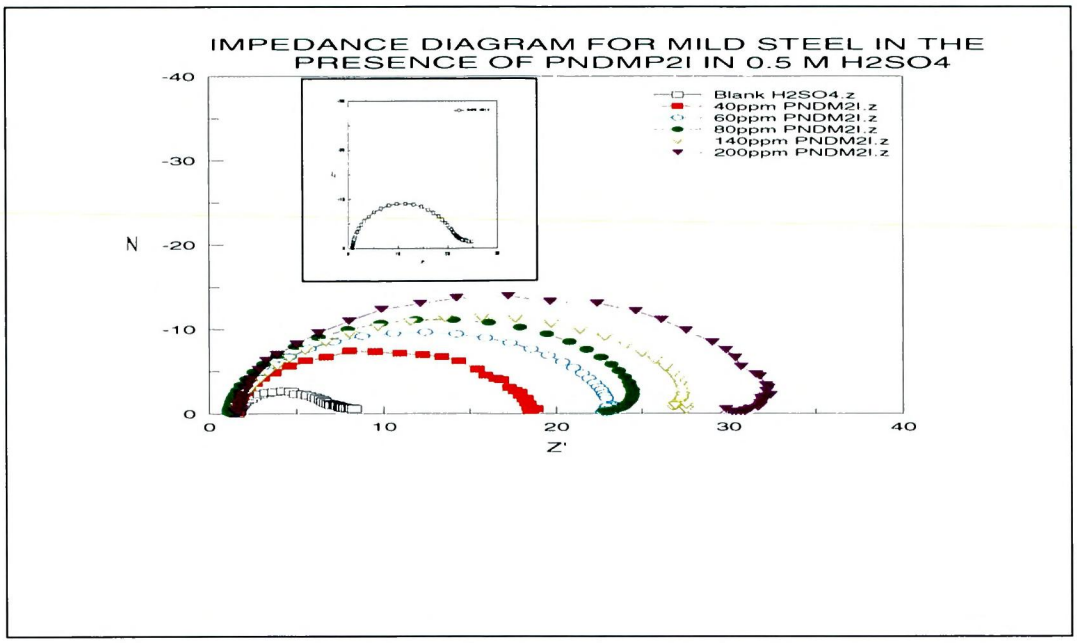

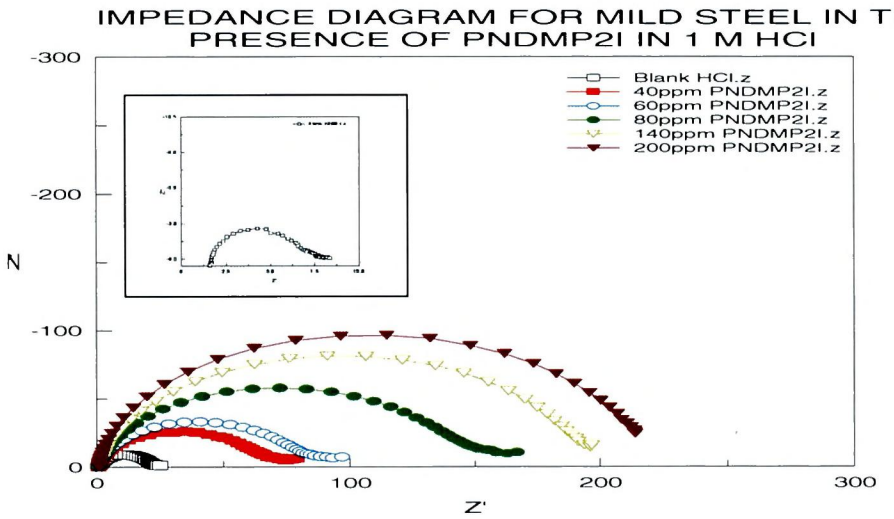

Figure - 63 Impedance diagram for mild steel in the presence of PNDMP2I in 0.5M H_2SO_4 and 1M HCl

Table - 43 Impedance parameters of Mild steel in the presence of PNDMP2I in 0.5M H_2SO_4 and 1M HCl

Conc in ppm	H_2SO_4				HCl			
	Rct ohmcm^2	IE %	Cdl µF/cm^2	θ	Rct ohmcm^2	IE %	Cdl µF/cm^2	θ
Blank	7.9	-	305	-	21.1	-	244	-
40	16.9	53.3	253	0.170	67.3	68.66	238	0.023
60	21.8	63.77	177	0.419	82.4	74.41	229	0.060
80	24.0	67.19	176	0.424	148.7	85.81	213	0.211
120	24.9	68.36	151	0.503	182.9	88.46	145	0.403
160	27.0	70.79	85	0.721	197.0	89.28	101	0.586
200	31.2	74.71	63	0.793	216.1	90.23	86	0.646

PNP2I

Electochemical impedance spectra for mild steel in H_2SO_4 and HCl in absence and presence of inhibitor were recorded and Nyquist plots of mild steel in uninhibited and inhibited acidic solutions containing various concentrations of PNP2I are shown in Figure- 64.

The impedance data from these investigations are given in table-44.

From the table – 44, it has been found that, the R_{ct} values increased with increase inhibitor concentration. The R_{ct} value increases from 3.13 Ohmcm^2 for the blank H_2SO_4 solution to 31.8 Ohmcm^2 and the R_{ct} value increases from 20.6 Ohmcm^2 for the blank HCl solution to 75.4 Ohmcm^2 for the maximum concentration of the inhibitor. The fact that impedance diagrams have an approximately semicircular appearance shows that the corrosion of mild steel in both the examined acid media is controlled by charge transfer process. Small distortion was observed , this distortion has been attributed to frequency dispersion. The diameters of the capacitve loop obtained increase in the presence of PNP2I derivative, and were indicative of the degree of inhibition of the corrosion process.

The analysis of the results presented in the table –44, reveals that C_{dl} decrease with the increase of concentration. The interfacial double layer capacitance C_{dl}

decreases from 249 μF/cm^2 for the blank H_2SO_4 solution to 95 μF/cm^2 and from 297 μF/cm^2 for the blank HCl solution to 67 μF/cm^2 for PNP2I at 200 ppm. The decrease in Cdl values increases the surface coverage (θ) from 0.002 to 0.62 in H_2SO_4 solution and from 0.093 to 0.774 in HCl solutions with the addition of various concentrations of PNP2I. The decrease in double layer is attributed to increase in thickness of electronic double layer.

The addition of inhibitor lowers the C_{dl} value, suggesting that the inhibition can be attributed to surface adsorption. The increase in R_{ct} value is attributed to the formation of protective film on the metal-solution interface. The decrease in C_{dl} value is attributed to increase in thickness of electrical double layer. These observations suggest that PNP2I molecules function by adsorption on the metal surface thereby causing increase in Rct value and decrease in Cdl value. **(Bentiss *et al.*, 2002, Ishtiaque Anamad *et al.*, 2010, Sathiyanarayana *et al.*, 2005).**

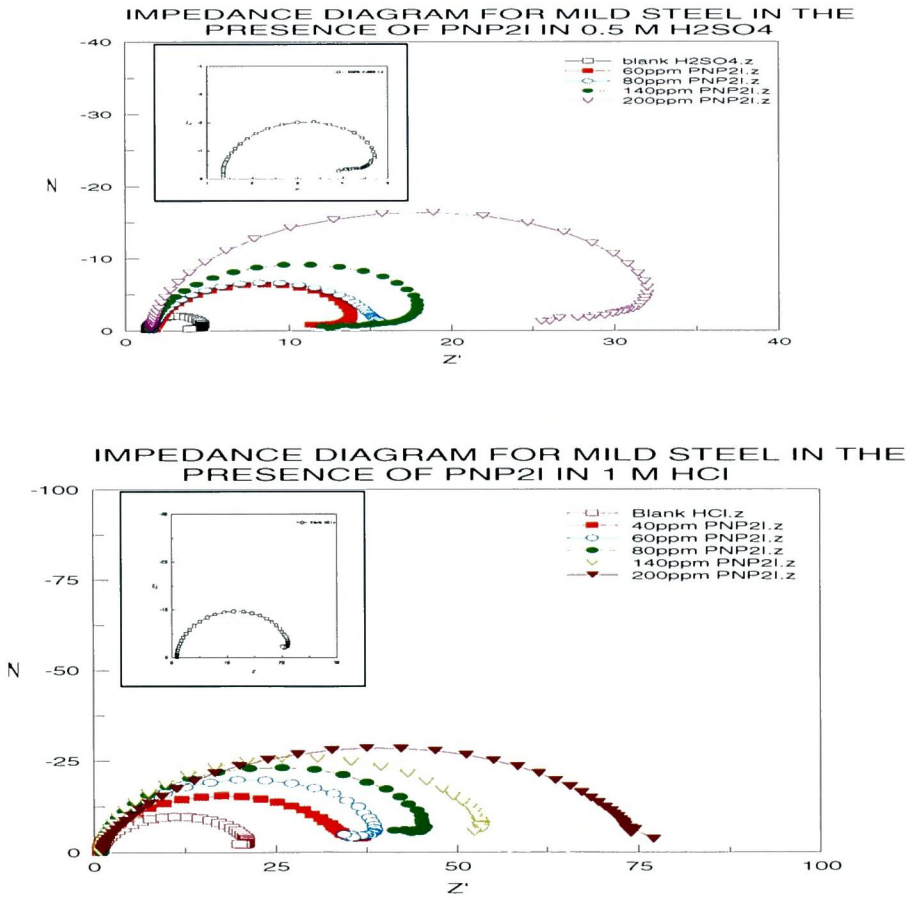

Figure -64 Impedance diagram for mild steel in the presence of PNP2I in 0.5M H_2SO_4 and 1M HCl

Table - 44 Impedance parameters of Mild steel in the presence of PNP2I in 0.5M H_2SO_4 and 1M HCl

Conc in ppm	H_2SO_4				HCl			
	Rct ohmcm^2	IE %	Cdl µF/cm^2	θ	Rct ohmcm^2	IE %	Cdl µF/cm^2	θ
Blank	3.13	-	249	-	20.6	-	297	-
40	12.5	74.9	248	0.002	35.1	41.1	270	0.093
60	14.15	77.8	237	0.048	37.5	44.9	222	0.254
80	16.52	81	158	0.362	44.8	53.8	213	0.283
140	18.43	83	110	0.555	53.8	61.5	163	0.452
200	31.8	90.1	84	0.66	75.4	72.5	67	0.774

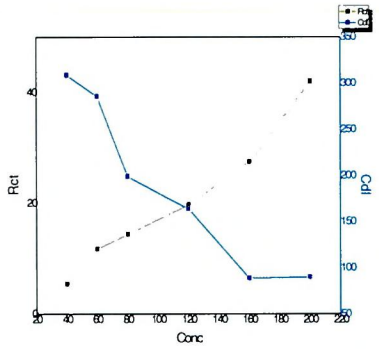

P2I

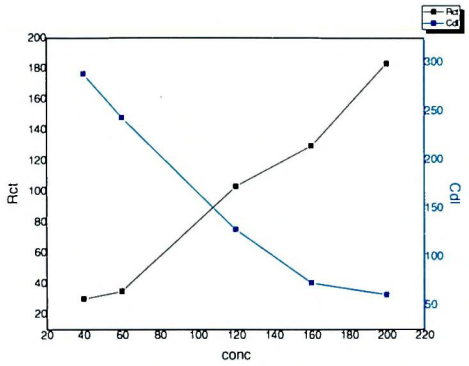

TMP2I

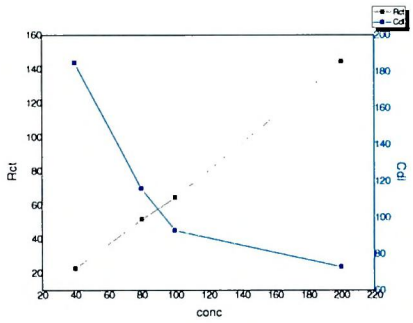

DMP2I

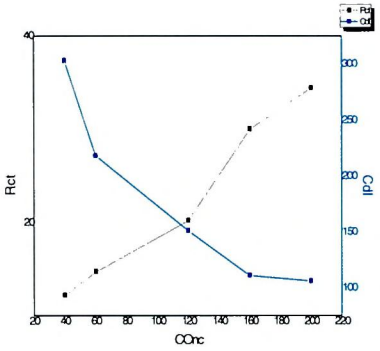

OCP2I

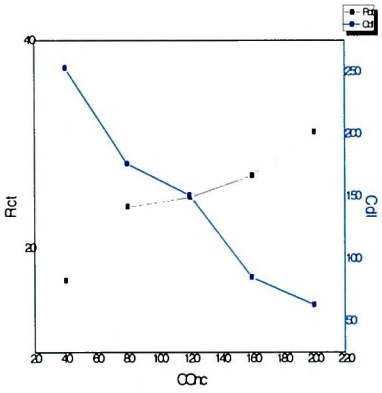

PNDMP2I

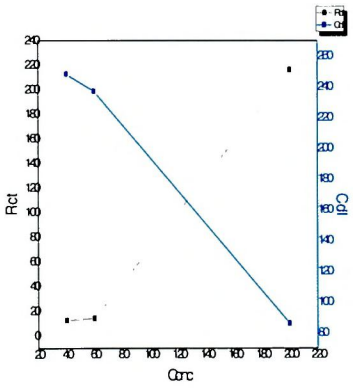

P2I

Figure- 65 Values of Rct and Cdl of mild steel in the presence of current inhibitors in H_2SO_4 medium

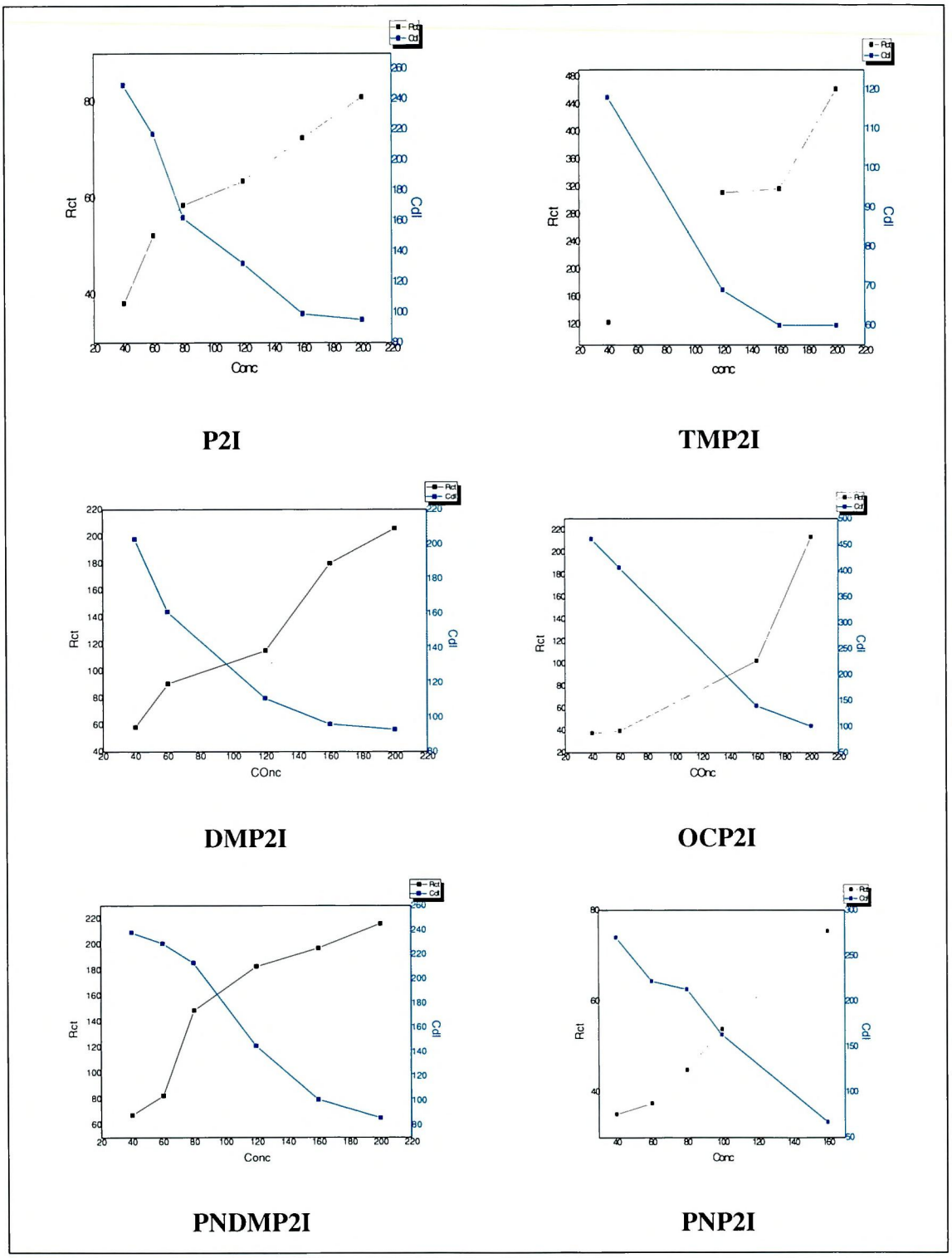

Figure- 66 Values of Rct and Cdl of mild steel in the presence of current inhibitors in HCl medium

Figure -65 & 66 demonstrate the increase in R_{ct} and decrease in C_{dl} of mild steel in the presence of studied inhibitors.

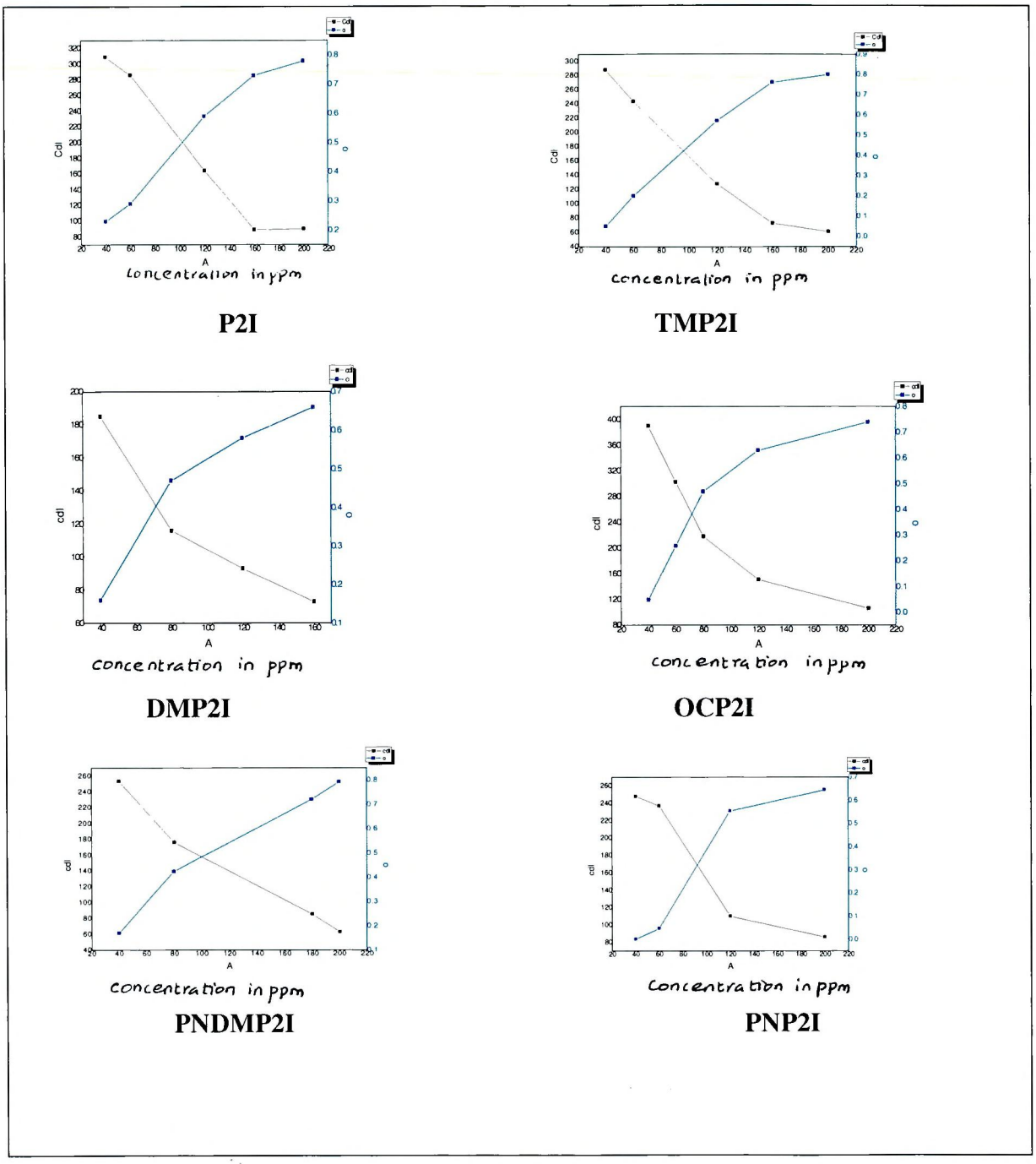

Figure- 67 Values of Cdl and θ of mild steel in the presence of current inhibitors in H_2SO_4 medium

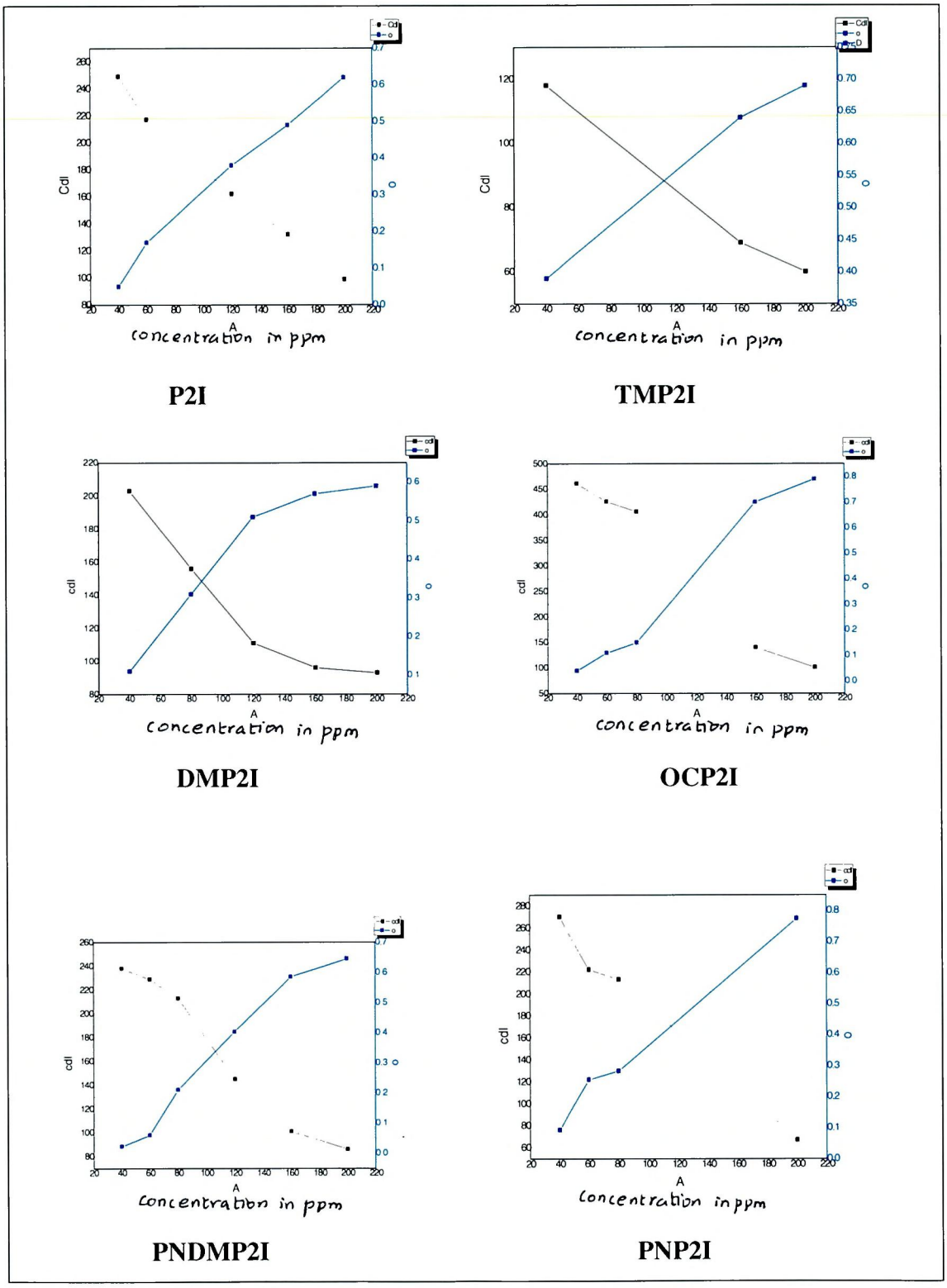

Figure- 68 Values of Cdl and θ of mild steel in the presence and absence of current inhibitors in HCl medium

A plot of C_{dl} values versus inhibitor concentration is drawn . A straight line is obtained. Similar plots are drawn for all the studied inhibitors which confirm that the inhibitor molecules adsorbed flatly on the metal surface.

Performance evaluation of imidazoline derivatives on mild steel acid corrosion in both acidic media by various techniques are depicted in Figure – 69.

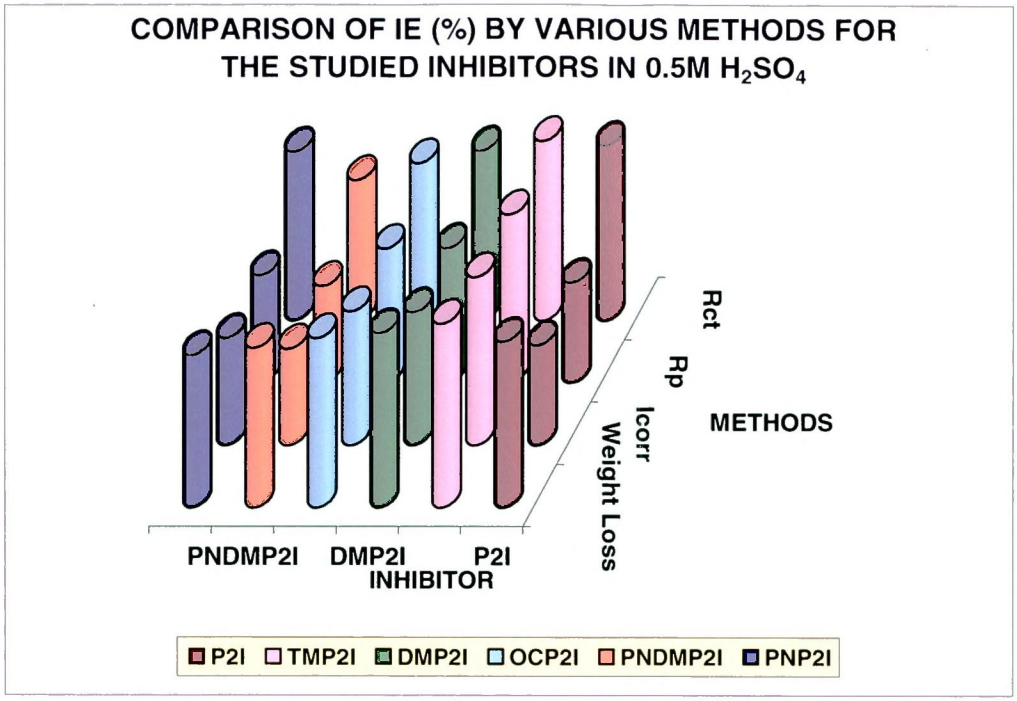

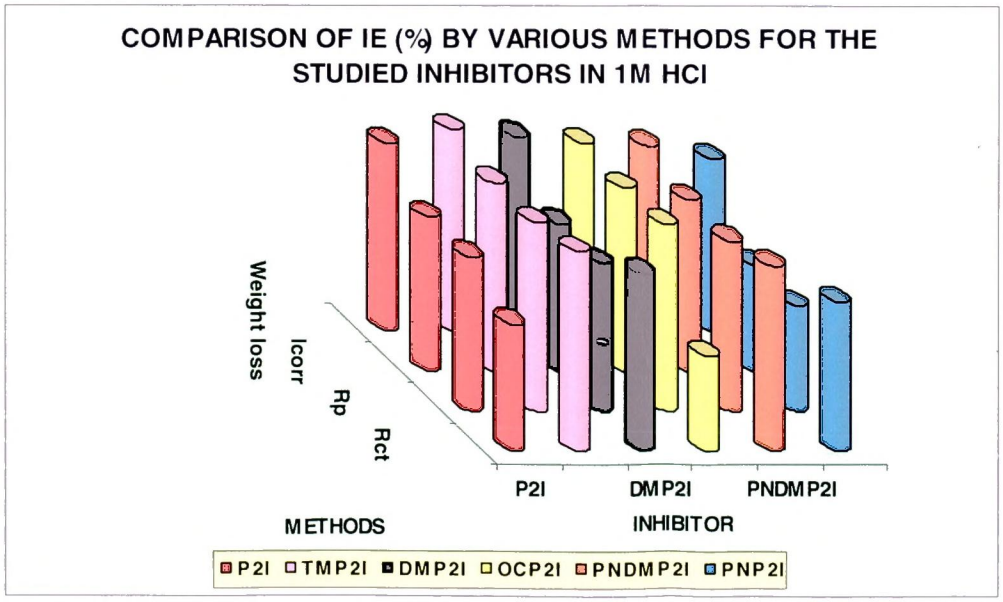

Figure – 69 Comparison of IE by various techniques.

4.4 Quantum Chemical Calculation

Quantum chemical methods and molecular dynamic simulation have become an effective way to study the correlation between molecular structure and inhibition properties . Quantum chemical calculations have proved to be a very powerful tool for studying corrosion inhibition mechanism and helped to design the novel high efficiency inhibitors by the Quantitative Structure-Activity Relationship (QSAR) method. Molecular dynamic simulation is adopted as a beneficial supplement of quantum chemical method, which is applied to study the interaction between inhibitors and metal surface

One of the aspects of recent corrosion inhibition studies is the use of quantum chemical methods to calculate electronic properties possibly relevant to explain the inhibiting action. Among all computer simulation methods, quantum chemistry calculation has been widely used to evaluate the inhibition performance of corrosion inhibitors, which can quantitatively study the relationship between inhibition efficiency and molecular reactivity. With this method, the capability of inhibitor molecules to donate or accept electrons can be predicted with analysis of global reactivity parameters, such as energy gap between Highest Occupied Molecular Orbital (HOMO) and Lowest Unoccupied Molecular orbital (LUMO), chemical potential, hardness, softness,dipole moment etc **(Khaled *et al.*, 2010).**

Quantitative structure-activity and structure property relationship studies are unquestionably of great importance in modern chemistry and biochemistry. The concept of Quantitative Structure-Activity Relationship (QSAR) and Quantitative Structure-Activity and Structure Property Relationship Studies (QSPR) is to transform searches for compounds with desired properties using chemical intuition and experience into mathematically quantified and computed form. Once a correlation between structure and activity/property is found, any number of compounds, including those not yet synthesized, can readily be screened on the computer. **(Jun Zhang et al., 2010)**

The reactive ability of the inhibitor is considered to be closely related to their frontier molecular orbitals, the HOMO and LUMO. Higher HOMO energy (E_{HOMO}) of the molecule means a higher electron donating ability to appropriate acceptor molecules with low-energy empty molecular orbital and thus explains the adsorption on metallic surfaces by way of delocalized pairs of π-electrons. E_{LUMO}, the energy of

the lowest unoccupied molecular orbital signifies the electron receiving tendency of a molecule.

In general, significant differences can be appreciated referring to the inhibitory efficiency of imidazoline. The understanding that the corrosion inhibition efficiency of organic compounds is related to their adsorption properties allows us to propose a possible mechanism. The inhibition efficiency depends strongly on the structures and chemical properties of the species formed under the experimental conditions studied. The extent of adsorption is dependent upon the electronic structure of the metal and the inhibitor.

Some organic compounds are found to be effective corrosion inhibitors for many metals and alloys. It has been commonly recognized that organic inhibitor usually promotes formation of a chelate on the metal surface, which includes the transfer of electrons from the organic compounds to metal, forming coordinate covalent bond during chemical adsorption process. In this way, the metal acts as an electrophile, whereas the nucleophilic centers of inhibitor molecule are normally hetero atoms with free electron pairs which are readily available for sharing, to form a bond. The most common organic substances with these characteristics are those containing N, O and/or S atoms

(Jian Fang *et al.*, 2002).

In research on organic corrosion inhibitors, attention is paid to the mechanism of adsorption and also to the relationship between inhibitor structures and their adsorption properties. It has been observed that the adsorption depends mainly on the electronic and structural properties of the inhibitor molecule such as functional groups, steric factors, aromaticity, electron density on donor atoms and π orbital character of donating electrons..

In the current investigation, to study the corrosion mitigation effect of the investigated inhibitor, theoretical calculations were performed for selected imidazoline derivatives – P2I, TMP2I and DMP2I. This study will give further insight into the experimental results. The P2I, TMP2I,DMP2I compounds have been fully optimized using the B3LYP hybrid functional and the 6-311 G basis set. The following quantum chemical parameters which indicate the structural characteristics of these inhibitors, were considered: E_{HOMO}, E_{LUMO}, ΔE and μ. The optimized geometry of the molecules and corresponding Frontier Molecular Orbital density

distribution of P2I, TMP2I and DMP2I are represented in Figure (71-73). It shows the values of some quantum chemical parameters, namely the energy of the highest occupied molecular orbital (E_{HOMO}), energy of the lowest unoccupied molecular orbital (E_{LUMO}), the energy gap ($_{ELUMO-HOMO}$) and dipole moment (μ) for the inhibitors P2I, TMP2I and DMP2I.

Phenyl-2-imidazoline (P2I) :

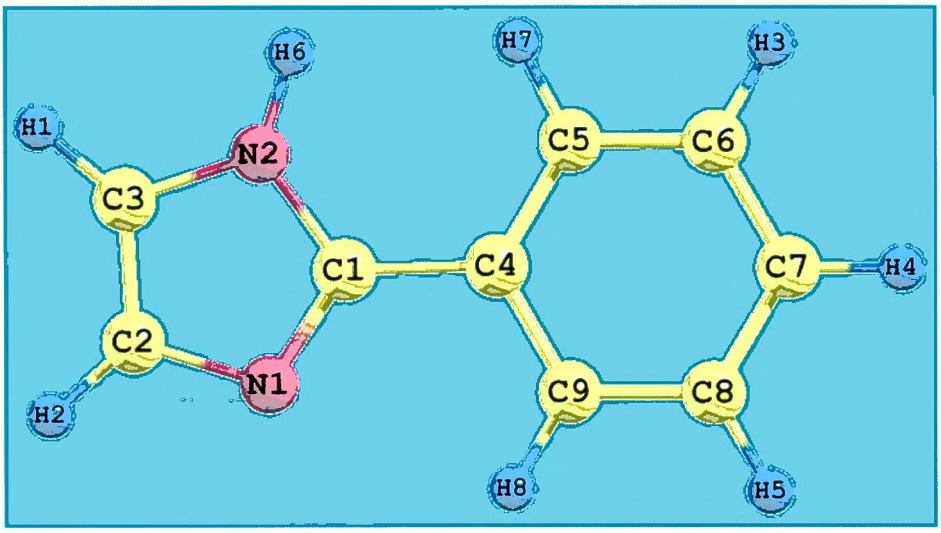

Figure – 71-a – Optimised structure of P2I

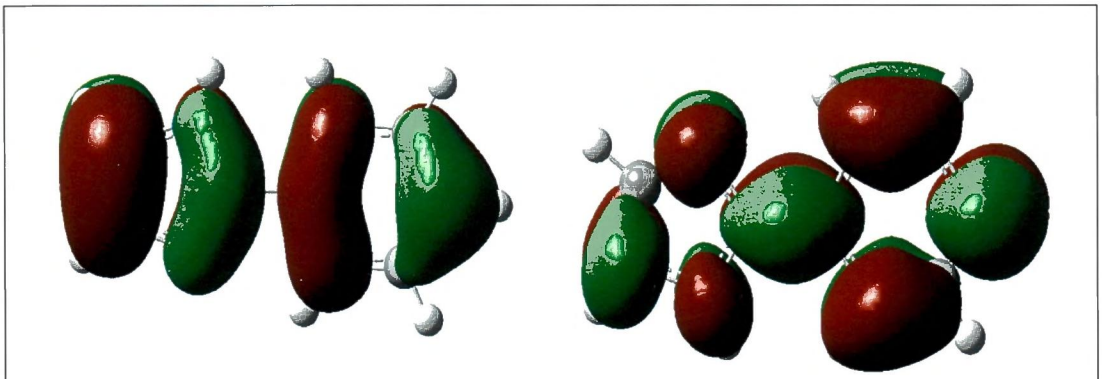

HOMO **LUMO**

Figure – 71 b & c Frontier Molecular orbital density distribution of P2I

2-(3',4',5'-Trimethoxyphenyl)-imidazoline (TMP2I):

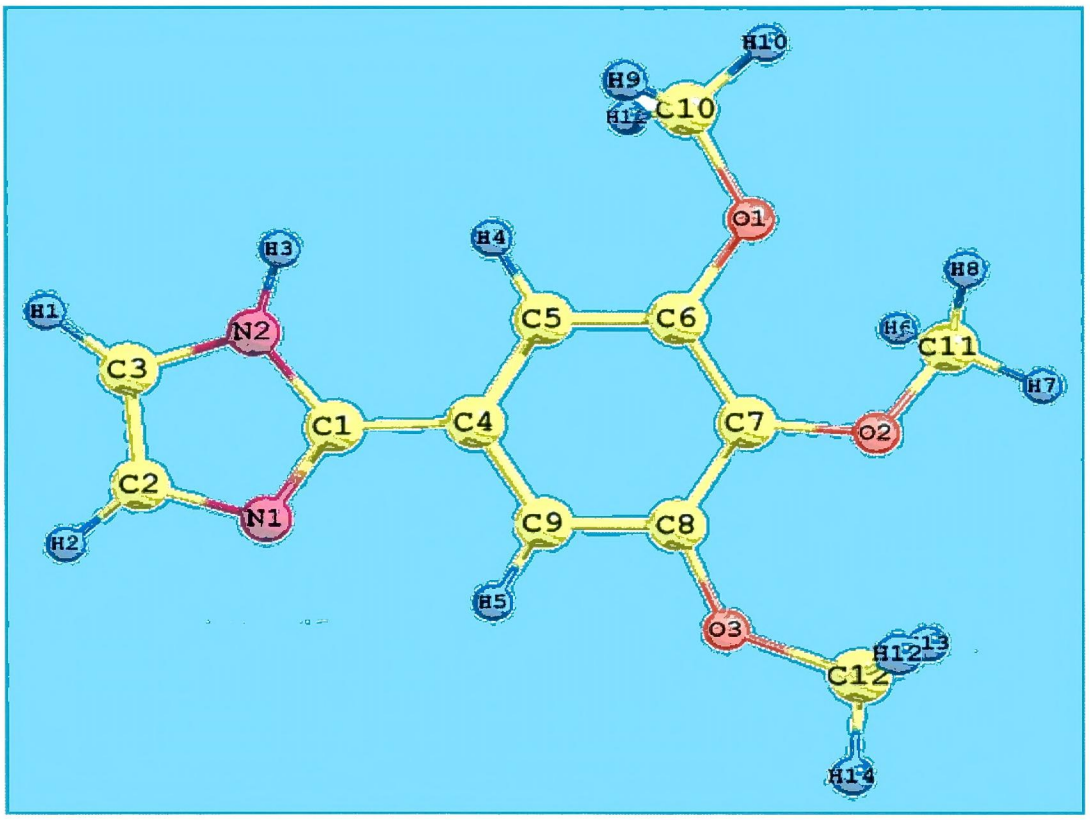

Figure – 72 –a Optimised structure of TMP2I

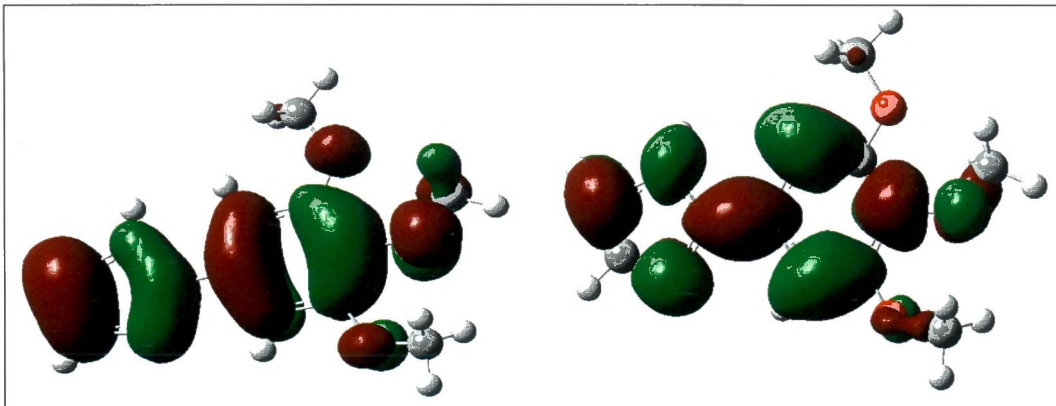

HOMO **LUMO**

Figure - 72 b&c Frontier Molecular orbital density distribution of TMP2I

2-(3',4',-Dimethoxyphenyl)-imidazoline (DMP2I):

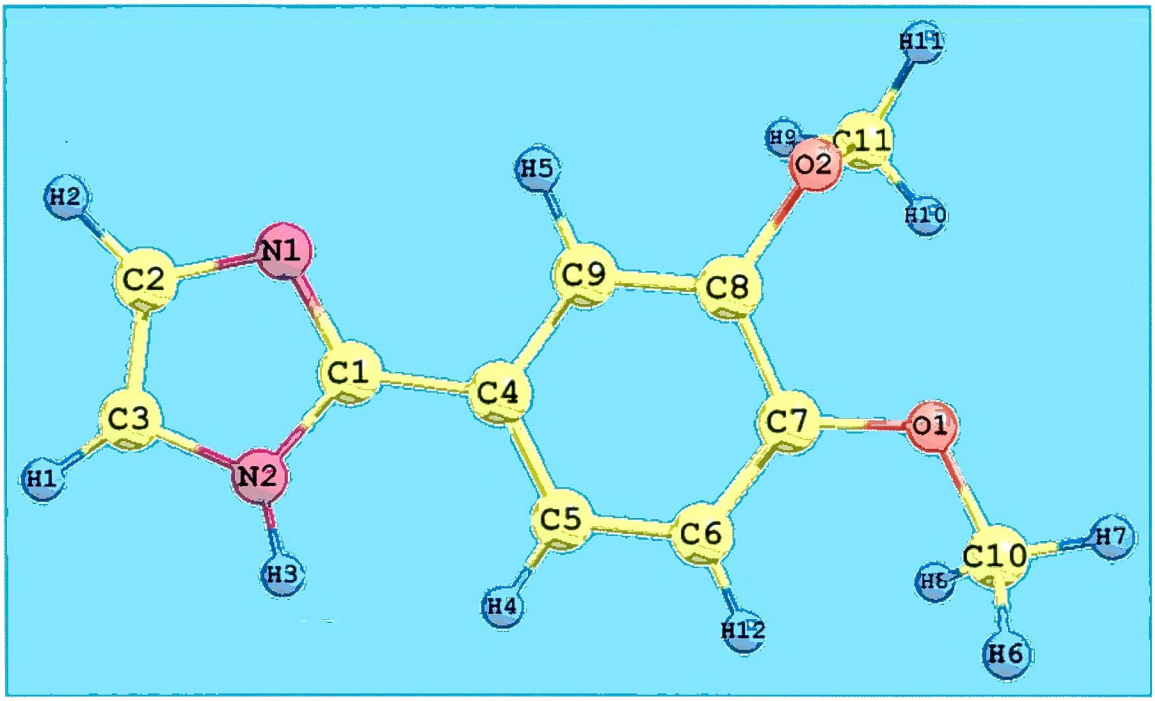

Figure – 73 a Optimised structure of DMP2I

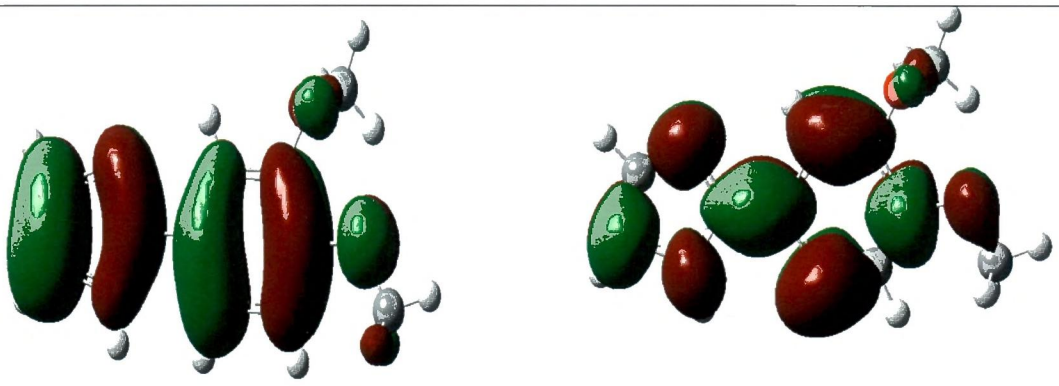

HOMO **LUMO**

Figure – 73 b& c Frontier Molecular orbital density distribution of DMP2I

Analysing the optimized geometry and Frontier Molecular orbital Denstiy Distribution of selected imidazoline derivatives, it is clear that the imidazoline ring being plane thus helping the interaction of imidazoline with the metal surface. The ground state geometry of the inhibitor as well as the nature of its molecular orbitals,

namely the HOMO and LUMO is involved in the acitivity properties of the inhibitors. When the frontier molecules are analysed, the HOMO are localized over the nitrogen atoms N2 and N5 of the plane imidazoline ring and the phenyl ring, consequently this is the preferred zone of the molecule interaction with the metal surface. Both the nitrogen atoms can coordinate with mild steel. Schematic representation of adsorption models of P2I, TMP2I and DMP2I are predicted based on this molecular interaction with the metal surface **(Curz *et al.*, 2004).**

4.4.1 Dipole Moment

The dipole moment (μ) is an index that can also be used for the prediction of the direction of a corrosion inhibition process. Dipole moment is the measure of polarity in a bond and is related to the distribution of electrons in a molecule. Although literature is inconsistent on the use of 'μ' as a predictor for the direction of a corrosion inhibition reaction, it is generally agreed that the adsorption of polar compounds possessing high dipole moments on the metal surface should lead to better inhibition efficiency. Comparison of the results obtained from quantum chemical calculations with experimental inhibition efficiencies indicated that the % inhibition efficiencies of the inhibitors increase with increasing value of the dipole moment **(Eno.E.Ebenso *et al.*, 2010).**

Our results indicate that the value of μ for the studied inhibitors according to the trend **TMP2I>DMP2I>P2I** obtained using weight loss and electrochemical techniques. Our experimental results using various techniques are strongly supported by theoretical Quantum chemical calculation **(Eno.E.Ebenso *et al.*, 2010).**

4.4.2 E_{HOMO} & E_{LUMO}

The HOMO energy (E_{HOMO}) is often associated with the electron density ability of the molecule, whereas the (E_{LUMO}) indicates the ability of the molecule to accept electron. Therefore, high values of the E_{HOMO} indicate an increased tendency of the inhibitor to donate electron to the vacant d orbital of Fe in mild steel. Similarly, E_{LUMO} represents the ability of the molecule to accept electrons. The lower the values of E_{LUMO}, the more probable it is that the molecule would accept electrons. According to Wang et al high values of the E_{HOMO} facilitate adsorption and enhance inhibition efficiency by influencing the transport process through the adsorbed layer. Large values of energy gap (EL-H = E_{LUMO} - E_{HOMO}) implies increased electronic stability

and low reactivity, while low values render good inhibiting efficiency because the energy to remove an electron from the last occupied orbital will be low.

Analysis of Table- 44, indicated that the values of E_{HOMO} of P2I, TMP2I, DMP2I compounds increased in the following order: **TMP2I>DMP2I>P2I.**

The values of ΔE decreased in the following order: **TMP2I<DMP2I<P2I.** The sequence of E_{HOMO} and ΔE support the results obtained from weight loss and electrochemical measurements. The inhibition efficiency increased with increase in the E_{HOMO} and decrease in ΔE. TMP2I has the highest E_{HOMO} and lowest ΔE among these compounds. Therefore, TMP2I has the strongest interaction with iron surface and affords best inhibition effect.

4.4.3 ΔN (number of electrons):

The number of electrons transferred (ΔN) from the inhibitor molecule to the metallic atom was also calculated using the following equation:

$$\Delta N = \frac{\chi_{Fe} - \chi_{inh}}{2(\eta_{Fe} + \eta_{inh})} \longrightarrow (1)$$

where χ_{Fe} and χ_{inh} represent the absolute electronegativity of iron and the inhibitor molecule, respectively and $\eta_{Fe} + \eta_{inh}$ represent the absolute hardness of iron and the inhibitor molecule. These quantities are associated with electron affinity (EA) and ionization potential (IP) which are useful in their ability to help chemical behaviour.

$$\chi = \frac{IP + EA}{2}$$

$$\eta = \frac{IP - EA}{2}$$

where IP and EA are related in turn to E_{HOMO} and E_{LUMO} as following equations:

$$IP = -E_{HOMO} \text{ and } EA = -E_{LUMO}$$

Inorder to calculate ΔN, a theoretical value for the electronegativity of bulk iron was used $\chi_{Fe} \approx 7$ eV and global hardness of $\eta_{Fe} \approx 0$, by assuming that for a metallic bulk IP = EA, because they are softer than the neutral metallic atoms. The values of ΔN for P2I, TMP2I, DMP2I are represented in Table- 45.

If $\Delta N < 3.6$, the inhibition efficiency increased with increasing electron donating ability at the metal surface. It can be inferred from the calculation results that inhibitors investigated in this current study were donating of electrons and the

iron surface was the acceptor. Order of ΔN is as follows: **TMP2I = DMP2I > P2I** which in accordance with the change in trends of E_{HOMO} and inhibition efficiency. The highest inhibition efficiency of TMP2I can be attributed to the strongest coordinate bonds formed between the lone electron pairs of heterocyclic atom/π electrons of imidazoline ring and the phenyl ring and the vacant d-orbitals of the metal surface (**Jia-jin Fu et al., 2010**)

Table – 44 Quantum chemical parameters for the studied inhibitors using Gaussian 03 W code of programs using B3LYP hybrid functional and the 6-311 G basis set

Inhibitor	HOMO eV	LUMO eV	TOTAL ENERGY eV	ΔE Change in energy eV	DIPOLE MOMENT (Debye)	ΔN Number of Electrons
P2I	-0.21517	-0.03702	-12446.589475	-0.17815	3.1939	1.666
TMP2I	-0.19307	-0.02318	-21797.68962	-0.16989	5.6758	1.739
DMP2I	-0.20182	-0.02655	-18680.83821	-0.17527	5.0548	1.739

Table -45 Calculated Quantum chemical parameters for the studied inhibitors using Gaussian 03 W code of programs using B3LYP hybrid functional and the 6-311 G basis set

Inhibitor	Ionisation Potential IP (eV)	Electron Affinity EA(eV)	Hardness η (eV)	Softness S (eV)	Electro negativity χ(eV)	Electrophilic Index ω
P2I	5.8	1.00	2.4	0.20	3	2.1
TMP2I	5.2	0.6	2.3	0.21	3	7.0
DMP2I	5.4	0.7	2.3	0.21	3	5.6

4.4.4 Global Softness

As expected, there are some similarities in the trends between the above parameters and frontier orbital molecular energies. The global softness S for the investigated inhibitors are the same, suggesting that softer molecules are stronger inhibitors. Calculated values of S and η are also presented in Table -45. From Table 45, it is evident that the inhibitor with the least value of global hardness (hence the highest

value of global softness) is the best and *vice versa*. This is because a soft molecule is more reactive than a hard molecule. This observation is consistent with the results obtained from experimental % inhibition efficiencies **(Eno.E.Ebenso *et al.*, 2010).**

4.4.5 Ionization Potential and Electron Affinity

Values of *IE* and *EA* calculated are presented in Table- 45. The results obtained indicate that the inhibition efficiencies of the inhibitors increase with increasing ionization energy but decrease with decreasing value of electron affinity. This is because IP is directly related with the *E*HOMO, while *EA* is related to the *E*LUMO. This explains why the trend for the variation of inhibition efficiencies of the inhibitors with IP and EA are similar to those obtained for E_{HOMO} and E_{LUMO} data. According to the data the trend in IE and EA are as follows:

TMP2I > DMP2I >P2I

Figure (71-73) represent the optimized structures and the HOMO and LUMO diagrams of P2I, TMP2I and DMP2I. The spatial distribution of the HOMO and the LUMO are important for understanding the adsorption preferences of the inhibitors. Considering that the inhibitors would be electron donors with respect to the steel surface, the HOMO distribution would be of particular importance. The HOMO distribution maps of P2I, TMP2I and DMP2I are very similar and the HOMO is localized on the imidazoline ring and the benzene ring suggesting strong docking to the imidazoline ring and benzene ring. The LUMOs of all three inhibitors have very similar spatial distribution **(Eno.E.Ebenso *et al.*, 2010).**

The quantum chemical parameters reveal that the inhibition efficiency of the studied inhibitors follow the same trend **TMP2I>DMP2I>P2I** as obtained from weight loss and electreochemical measurements. It is evident from Quantum Chemical Calculation, that our experimental results and theoretical calculations could go hand to hand.

4.5 Surface Analytical Techniques

4.5.1 FTIR Spectra:

FTIR studies help to predict the functional groups of the adsorption bands and the arrangement of the inhibitor molecules on the surface of the metal. To find out the types of bonding for organic molecule adsorbed on the surface of solid, FTIR study has been conducted. Several researchers have confirmed that FTIR spectrometry is a powerful tool that can be used to determine the type of bonding for organic inhibitors.

In this paper, FTIR spectrometry was used to identify whether there was adsorption and to provide new bonding information on the steel surface after immersion in inhibited acid solutions. In the present investigation FTIR spectra of the inhibitors, corrosion product obtained in H_2SO_4 and HCl medium for all the investigated inhibitors are presented and discussed.

P2I:

The FT IR spectra of P2I, corrosion product in both medium are depicted in Figure - 74

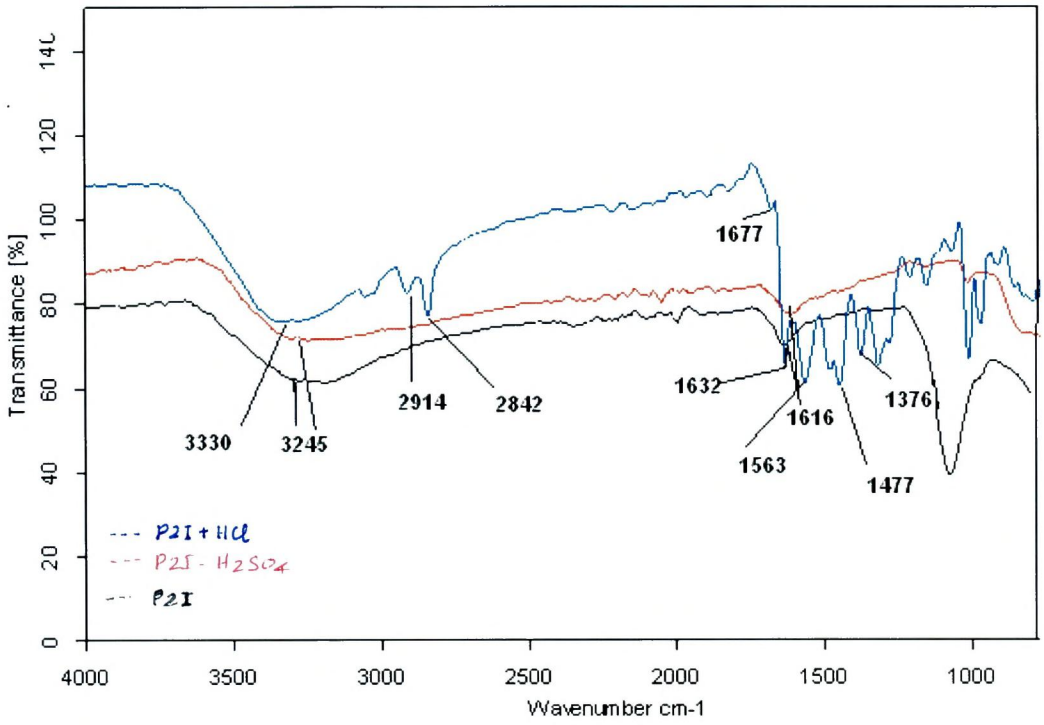

Figure -74 FT IR spectra of P2I and the corrosion products of P2I in 0.5 M H_2SO_4 and in 1M HCl

The IR spectrum of the compound P2I showed the characteristic peaks of the imidazoline ring with wave numbers of 1677 cm^{-1} for stretching vibration of C=N, 1632 cm^{-1} for stretching vibration of N=C-C, 1563, 1477 and 1376 cm^{-1} for C-N-C stretching vibrations, N-H group is confirmed by the peak at 3330 cm^{-1} . Peaks at 2914 cm^{-1} and 2842 cm^{-1} are due aromatic and aliphatic C-H stretching vibrations respectively.

Frequencies and peaks of adsorption of IR for the corrosion product of P2I adsorbed on the mild steel in the presence of H_2SO_4 and HCl were discussed as follows:

From the results it was found that the N-H stretch at 3330 cm^{-1} was shifted to 3245 cm^{-1} and N=C-C stretch at 1632 cm^{-1} was shifted to 1616 cm^{-1} indicating that there interaction between the inhibitor and the mild steel surface. Other functional groups were missing suggesting that the adsorption of the inhibitor on the mild steel surface might have occurred through the missing bonds.

TMP2I:

Infrared spectroscopy is a useful technique in characterizing structures of materials. FTIR analysis was done to study the adsorption of TMP2I in both acidic media. FTIR spectra of TMP2I, TMP2I-H_2SO_4 and TMP2I-HCl are shown in Fig -75. The FTIR analysis of TMP2I shows major peaks related to imidazoline and aromatic ring.. The peaks at 1636 cm^{-1} is assigned to C=N stretching vibration. The absorption peaks at 3005 cm^{-1}, 2919 cm^{-1}, 2827 cm^{-1} are due to aromatic & aliphatic C-H stretching vibrations respectively.. A broad singlet observed at 3370cm^{-1} is due to N-H vibrations . The peak at 1227 cm^{-1} can be assigned to Ar-O-CH_3 vibration. The C-N-C vibrations are observed at 1577 cm^{-1}, 1498 cm^{-1}, 1367 cm^{-1}.

Figure – 75 shows the FTIR spectrum of the corrosion product of mild steel in H_2SO_4 in the presence of TMP2I. The slight shift in N-H and C=N bands to 3132 cm^{-1} and 1616 cm^{-1} are observed. The peaks due to aromatic ring disappeared. So, the Π–electronic cloud of phenyl ring and the lone pair electron of the nitrogen atom may act as electron donors and forms a complex with Fe^{2+} and prevents corrosion.

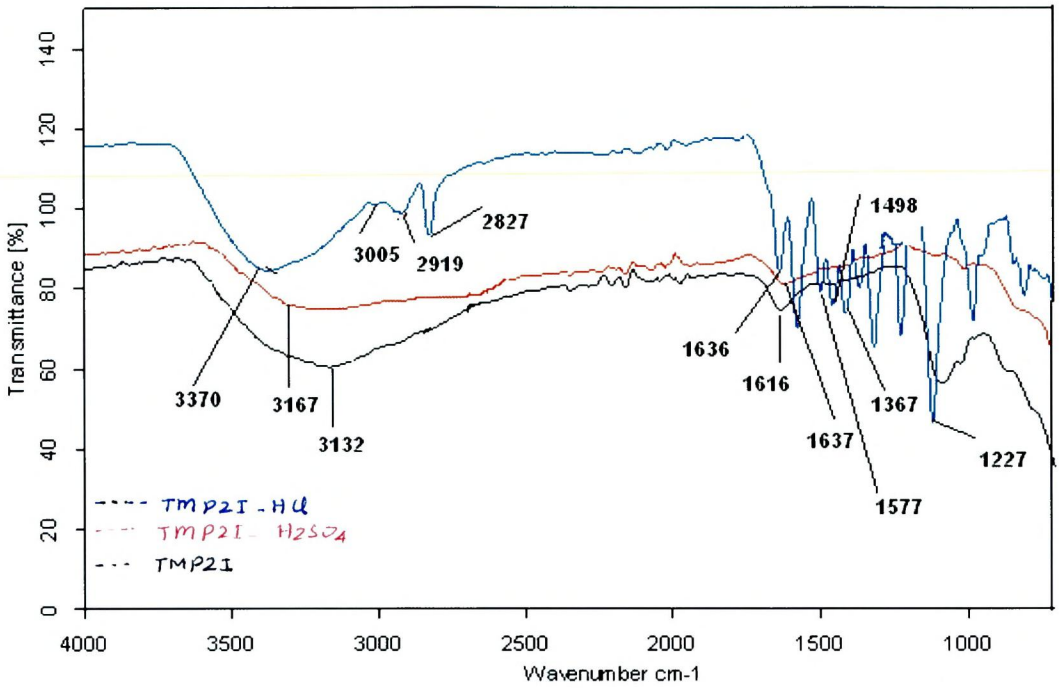

Figure-75 **FT IR spectra of TMP2I and the corrosion products of TMP2I in 0.5 M H_2SO_4 and 1M HCl**

DMP2I:

The FT IR spectra of DMP2I is as shown in the Figure- 76

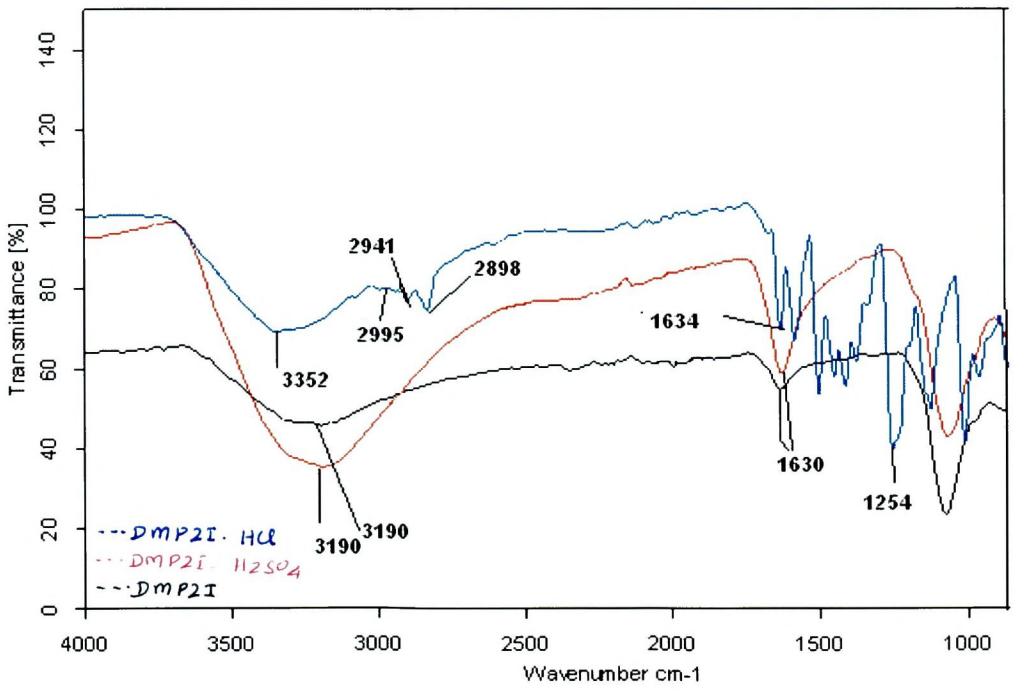

Figure- 76 FT IR spectra of DMP2I and the corrosion products of DMP2I in 0.5 M H_2SO_4 and 1M HCl

The FT IR spectra for DMP2I shows characteristic peaks for imidazoline and the aromatic ring. The absorption peak at 1634 cm^{-1} is assigned to C=N stretching vibration. The presence of aromatic ring is confirmed by the peaks at 2995 cm^{-1}, 2941 cm^{-1} and 2898 cm^{-1}. A broad, strong band at 3352 cm^{-1} is the characteristic peak of N-H vibration. The peak at 1254 cm^{-1} is attributed to the Ar-O-CH_3 vibration .

Analysis of the FT IR spectra of the corrosion product of DMP2I in acidic media, it was found that the N-H strech at 3352 cm^{-1} was shifted to 3190 cm^{-1} and the C=N was shifted from 1634 cm^{-1} to 1630 cm^{-1}. Other functional groups were missing suggesting and the adsorption of the inhibitor on the surface of mild steel might have occurred through the missing bonds.

OCP2I:

FT IR spectral studies were carried out for OCP2I and mild steel surface immersed in 0.5M H_2SO_4 and 1M HCl with OCP2I and their respective FT-IR spectra are as shown in Figure- 77

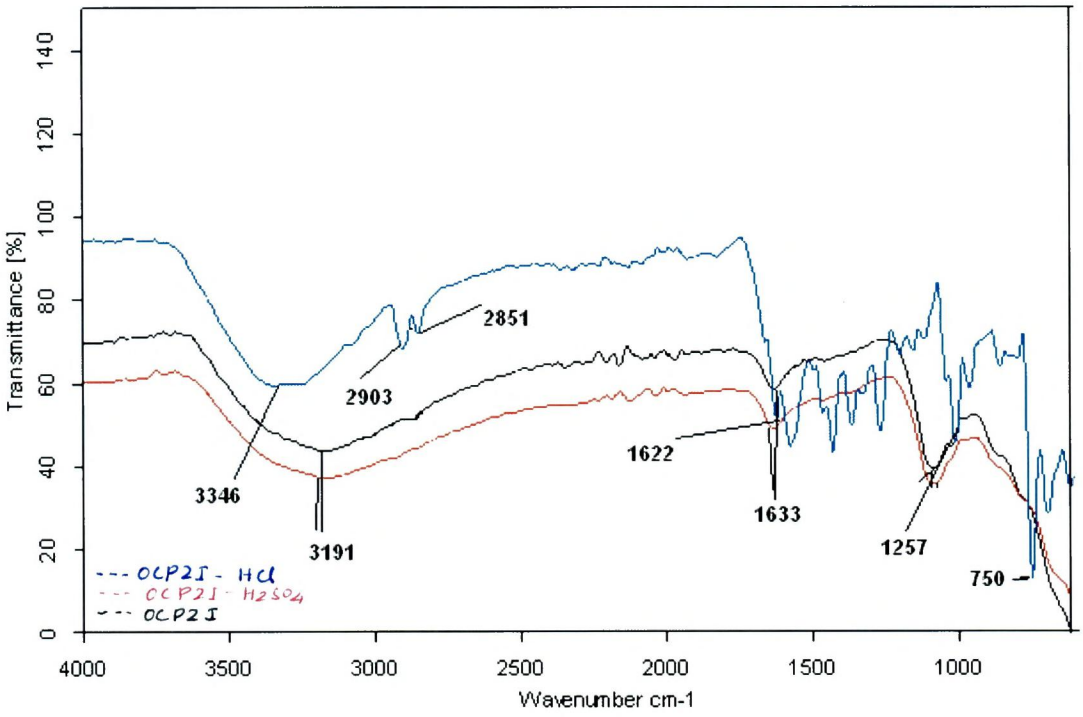

Figure – 77 **FT IR spectra of OCP2I and the products of OCP2I in 0.5 M H_2SO_4 and 1M HCl**

The formation of OCP2I is confirmed by the storng broad absorption peak at 3346 cm^{-1} due to N-H vibrations, peak at 1622 cm^{-1} is due to C=N stretching frequency and the peaks at 2903 cm^{-1} and 2852 cm^{-1} indicate the presence of aromatic ring and the Ar-Cl bond is confirmed by the peak at 750 cm^{-1}.

Analysis of the FT IR spectra of the products of OCP2I in 0.5 M H_2SO_4 and 1M HCl indicate there is shift in the peak due to N-H vibration from 3346 cm^{-1} to 3191 cm^{-1} and the peak due to C=N from 1622 cm^{-1} to 1633 $cm^{-1}$and the peaks due to other functional groups were missing confirming the formation of complex with Fe^{2+} and prevents corrosion.

PNDMP2I:

FT IR spectra of PNDMP2I and corrosion product of mild steel in 0.5 M H_2SO_4 and 1M HCl containing PNDMP2I is shown in Figure- 78

Figure-78 FT IR spectra of PNDMP2I and the co

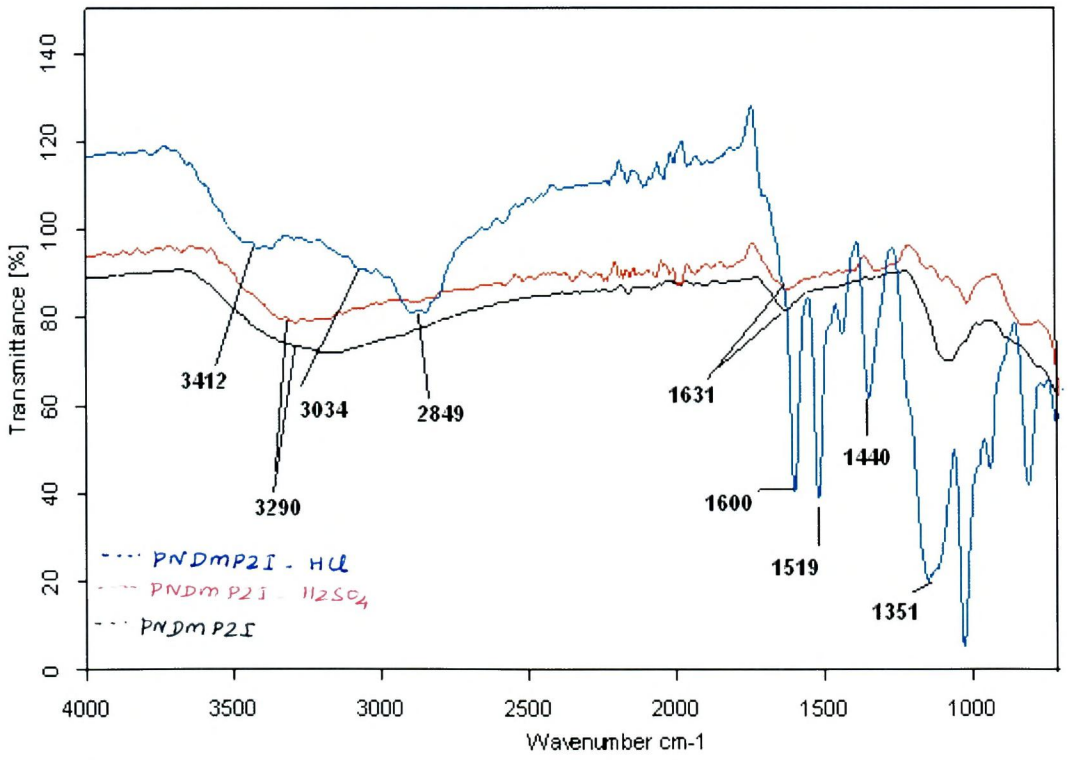

Figure – 78 FT IR spectra of PNDMP2I and the corrosion products of PNDMP2I in 0.5 M H_2SO_4 and 1M HCl

The spectrum show a broad singlet peak at 3412 cm^{-1} which is attributed to N-H stretching vibration.Appearance of absorption peaks at 3034 cm^{-1} and 2849 cm^{-1} are due to aromatic and aliphatic stretching frequencies. The C-N-C vibrations are observed at 1519 cm^{-1}, 1440 cm^{-1} and 1351 cm^{-1}. A band arising from C=N stretching is observed at 1631 cm^{-1}. The peak at 1351 cm^{-1} is the characteristic peak of tertiary amine ($-N(CH_3)$).

The FT IR spectrum of the corrosion product of mild steel in acid media containing PNDMP2I show a shift in the band due to N-H and C=N from 3412 cm^{-1} to 3290 cm^{-1} and from 1631 cm^{-1} to 1600 cm^{-1} respectively. The disappearance of peaks due to other functional groups proves the formation of complex with Fe^{2+} and prevents corrosion.

PNP2I:

Figure –79 shows the FT IR spectra of PNP2I .

The IR spectrum of PNP2I shows a broad singlet in the region 3340 cm^{-1} due to N-H stretching frequency. The peak at 1571 cm^{-1} can be assigned to C=N group. The aromatic and aliphatic C-H frequencies are characterized by peaks at 3100 cm^{-1}, 2903 cm^{-1} and 2852 cm^{-1} . The peak at 1488 $cm^{-1}$and 1410 cm^{-1} are attributed to the stretching frequencies of C-N-C . The FT IR confirms the formation of PNP2I.

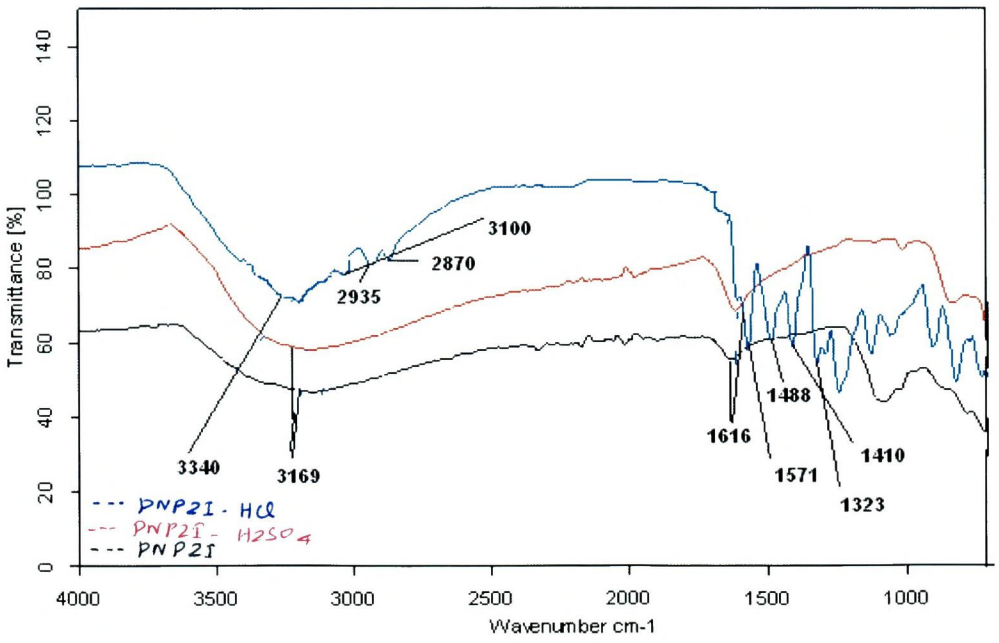

Figure – 79 FT IR spectra of PNP2I and the corrosion products of PNP2I in 0.5 M H_2SO_4 and 1M HCl

The FT IR spectrum of the corrosion product of mild steel in 0.5 M H_2SO_4 and 1M HClreveals that frequencies and absorption due to C=N and N-H are shifted to 1616 cm^{-1} and 3169 cm^{-1} respectively. The formation of Fe^{2+} complex is confirmed by the disappearance of peaks due to other functional groups and there is interaction between the PNP2I and the mild steel surface. **(Nnabuk Okon Eddy 2009).**

4.5.2 UV-Visible Spectroscopy:

A substantial support for the formation of metal complexes is often obtained by UV-visible spectroscopic investigation. Since there is often a certain quantity of metal cation in the solution that is first dissolved from the metal surface, such procedures were conducted in the present work to confirm the possibility of the formation of [Imidazoline-Fe^{2+}] complexes as described by **Obi *et al.*, (2010).** Furthermore, it has been reported that change in position of the absorbance maximum and change in the value of absorbance indicate the formation of a complex between two species in solution.

In order to confirm the possibility of the formation of Imidazoline-Fe^{2+} complex, UV-Visible absorption spectra obtained from 0.5 M H_2SO_4 and 1M HCl solution containing 200 ppm of the inhibitors before and after three days of mild steel immersion are shown in Figures (-80-85).

P2I

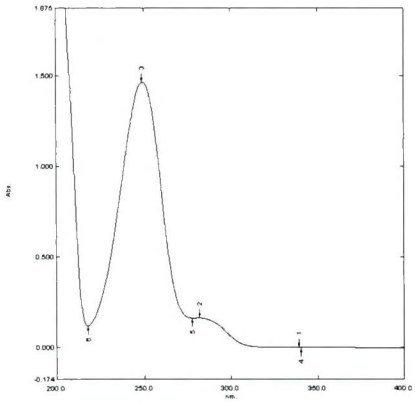

Fig – a

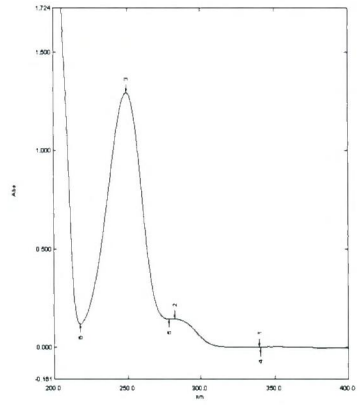

Fig – b

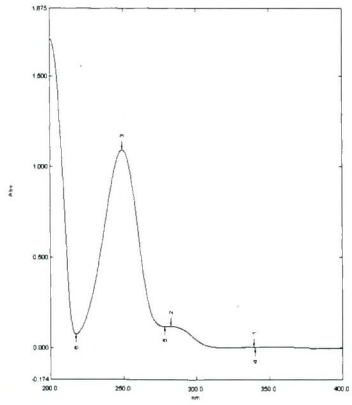

Fig – c

UV-Visible Spectra of P2I (Fig – 80 a), the solution containing H_2SO_4 +P2I (Fig - 80b), HCl + P2I (Fig – 80 c) after three days of mild steel immersion

TMP2I

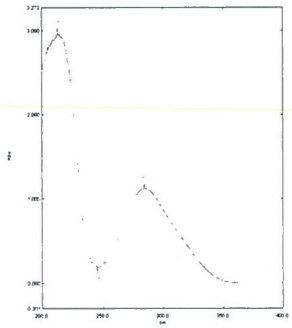

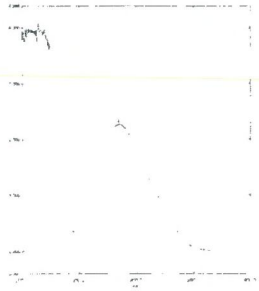

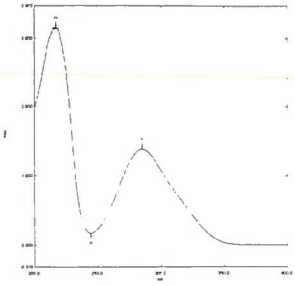

Fig – a **Fig – b** **Fig – c**

UV-Visible Spectra of TMP2I (Fig –81 a), the solution containing H_2SO_4 + TMP2I (Fig - 81b), HCl + TMP2I (Fig –81 c) after three days of mild steel immersion

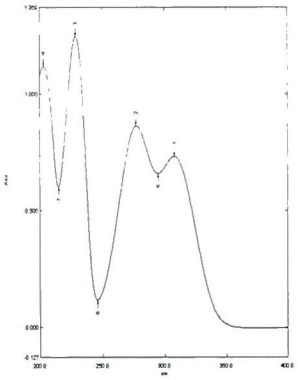

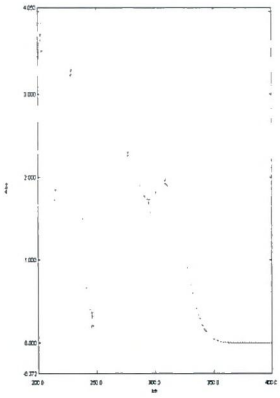

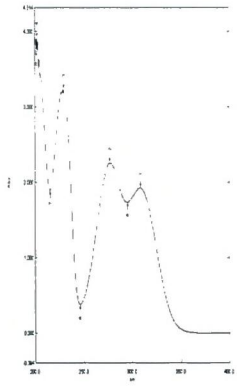

UV-Visible Spectra of DMP2I (Fig –82 a), the solution containing H_2SO_4 + DMP2I (Fig -82 b), HCl + DMP2I (Fig – 82c) after three days of mild steel immersion

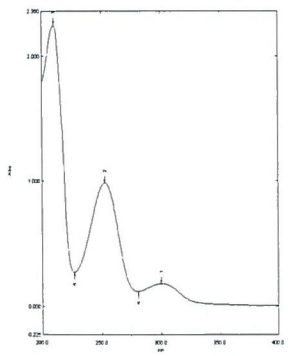

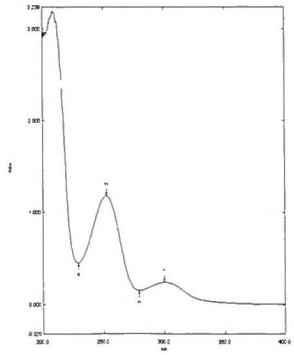

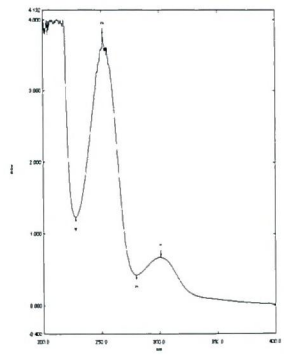

UV-Visible Spectra of OCP2I (Fig – 83a), the solution containing H_2SO_4 + OCP2I (Fig - 83b), HCl + OCP2I (Fig – 83c) after three days of mild steel immersion

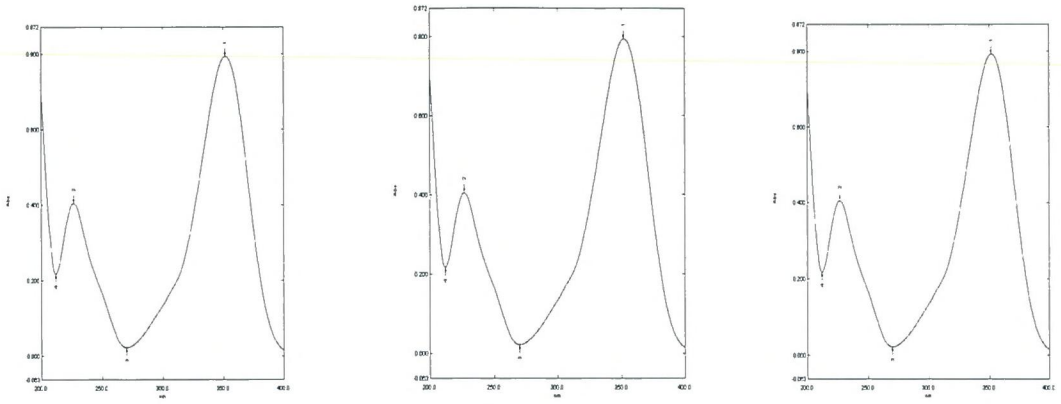

Fig – a **Fig – b** **Fig – c**

UV-Visible Spectra of PNDMP2I (Fig –84 a), the solution containing H_2SO_4 + PNDMP2I (Fig - 84b), HCl + PNDMP2I (Fig – 84c) after three days of mild steel immersion

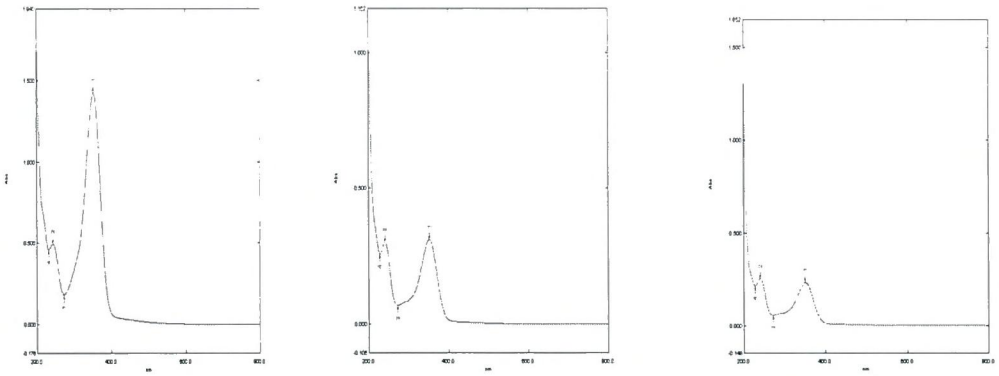

UV-Visible Spectra of PNP2I (Fig – 85a), the solution containing H_2SO_4 + PNP2I (Fig - 85b), HCl+ PNP2I (Fig –85 c) after three days of mild steel immersion

The UV spectra of P2I displayed two bands at 282.5 nm and 294.4 nm due to π- π^* transition and n- π^* transition respectively.

For the UV spectra of TMP2I displayed two bands at 284.4 nm due to π- π^* transition and 216.7 nm due to n- π^* transition.

For DMP2I, the UV spectra displayed bands at 228.8 nm and 277.0 nm for the π- π^* transition and n- π^* transition respectively.

Bands at 252.5 nm and 210.1 nm correspond to the π- π^* transition and n- π^* transition respectively for OCP2I.

π- π* transition and n- π* transition are confirmed by two bands at 231.1nm and 351.8 nm respectively for PNDMP2I .

The UV spectra of PNP2I displayed two bands at 243.2 nm and 351.8 nm due to π- π* transition and n- π* transition respectively.

After three days of steel immersion it is clearly seen that the band maximum underwent a blue shift suggesting the interaction between imidazoline derivative and Fe^{2+} ions in the solution. Furthermore there is an increase in the absorbance of this band. These experimental findings furnish a strong evidence for the possibility of the formation of a complex between Fe^{2+} cation and imidazoline in 0.5M H_2SO_4 and 1M HCl. **(Obi-Egbedi *et al.*, 2010).**

4.5.3 Scanning Electron Microscopy

Scanning electron microscope (SEM) Model JEOL MODEL JSM 6360 was used to study the morphology of corroded surface in presence and absence of inhibitors. The specimens were thoroughly washed with double distilled water. They were photographed at appropriate magnifications. To understand the morphology of the mild steel surface in absence and presence of inhibitors, the following cases have been examined.

i) Polished mild steel specimen

ii) Mild steel specimen immersed in O.5M H_2SO_4

iii) Mild steel specimen immersed in 0.5M H_2SO_4 containing 200 ppm concentration of the inhibitors P2I, TMP2I, DMP2I OCP2I, PNDM2I, and PNP2I.

SEM images of the mild steel specimens confirms the formation of adsorbed layer on the metal surface. The SEM photographs are given in Figure -93. The surface morphology of the sample before immersion in 0.5 M H_2SO_4 solutions show a freshly polished steel surface (Figure -93), and the scratches are from mechanical polishing treatment. Figure – 93 shows the surface morphology in the absence of the inhibitor, the mild steel surface was highly corroded with areas of corrosion. SEM images of the mild steel surface after immersion in 1M HCl with 200 ppm inhibitor of P2I, TMP2I, DMP2I, OCP2I, PNDMP2I and PNP2I are shown in Figure – 93 where it can be seen that the rate of corrosion is suppressed, and there is little acid corrosion product on the steel surface, even the original polishing scratches are see,.

This clearly reveals that there is a good protective layer on the mild steel surface, decreasing the extent of corrosion. **(Wei-hua Li *et al.*, 2008).**

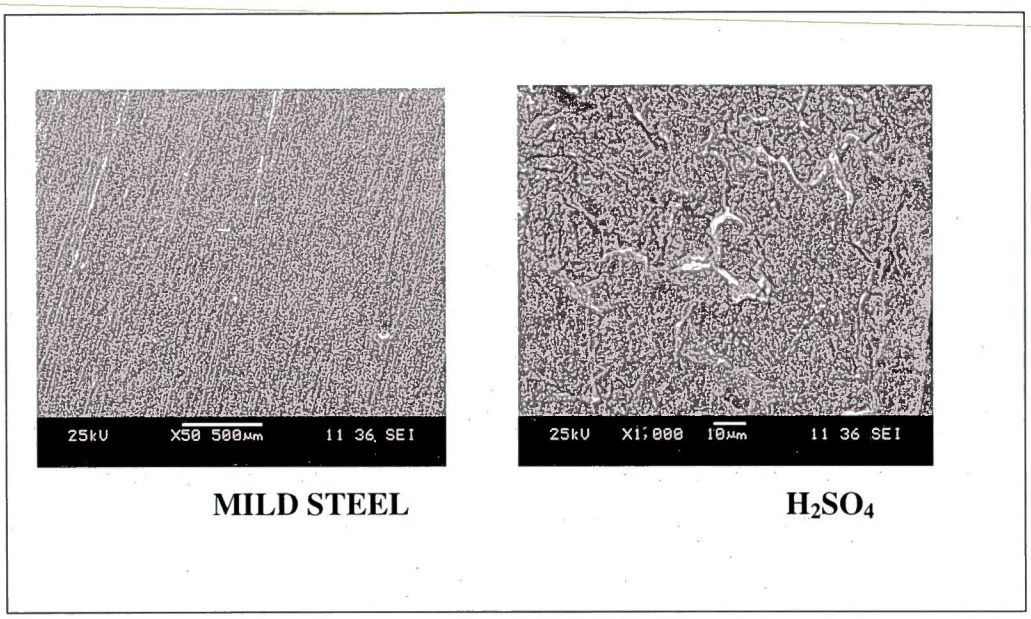

MILD STEEL **H_2SO_4**

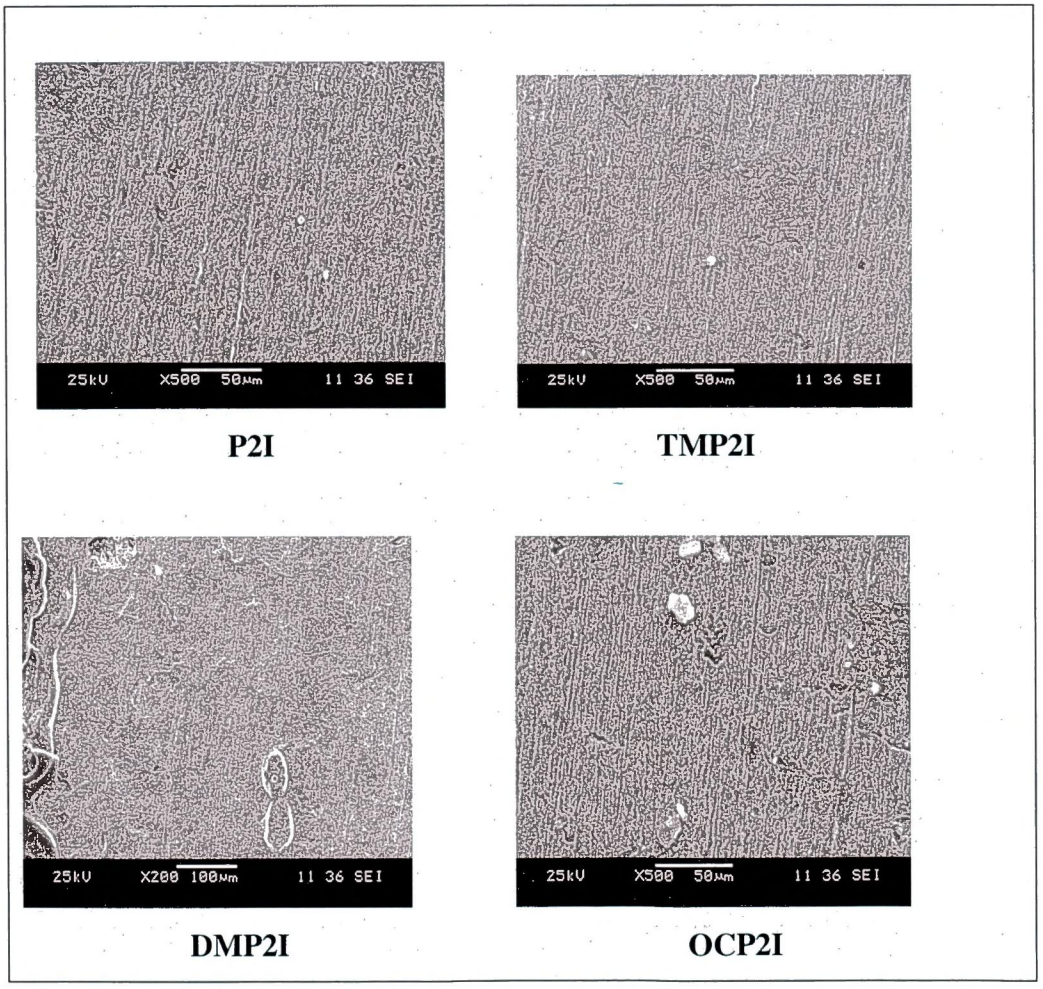

P2I **TMP2I**

DMP2I **OCP2I**

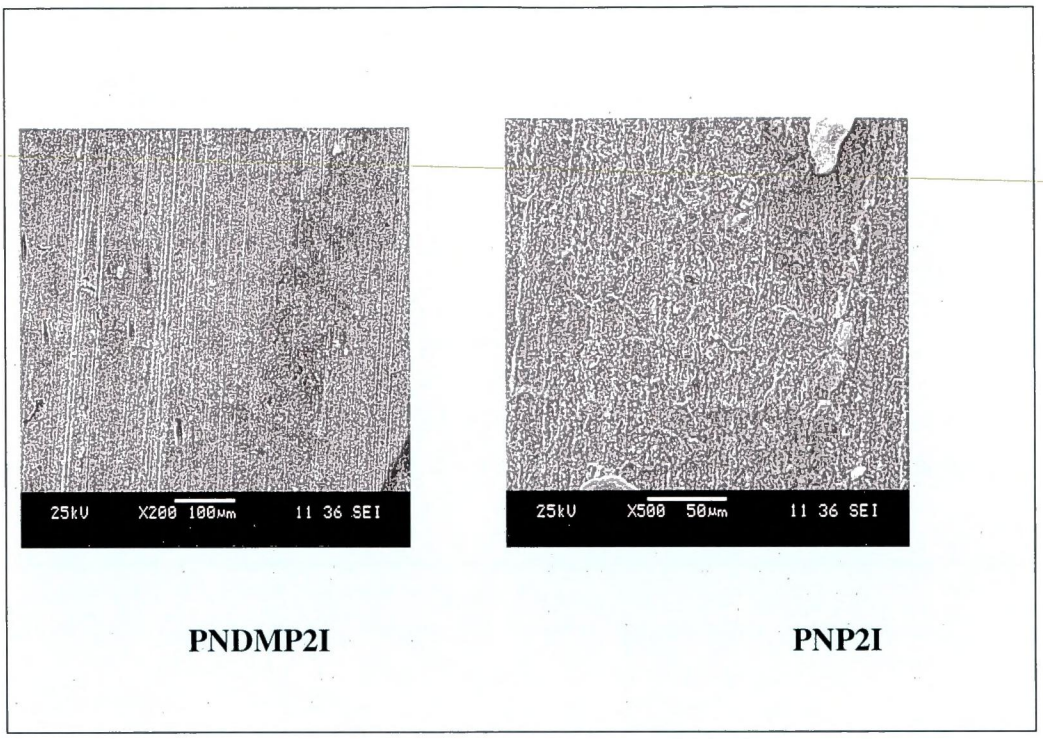

Figure – 93 SEM images of mild steel in the presence and absence of studied inhibitors

4.6 Mechanism of Corrosion:

Mechanism of the inhibition process can be discussed on the basis of the experimental findings from weight loss, electrochemical measurements, surface analytical techniques and quantum chemical studies.

In the present investigation on corrosion inhibition of mild steel using the imidazoline derivatives could furnish the following results:

All the investigated inhibitors obey Langmuir and Temkin adsorption isotherm indicating that the imidazoline derivatives are adsorptive type. The inhibition process is due to the adsorption of the inhibitor molecule onto the mild steel surface.

The large and negative values of ΔG_{ads} could confirm that the adsorption process is comprehensive adsorption (i.e both physical and chemical adsorption)

Inspection of the data from El Awady adsorption isotherm shows that the values 'x' are less than one and are approximately equal to one which mean that a given inhibitor molecule will occupy more than one active site. Values show that the imidazoline molecules occupy more than one active site.

Values of cathodic and anodic Tafel constant confirmed that the imidazoline derivatives under study act as mixed type of inhibitors.

Surface analytical techniques using FTIR spectroscopic studies confirm the adsorption of the imidazoline molecules and thus prevents the mild steel corrosion by the donation of π-electrons of the nitrogen atoms and the phenyl ring.

Surface analysis of the mild steel using SEM and UV-Visible spectrophotometer also confirm the adsorption of the inhibitor on the mild steel.

The results of quantum chemical studies, i.e the optimized structures of the studied inhibitors also confirm the donation of π-electrons to the mild steel surface.

A clarification of the mechanism of inhibition requires full knowledge of the interaction between the protective compound and the metal surface. Many of the organic corrosion inhibitors have at least one polar unit with atoms of nitrogen,

sulphur, oxygen and in some cases phosphorous. The polar unit is regarded as the reaction centre for the chemisorption process. Furthermore, the size, orientation, shape and electric charge on the molecule determine the degree of adsorption and hence the effectiveness of inhibitor. On the other hand, iron is well known for its co-ordination affinity to heteroatom bearing ligands.

Organic materials act as corrosion inhibitors according to their functional group, which are adsorbed on the metal surface. Organic compounds having π bonds are found to inhibit corrosion of steel by getting adsorbed over the electronic surface through electron sharing. Presence of functional groups such as NH, N-N, -CHO, ROH etc in the inhibitor molecule and also the steric factor, aromaticity, electron density at the donor atoms are found to influence the adsorption of the inhibitor molecule over corroding electrode surface.

From the various results of weight loss, electrochemical techniques surface analytical techniques and quantum chemical calculations, it was concluded that imidazoline derivatives P2I, TMP2I, DMP2I, OCP2I, PNDMP2I and PNP2I inhibit the corrosion of mild steel in 0.5M H_2SO_4 and 1M HCl by the adsorption at the metal/solution interface. The essential effect of these compounds as corrosion inhibitors is due to the presence of several potential sources like free electron pair on the nitrogen atom, capable of forming a co-ordination bond with Fe. Secondly, the π-electrons from the aromatic ring may interact with the metal surface. The unshared and π-electrons interact with the d-orbital of Fe to provide a protective film. The inhibitive properties of such compounds depend on the electron densities at the active centres, the more effect is the inhibitor.

1. The inhibition of active dissolution of the metal is due to the adsorption of the inhibitor molecules on the metal surface forming a protective layer. In general, the rate of adsorption is quite swift and as a result, the metal surface is shielded from the corrosive environment. The inhibitor molecules can be adsorbed onto the metal surface through the electron transfer from the adsorbed species to the vacant electron orbit of low energy in the metal to form a coordinate type link. As stated before, the adsorption process is often displacement reaction between water and inhibitor molecules. Iron is quite well known for its coordination affinity towards nitrogen and oxygen bearing ligands. Therefore, adsorption on the metal surface can be attributed to

coordination of the organic compounds via phenolic and iminic groups in all three cases. During chemisorption of the compounds, electron transfer can be expected with compounds having relatively loose band electrons.The π electrons in the system is then likely to be determining factor in the adsorption process **(Kaan *et al.*, 2006).**

2. Increase in inhibition efficiencies with the increase of concentration of imidazoline derivatives show that the inhibition action is due to adsorption on the metal surface. Four types of adsorption may take place by organic molecules at metal/solution interface namely.
    i) Electrostatic attraction between the charged molecules and charged metal.
    ii) Interaction of the unshared electron pairs in the molecule with th metal.
    iii) Interaction of π-electrons with the metal.
    iv) Combination of i) and iii)

Further, imidazoline molecules are chemically adsorbed due to interaction of π-orbitals with metal surface. (**Ashish Kumar Singh *et al.*, 2010).**

3. The lone pair of electrons in the nitrogen atom can form co-ordination bond with the iron by sharing the electrons with the unfilled levels.
4. The π-electrons on the aromatic ring **(Sathyanarayanan *et al.*, 2005)**

The reason for which imidazoline was better corrosion inhibitor is due to the plane geometry of the heterocyclic ring, thus favouring adsorption through the double iminic bond N=C. The iminic nitrogen seems to be directly involved in the coordination of the cycle with the metal surface. The π-electron is easily translated to an Fe atom and is more favourable for chemical adsorption of the N atom on the metal surface. It is also evident from the C_{dl} values. **(Curz *et a.*.2004)**

The adsorption of imidazoline on the mild steel surface can be visualized as shown in the Fig -86 (a-b)

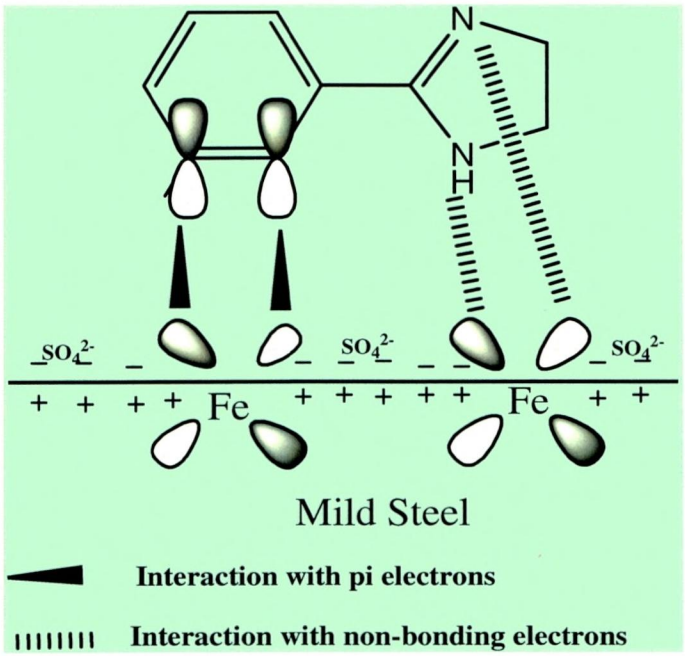

Figure -86 -a The schematic illustrations of different modes of adsorption of mild steel/acid interface in H_2SO_4

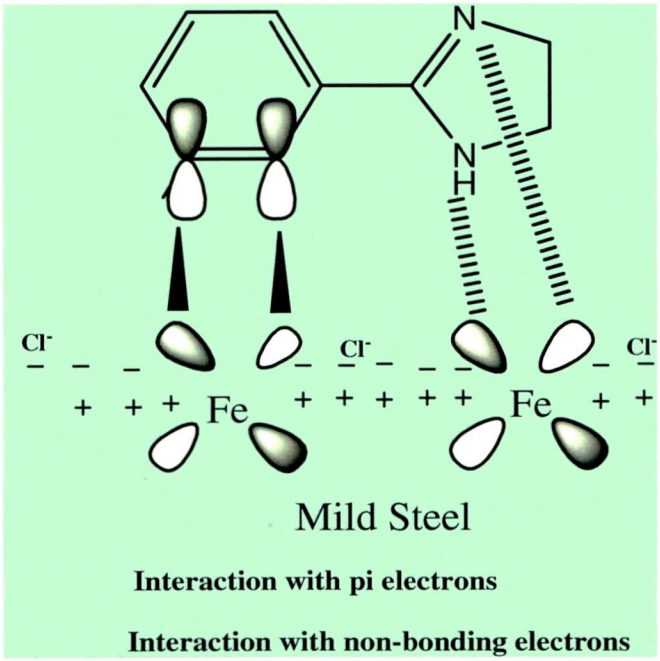

Figure – 86 b The schematic illustrations of different modes of adsorption of mild steel/acid interface in HCl

ADSORPTION MODELS

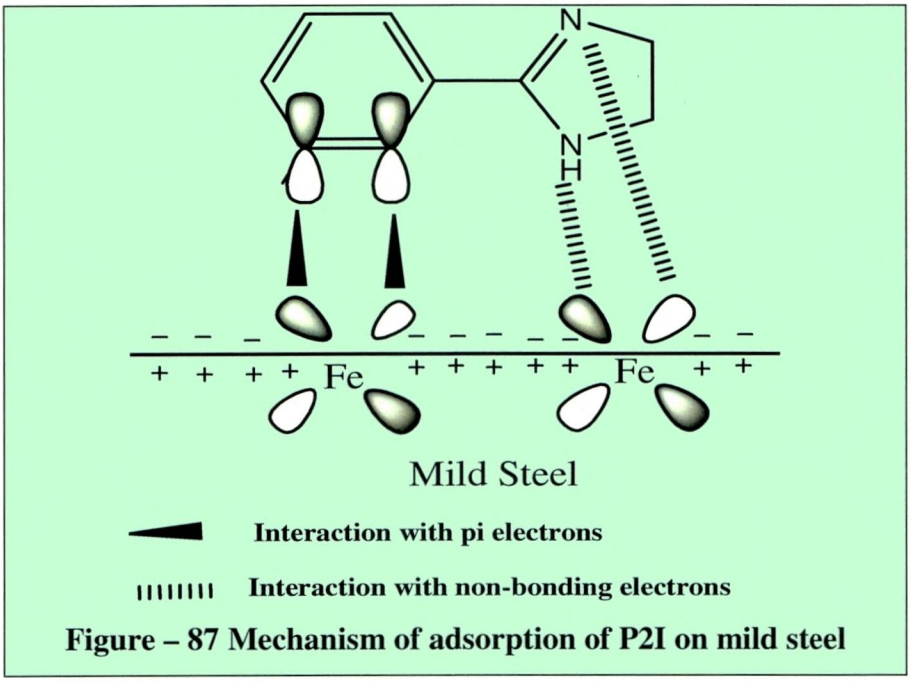

Figure – 87 Mechanism of adsorption of P2I on mild steel

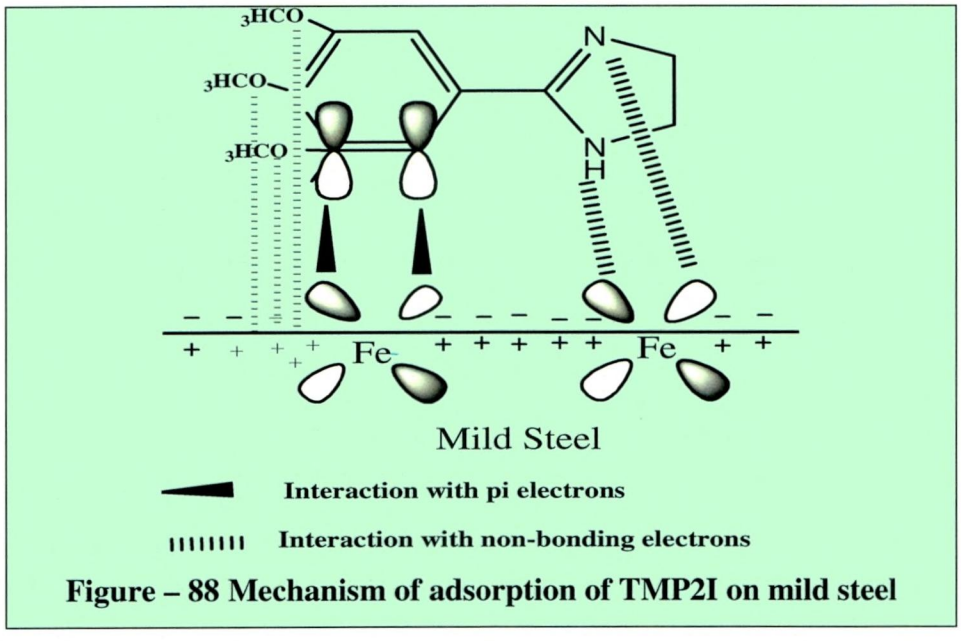

Figure – 88 Mechanism of adsorption of TMP2I on mild steel

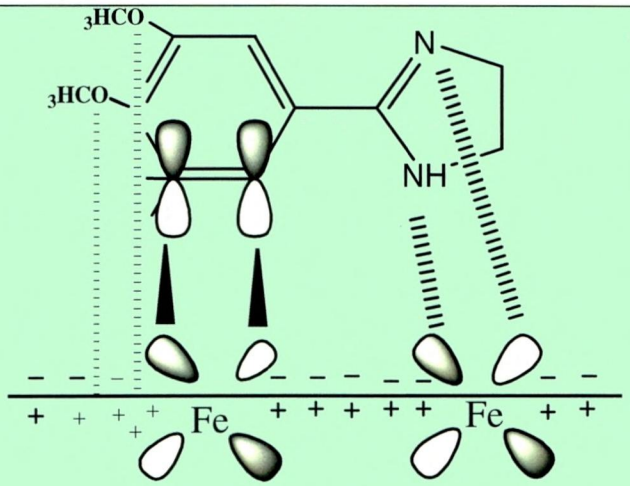

Figure – 89 Mechanism of adsorption of DMP2I on mild steel

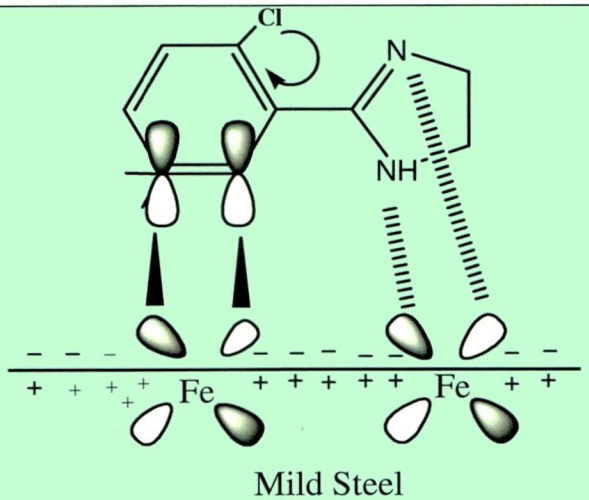

Figure – 90 Mechanism of adsorption of OCP2I on mild steel

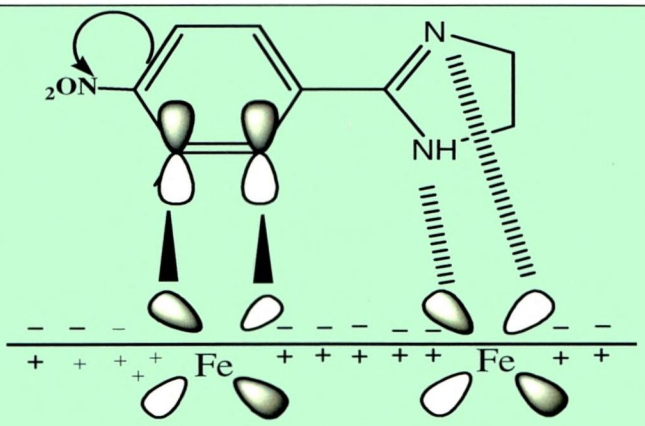

Figure – 91 Mechanism of adsorption of PNP2I on mild steel

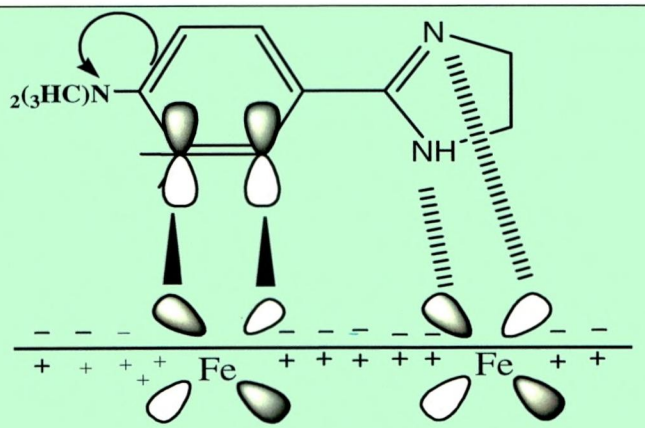

Figure – 92 Mechanism of adsorption of PNDMP2I on mild steel